

AD-A075 809 NAVAL SURFACE WEAPONS CENTER WHITE OAK LAB SILVER SP--ETC F/G 19/4  
DYNAMICAL MODEL FOR EXPLOSION INJURY TO FISH.(U)  
DEC 78 J F GOERTNER  
UNCLASSIFIED NSWC/WOL/TR-76-155

NL

1 OF 2  
AD  
A075809



NSWC/WOL TR 76-155

12

LEVEL #

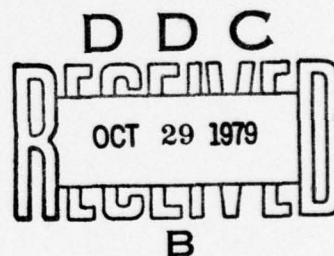
## DYNAMICAL MODEL FOR EXPLOSION INJURY TO FISH

BY JOHN F. GOERTNER

RESEARCH AND TECHNOLOGY DEPARTMENT

18 DECEMBER 1978

Approved for public release, distribution unlimited



ORIGINAL CONTAINS COLOR PLATES: ALL DDC  
REPRODUCTIONS WILL BE IN BLACK AND WHITE



**NAVAL SURFACE WEAPONS CENTER**

Dahlgren, Virginia 22448 • Silver Spring, Maryland 20910

79 10 29 054

AD A 075809

DDC FILE COPY



UNCLASSIFIED

SECURITY CLASSIFICATION OF THIS PAGE (When Data Entered)

REPORT DOCUMENTATION PAGE		READ INSTRUCTIONS BEFORE COMPLETING FORM
1. REPORT NUMBER (14) NSWC/WOL/TR-76-155	2. GOVT ACCESSION NO.	3. RECIPIENT'S CATALOG NUMBER
4. TITLE (and Subtitle) (6) Dynamical Model for Explosion Injury to Fish,	5. TYPE OF REPORT & PERIOD COVERED (9) Final Repts	
7. AUTHOR(s) (10) John F. Goertner	6. PERFORMING ORG. REPORT NUMBER	
9. PERFORMING ORGANIZATION NAME AND ADDRESS Naval Surface Weapons Center White Oak, Silver Spring, Maryland 20910	8. CONTRACT OR GRANT NUMBER(s) (16) S0400	
11. CONTROLLING OFFICE NAME AND ADDRESS (12) 352	10. PROGRAM ELEMENT, PROJECT, TASK AREA & WORK UNIT NUMBERS 63721N; S0400; S040001 CR14CA501 (17)	
14. MONITORING AGENCY NAME & ADDRESS (if different from Controlling Office)	12. REPORT DATE (11) 18 December 1978	
	13. NUMBER OF PAGES 137	
	15. SECURITY CLASS. (of this report) UNCLASSIFIED	
	15a. DECLASSIFICATION/DOWNGRADING SCHEDULE	
16. DISTRIBUTION STATEMENT (of this Report) Approved for public release, distribution unlimited.		
17. DISTRIBUTION STATEMENT (of the abstract entered in Block 20, if different from Report)		
18. SUPPLEMENTARY NOTES		
19. KEY WORDS (Continue on reverse side if necessary and identify by block number) Underwater Explosions      Cavitation Swim Bladder Fish      Sound Ranging Fish-kill      Lethal Ranges Explosion Effects		
20. ABSTRACT (Continue on reverse side if necessary and identify by block number) A new method is given for calculating kill probability for bladder fish subjected to the rapidly varying pressure field of an underwater explosion. The method consists of an approximate calculation for the extreme values of compression and extension of the fishes' gas-filled swim bladder in response to the explosion pressure wave. The calculations are made for the damped radial oscillations of a spherical air bubble in water. The kill probability is then calculated as an experimentally (Cont)		

DD FORM 1473  
1 JAN 73EDITION OF 1 NOV 65 IS OBSOLETE  
S/N 0102-014-6601

UNCLASSIFIED

SECURITY CLASSIFICATION OF THIS PAGE (When Data Entered)

391 596

alt

UNCLASSIFIED

SECURITY CLASSIFICATION OF THIS PAGE(When Data Entered)

determined function of the ratio of maximum to minimum radius during the oscillatory response. For each species of fish the effective bubble radius for the calculations is determined thru correlating the observed injuries with the calculated radius ratio.

The method was used to satisfactorily describe dissection results from 1500 Spot and White Perch caged at depths from 5 to 100 feet and subjected to pentolite explosions of from 1 to 70 lbs submerged at depths ranging from 5 to 70 feet. An approximate method for calculating the pressure signature from an underwater explosion subject to surface effects - including cavitation - is given in an appendix.

UNCLASSIFIED

SECURITY CLASSIFICATION OF THIS PAGE(When Data Entered)

FOREWORD

This report deals with the prediction of explosion injury to fish with swim bladders and is part of a continuing study of the effects of underwater explosions on marine life. Swim bladder fish are particularly vulnerable to explosions, and this group includes the majority of fish with sports and commercial value. This study will result in an improved capability to predict such effects, and will be useful in connection with the testing of new explosives and of warheads at sea.

This study is part of the ordnance pollution abatement program of the Naval Sea Systems Command and was supported by SEA TASK SSL 55001/19373.

The author is indebted to Ermine A. Christian and George A. Young for many valuable suggestions during the course of this work.

*Julius W. Enig*

JULIUS W. ENIG  
By direction

ACCESSION for		
NTIS	White Section	<input checked="" type="checkbox"/>
DDC	Buff Section	<input type="checkbox"/>
UNANNOUNCED		<input type="checkbox"/>
JUSTIFICATION		
BY		
DISTRIBUTION/AVAILABILITY CODES		
Dist.	AVAIL.	and/or SPECIAL
A		



## CONTENTS

	Page
1 INTRODUCTION AND SUMMARY .....	13
2 DYNAMICAL MODEL .....	14
2.1 The Swim Bladder .....	14
2.2 Preliminary Calculations of Bladder Oscillation ....	14
2.3 Current Method for Calculating Bladder Oscillation .....	14
3 CORRELATIONS WITH EXPERIMENTAL DATA .....	23
3.1 Summary of Test Data and Computation Results .....	23
3.2 Observed Injuries to Spot vs Calculated Oscillation Parameter Z .....	38
3.3 Observed Injuries to White Perch vs Calculated Oscillation Parameter Z .....	42
3.4 Comparison of Shockwave Impulse and Calculated Bladder Oscillation as Damage Parameters .....	47
3.5 Discussion of Injury Correlations .....	49
4 APPLICATIONS .....	53
4.1 Fish-Kill Contours .....	53
4.2 Kill Probabilities as a Function of Depth for Different Sized Fish .....	57
4.3 Total Fish-Kill and its Spatial Distribution .....	59
REFERENCES .....	63
LIST OF SYMBOLS .....	6
APPENDIX A RESPONSE OF GAS BLADDER TO UNDERWATER EXPLOSION PRESSURES: SQUARE STEP APPROXIMATION .....	A-1
APPENDIX B METHOD FOR CALCULATING GAS BLADDER RESPONSE TO EXPLOSION PRESSURE WAVE .....	B-1
APPENDIX C APPROXIMATE METHOD FOR CALCULATING THE PRESSURE- TIME SIGNATURE .....	C-1
APPENDIX D LOCATION OF FISH CAGES BY SOUND RANGING .....	D-1
APPENDIX E NOTE ON FISH CLOSE TO THE WATER SURFACE .....	E-1



## ILLUSTRATIONS

<u>Figure</u>		<u>Page</u>
2.1.1	Body Tracing of Spot .....	15
2.1.2	Swim Bladder Removed from Spot .....	16
2.1.3	Body Tracing of White Perch .....	17
2.3.1	Bladder Pressure and Size as a Function of Time .....	18
2.3.2	Approximating Step Wave for Calculating Oscillatory Response .....	21
3.1.1	Sketch Showing Calculated Pressure-Time Signature .....	33
3.1.2	Sketch Depicting Injury Code for Evaluating Visible Fish Damage .....	37
3.2.1	Observed Injuries to Spot as a Function of Z .....	39
3.2.2	Observed Cumulative Injury to Spot as a Function of Z .....	41
3.3.1	Observed Injuries to White Perch as a Function of Z .....	43
3.3.2	Observed Cumulative Injury to White Perch as a Function of Z .....	45
3.3.3	Observed Cumulative Injury as a Function of Z - Spot and White Perch Combined Data .....	46
3.4.1	Correlations of Level 3 Injuries for Spot and White Perch with Impulse Damage Parameter and with Bladder Oscillation Parameter .....	48
3.5.1	Sketch Illustrating Bubble Response to a Pressure Wave of Very Short Duration .....	51
4.1.1	Region of Greater than 50% Kill for 18 cm Spot - 32 KG Pentolite at 9 M Depth.....	54
4.1.2	Regions of Greater than 10%, 50%, and 90% Kill for 21.5 cm White Perch - 32 KG Pentolite at 9 M Depth.....	56
4.2.1	Predicted Kill Probabilities as a Function of Depth for Different Size Fish - 32 KG Charge at 9 M Depth - Horizontal Range: 91 Meters.....	58

## TABLES

<u>Table</u>		<u>Page</u>
3.1.1	Applied Pressure Parameters and Bladder Oscillation Response for Spot .....	24
3.1.2	Applied Pressure Parameters and Bladder Oscillation Response for White Perch .....	26
3.1.3	Observed Injuries for Spot and Calculated Oscillation Parameter Z .....	28
3.1.4	Observed Injuries for White Perch and Calculated Oscillation Parameter Z .....	30
3.1.5	Code for Evaluating Visible Fish Damage .....	36
3.2.1	Averaged Observed Injury Probability for Spot as a Function of Calculated Oscillation Parameter Z .....	40
3.3.1	Averaged Observed Injury Probability for White Perch as a Function of Calculated Oscillation Parameter Z .....	44
4.1.1	Bladder Oscillation Parameter Z as a Function of Fishes' Depth and Horizontal Range.....	55
4.3.1	Bladder Oscillation Parameter and Kill Probability as a Function of Fishes' Depth and Horizontal Range .....	60
4.3.2	Fish Present and Number Killed as a Function of Water Depth and Horizontal Range .....	61

LIST OF SYMBOLS

$A$	Swimbladder or bubble radius
$A_i$	Bladder or bubble radius corresponding to ambient pressure $p_i$
$(A_i)_0$	Bladder or bubble radius corresponding to zero depth, i.e., one atmosphere pressure
$\bar{A}$	Bladder or bubble radius at "equilibrium" (radius after oscillation has damped out, Equation A-19)
$A_M$ or AMAX	Maximum bubble radius
$A_m$ or AMIN	Minimum bubble radius
$A_{c_n}, t_{c_n}, V_{c_n}, P_{c_n}$	Radius, time, volume, and internal air pressure when ambient pressure jump from $p_n$ to $p_{n+1}$ occurs
$P_M$	Bubble internal air pressure at maximum size
$P_m$ or PMIN	Bubble internal air pressure at minimum size
$P_O$	Bubble internal air pressure at "equilibrium" (= $p_n$ )
$A_{Mm}, V_{Mm}, P_{Mm}$	Bubble radius, volume, or internal air pressure at either extremum of the bubble oscillation (Appendixes A and B)



$P_o$	Ambient water pressure = constant = $p_i, p_1, p_2, \dots$
$p_i$	Initial value of ambient water pressure
$p_n$	$n^{th}$ value of ambient water pressure = constant
$P(A)$	Air pressure inside bubble of radius A
$V(A)$	Volume of bubble of radius A
$E(A)$	Internal energy of air inside bubble
$Y$	Total energy of oscillating bubble (Equation A1)
$Y_i$	Initial value of total energy of at-rest bubble
$Y_n$	$n^{th}$ value of total energy of oscillating bubble = constant (Equations A7, A10, B15)
$\bar{Y}_n$	$n^{th}$ value of total energy of non-oscillating equilibrium bubble (Equation B17)
$Y'_n$	$Y_n - \bar{Y}_n$ = oscillation energy of bubble (Equation B18)
$\rho$	Density of water = constant
$\gamma$	Exponent in adiabatic P-V relationship = 1.4 (for air)
$a$	Dimensionless bubble radius = $A/L$
$L$	Fork length of fish - length measured from most anterior part of head to deepest point of notch in tailfin



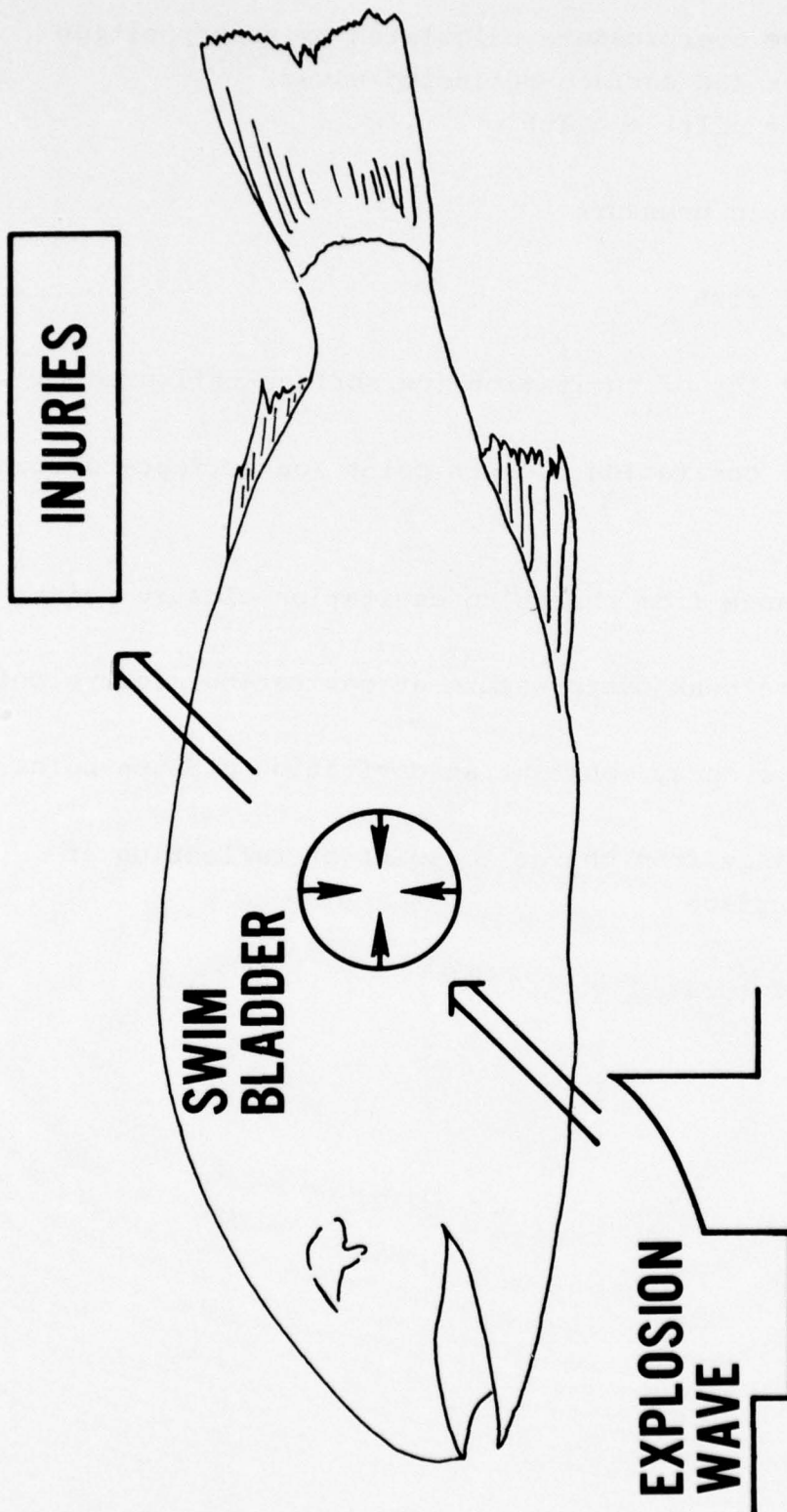
L	Length scale factor (Equation A-5)
t'	Dimensionless time = $t/C$
C	Time scale factor (Equation A-6)
T, T'	Bubble period of oscillation and dimensionless bubble period
$\bar{T}$ , $\bar{T}'$	Equilibrium bubble period and dimensionless equilibrium bubble period (for vanishingly small oscillations about the equilibrium radius, Equation B-9)
k	Bubble oscillation parameter (Equations A-4 and A-13)
X	$\frac{P_{Mm}}{P_o(\gamma-1)}$ , parameter used in Appendix A to compute other bubble oscillation parameters, where $P_{Mm}$ is the internal pressure at either extremum of the bladder oscillation
X	$-100 \ln AMIN/A_i$ (Equation 3.1.3)
Y	$100 \ln AMAX/A_i$ (Equation 3.1.4)
Z	$X + Y = 100 \ln AMAX/AMIN$ = Bladder Oscillation Parameter (damage parameter used for fish-kill and injury correlations) - (Equation 3.1.5)
$Z_I$	$80 \ln \left[ I/M^{1/3} \right]$ = Impulse Damage Parameter (damage parameter used for fish-kill and injury correlations)
ln	Natural logarithm

I	Impulse of positive portion of pressure wave in psi-mec
M	Mass of fish in grams
$Z_{50\%}$	Value of Bladder Oscillation Parameter corresponding to 50% kill probability
TPOS	Time corresponding to end of positive pressure phase (Figure 3.1.1)
$(\Delta t/T)_{PC}$	The fraction portion of the number of oscillation cycles during the positive phase
DTNEG	Duration of the negative pressure phase (Figure 3.1.1)
$T_{neg}$	Bubble period of oscillation during negative pressure phase
$(\Delta t/T)_{NP}$	Parameter which locates the end of the negative phase in terms of bubble oscillation cycles (Equations B-13 thru B-16)
$\alpha$	Coefficient used to estimate the bubble period of oscillation (Equation B-10)
$\beta$	Fraction of oscillation energy removed each half-cycle to achieve damped oscillations (Equation B-23)
$\alpha, \beta$	Exponents in the shockwave similitude equations for P <sub>MAX</sub> and $\theta$ (Equations C-2 and C-3)
$k, \ell$	Coefficients in the shockwave similitude equations for P <sub>MAX</sub> and $\theta$ (Equations C-2 and C-3)

PMAX	Shockwave peak overpressure referenced to initial ambient pressure, $p_i$ , but generally referred to as "shockwave peak pressure"
$\theta$	Shockwave decay constant (Figure 3.1.1)
PCORR	Coefficient used to adjust shockwave peak overpressure for batch-to-batch variations in explosive charges (Equation 3.1.1)
PNEG	Pressure during negative phase (measured from hydrostatic) (Figure 3.1.1)
R	Slant range from charge
$R_o$	Radius of charge
$R_1$	Slant range from image of charge reflected in water surface
$c_o$	Sound speed in water
U	Shock velocity in water
D	Detonation velocity in charge
PVAP	Vapor pressure of water
$p_{ABS}$	Absolute pressure
g	Acceleration of gravity
$p_D(t)$	Free-field or direct-arrival shockwave overpressure
$p_r(t)$	Surface-reflected overpressure wave

$p_{SUM}(t)$	Shockwave overpressure calculated by superposition of direct and surface-reflected waves, $p_{SUM}(t) = p_D(t) + p_R(t)$
$P_{ATM}$	Atmospheric pressure
$y$	Depth of fish
$y_t$	Depth of top of cavitation (on surface-reflected ray)
$y_c$	Depth of cavitation closure point (on surface-reflected ray)
$R_c$	Slant range from charge to cavitation closure point
$P_{MAX}_c$	Shockwave peak overpressure at cavitation closure point
$\theta_c$	Shockwave decay constant at cavitation closure point
$R_z$	Slant range from charge to point of reflection at water surface
$DOB$	Depth of burst





FRONTISPIECE: THE DAMAGE MECHANISM

This sketch illustrates the fundamental hypothesis of this report. For bladder fish the fish-kill correlates with injuries caused by the oscillatory response of the fish's swim bladder to the incident explosion pressure wave. How these injuries come about--whether they are due to displacements associated with the motion or to the radiated pressure field--is not known.

## DYNAMICAL MODEL FOR EXPLOSION INJURY TO FISH

## 1 INTRODUCTION AND SUMMARY

This report describes a method for calculating the kill probability for bladder fish subjected to an underwater explosion. The method consists of an approximate calculation for the extreme values of compression and extension of the fishes' gas-filled swim bladder in response to the explosion pressure wave. The calculations are made for the damped radial oscillations of a spherical air bubble in water. The kill probability is then calculated as an experimentally determined function of the ratio of maximum to minimum radius during the oscillatory response. For each species of fish the effective swim bladder radius needed for the calculations is determined by trial and error thru correlating the observed injuries with the calculated ratio of maximum to minimum radius.

The method is used to describe dissection results from 1500 Spot and White Perch caged at depths from 5 to 100 feet and subjected to pentolite explosions of from 1 to 70 lbs submerged at depths ranging from from 5 to 70 feet.<sup>1,2</sup>

These results are then used to calculate several examples of kill-probability and fish-kill distributions for a particular explosion geometry and several species and sizes of fish. Details of the computations are given in the appendices. Appendix C gives an approximate method for calculating the pressure signature from an underwater explosion subject to surface effects including cavitation.

- 
1. Gaspin, Joel B., "Experimental Investigations of the Effects of Underwater Explosions on Swim Bladder Fish, I: 1973 Chesapeake Bay Tests", NSWC/WOL TR 75-58, 1975.
  2. Gaspin, J. B., Wiley, M. L., and Peters, G. B., "Experimental Investigations of the Effects of Underwater Explosions on Swim Bladder Fish, II: 1975 Chesapeake Bay Tests", NSWC/WOL TR 76-61, 1976.

## 2. DYNAMICAL MODEL

2.1 THE SWIM BLADDER. Figure 2.1.1 shows a life-size tracing of a Spot (Leiostomus xanthurus Lacepède) which depicts the swim bladder and the surrounding internal organs. Figure 2.1.2 shows a swim bladder removed from a Spot. In our work we depicted the motion of this organ by that calculated for a spherical bubble of air. The size of this "equivalent spherical bubble" was first estimated by equating its volume to that of the fishes' swim bladder -- then later we adjusted the size of the equivalent bubble to optimize the correlation between the calculated motion and the observed injuries.

Figure 2.1.3 shows a life-size tracing of a White Perch (Morone americana Gmelin), the other species of fish used in the work reported here. The inset shows the shape of the forward portion of the swim bladder in-place in the fish.

2.2 PRELIMINARY CALCULATIONS OF BLADDER OSCILLATION. We began this study by making order of magnitude calculations which approximated the explosion pressure field with a step increase followed by a step decrease in pressure. The fishes' swim bladder was approximated by a spherical bubble of air in an infinite body of water -- and, we calculated its undamped oscillatory response. These order of magnitude calculations showed that the oscillatory response of the swim bladder was a likely source of the fishes' injuries. They also pointed out a strong resonance which occurs when surface cut-off (the arrival of the rarefaction wave reflected from the water surface) happens at the instant of maximum bladder compression. This work was described in an internal Center report which is reproduced as Appendix A of this report.

2.3 CURRENT METHOD FOR CALCULATING BLADDER OSCILLATION. The method developed for calculation of the oscillatory response to the changing pressure field generated by an underwater explosion is described in detail in Appendix B. Here, we attempt to give the reader a feel for this computation and its approximate nature. Figure 2.3.1 shows the idealized pressure signature measured on an underwater explosion test together with the calculated pressure inside a fish's swim bladder



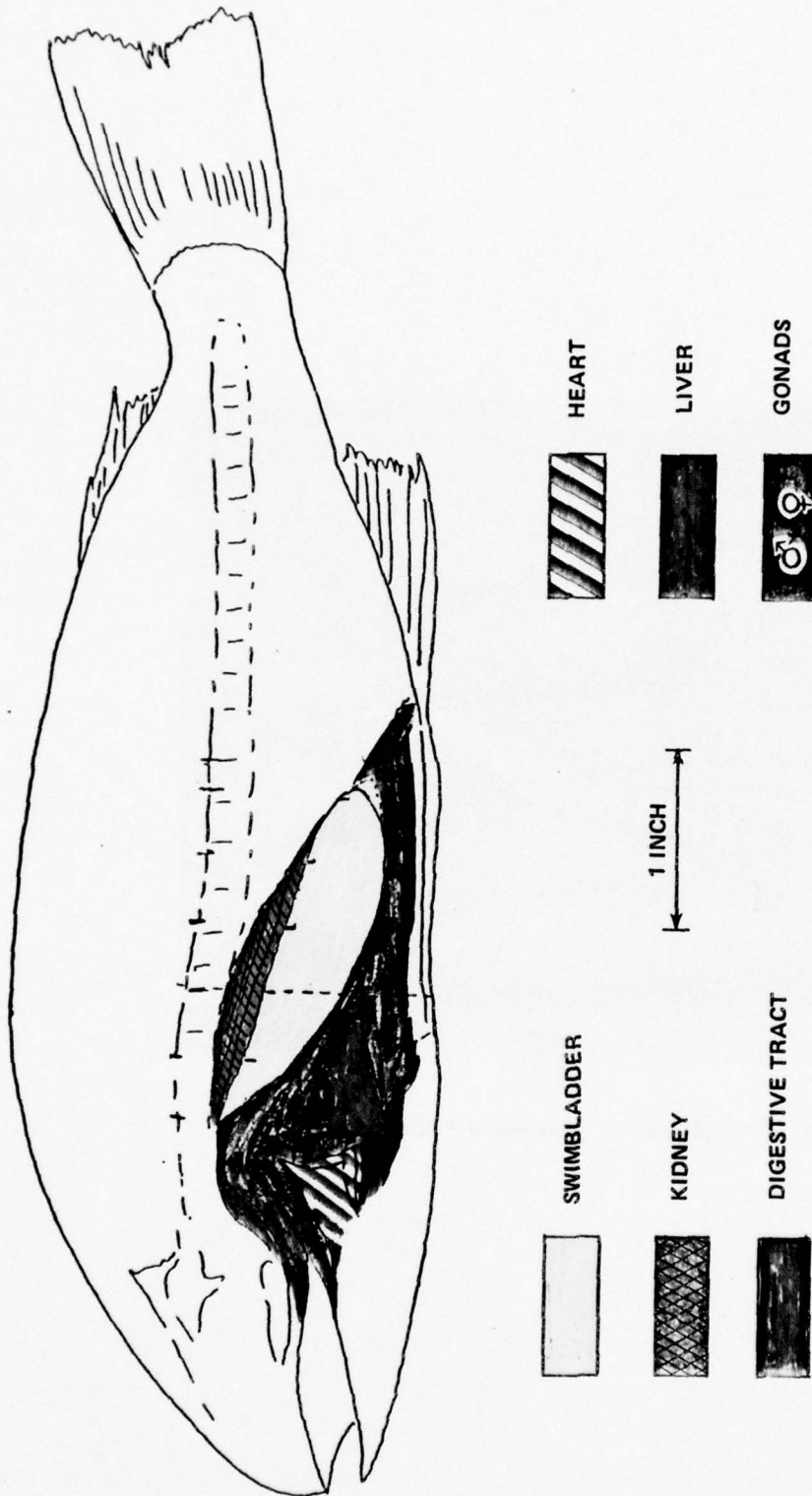


FIG. 2.1.1 BODY TRACING OF SPOT

This is a life-size body tracing of a frozen fish which has been sawed in half.



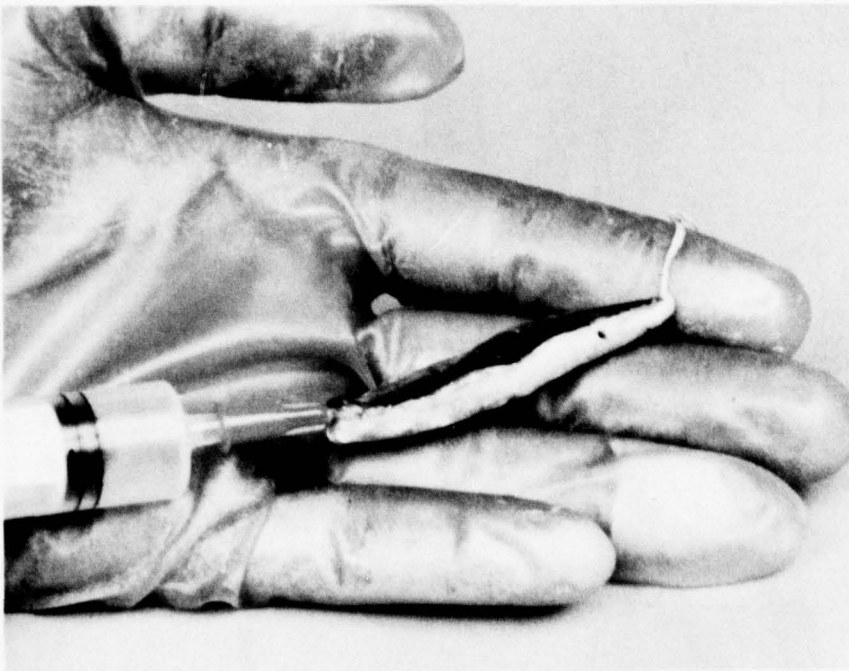


FIG. 2.1.2 SWIM BLADDER REMOVED FROM SPOT

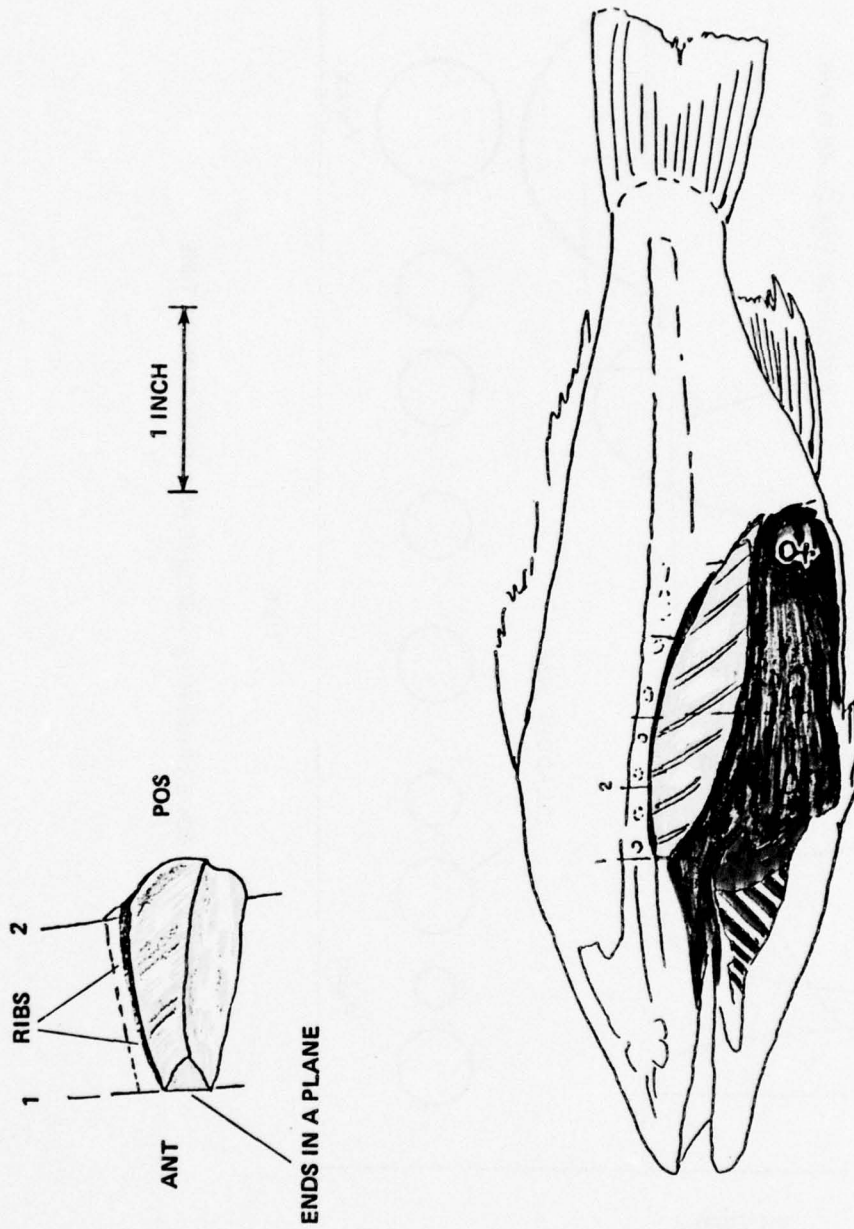


FIG. 2.1.3 BODY TRACING OF WHITE PERCH (LIFE-SIZE)

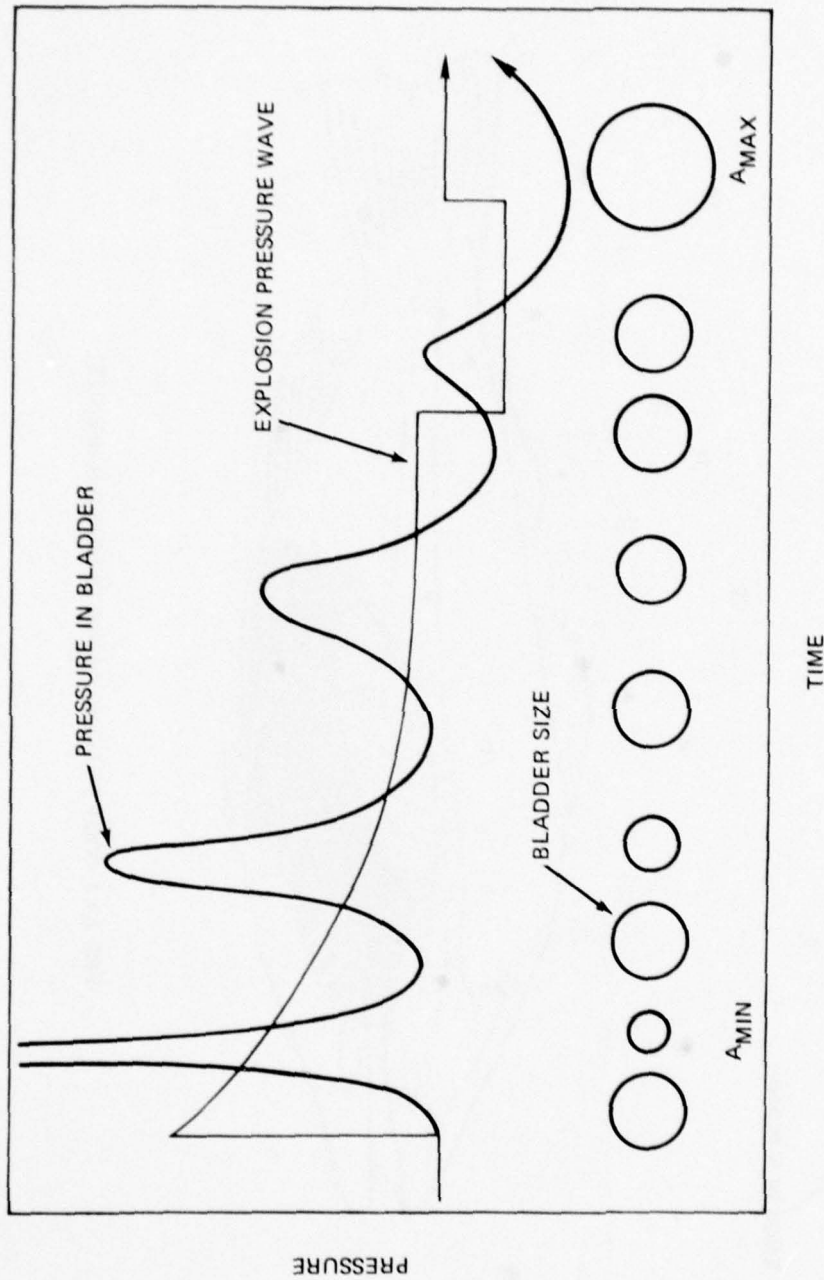
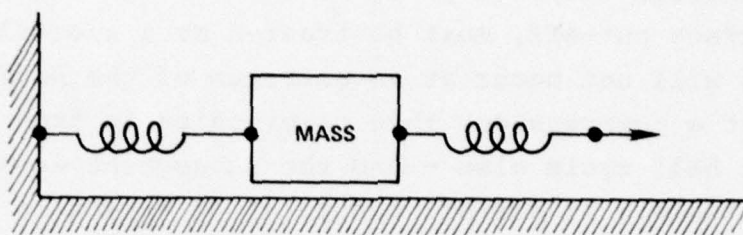


FIG. 2.3.1 BLADDER PRESSURE AND SIZE AS A FUNCTION OF TIME

as it responds to this applied pressure. Below the pressure traces are corresponding sizes calculated for the spherical air bubble used to represent the fish's swim bladder.

This fluid motion can be likened to a mass attached between two springs, the end of one being fixed, the end of the other movable.



The first spring is analogous to the internal gas pressure; the second to the changing external water pressure. Let us imagine the mass resting on a frictionless block of ice. It is at rest in a position of equilibrium. If at  $t=0$  we quickly displace the movable spring to a new position, the mass will oscillate about a new position of equilibrium determined by the displacement of the end of the spring. The mass will oscillate about this new equilibrium position with an amplitude equal to the displacement of this equilibrium position from the initial at-rest position of the mass.

This initial at-rest position now becomes an extremum of the oscillatory motion. Since, at each extremum of the motion the mass is instantaneously at rest, a subsequent jump displacement of the end of the spring occurring at an extremum simply shifts the motion to an oscillation about a new equilibrium position - and the new amplitude is just the distance of the mass at the time of the jump from this new equilibrium position.

Likewise, for the bubble, step changes in the outside water pressure occurring at half-period intervals simply change the equilibrium pressure (equal to the outside pressure) of the oscillating



bubble flow - and the new amplitude is just the instantaneous excursion of the bubble pressure from the changed outside pressure. We made use of this property of the motion to calculate the motion as the response to a series of pressure steps as shown in Figure 2.3.2. (Appendix B describes the way we estimated successive half-periods in order to construct the approximating step wave.)

The transition from the positive to the negative pressure phase, i.e., surface cut-off, must be treated as a special case, since in general, this will not occur at an extremum of the motion. If cut-off occurs at a compression, this compression is then the compression of the next half cycle also - and the subsequent expansion is the greatest possible. If cut-off occurs at an expansion and the new outside pressure is lower than that inside, this expansion becomes the compression of the next half cycle, there occurs a 180 degree phase shift, and the subsequent expansion is the smallest possible. In general, cut-off occurs somewhere in between and there is an intermediate phase shift and subsequent expansion or compression. In such cases we calculated this next half cycle at lowered pressure as starting at the time of the previous extremum but at a fictitious amplitude interpolated as a function of the time at which cut-off occurred. (The details of this procedure are described in Appendix B.)

Finally, at the end of the negative phase, the return to ambient pressure can cut short or even prevent the final expansion. This was handled in an analogous manner to surface cut-off and is also described in Appendix B.

To approximate the dissipation of energy which in nature must occur during the oscillation, we arbitrarily extracted a fraction — 30% — of the remaining oscillation energy at each half cycle of the motion.

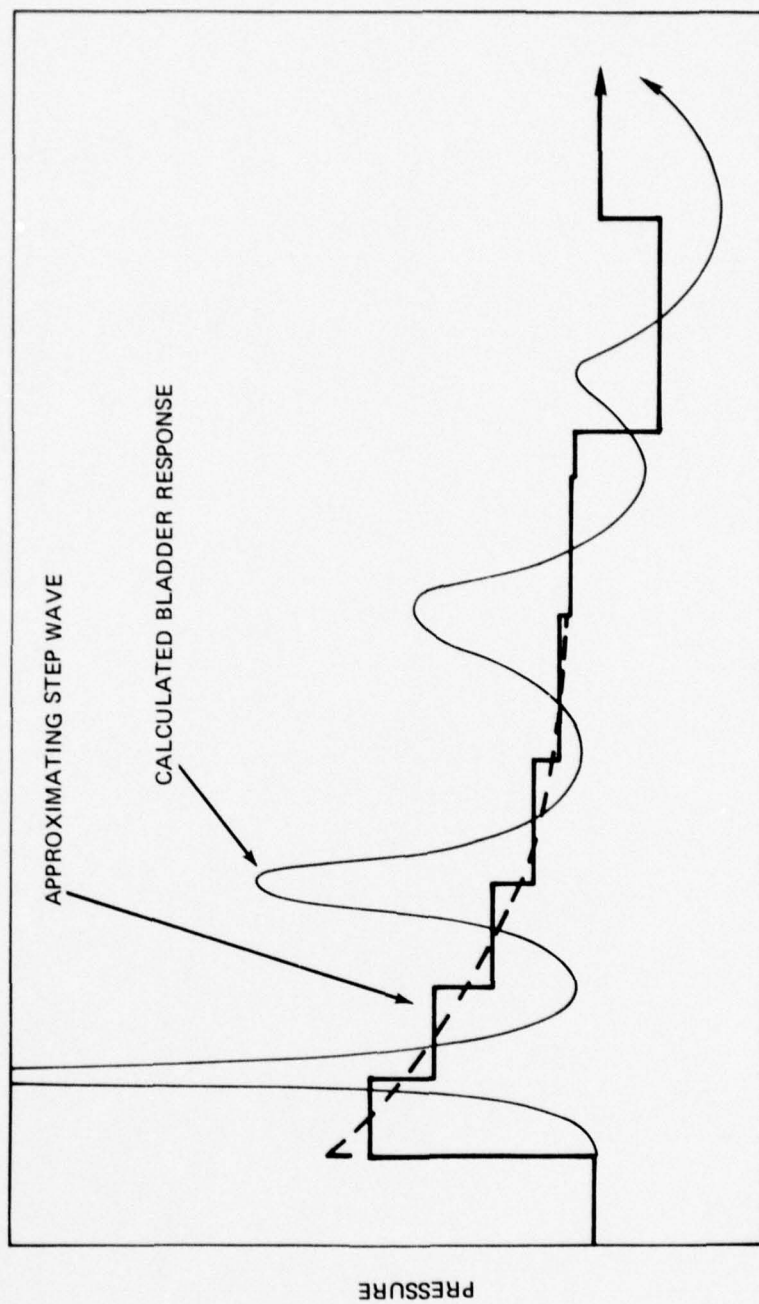


FIG. 2.3.2 APPROXIMATING STEP WAVE FOR CALCULATING OSCILLATORY RESPONSE

## 3. CORRELATIONS WITH EXPERIMENTAL DATA

3.1 SUMMARY OF TEST DATA AND COMPUTATION RESULTS. Tables 3.1.1 thru 3.1.4 summarize the input and output parameters of the computations of this report. These tables include all the test data for Spot and White Perch obtained on the 1973 and 1975 test series in the Chesapeake Bay. For the 1973 test data (the "500" Shot Numbers) the fishes' horizontal ranges and depth which are listed in the tables are the preset or intended values.<sup>1</sup> On the 1975 tests, shots 783 thru 786, water currents caused significant deviations in horizontal range and depth. For these shots the preset values<sup>2</sup> have been corrected as described in Appendix D. (Tables D-2 thru D-7 list corrected values for charge depth and fish and pressure gage locations for all shots of the 1975 test series.)

The ambient pressure (Tables 3.1.1 and 3.1.2) is the total hydrostatic head at fish depth calculated for fresh water, density = 1000 kg/m<sup>3</sup>, and nominal atmospheric pressure,  $1.013 \times 10^5$  pascals. The vapor pressure was calculated from the measured water temperature (1975 tests) or estimated water temperature (1973 tests).

The peak pressure P<sub>MAX</sub> in pascals and time constant  $\theta$  in milliseconds are calculated from the similitude relations for pentolite

$$P_{MAX} = PCORR \times 5.62 \times 10^7 \left( \frac{W^{1/3}}{R} \right)^{1.14} \quad (3.1.1)$$

$$\theta = 0.084 W^{1/3} \left( \frac{R}{W^{1/3}} \right)^{0.23} \quad (3.1.2)$$

where W is the explosive mass in kilograms, R is the slant range from the charge in meters, and PCORR is an empirical constant that was used to adjust Equation 3.1.1 for batch-to-batch variations in the explosive charges. For the 1973 test series PCORR = 1.10 — for the 1975 tests PCORR = 0.95.

(Text continued on page 32)



TABLE 3.1.1 APPLIED PRESSURE PARAMETERS AND BLADDER OSCILLATION RESPONSE FOR SPOT  
(1 bar =  $10^5$  pascals = 14.50 psi)

SHOT	FISH HOR. RANGE (M)	FISH DEPTH (M)	AMBIENT PRESS. (BARS)	VAPOR PRESS. (BARS)	PEAK PRESS. (BARS)	TIME CONST. (MSEC)	APPLIED PRESSURE		BLADDER OSCILLATION RESPONSE					
							POSITIVE PRESS. DURATION (MSEC)	NEG. DURATION (MSEC)	POS. CYCLES	NEG. CYCLES	OSCILLATION X	OSCILLATION Y	OSCILLATION Z	
517	12.8	1.5	1.16	.034	25.2	.12	.24	-1.13	2.75	1.32	.67	161.	40.	201.
	12.8	6.1	1.61	.034	23.5	.12	.87	-.97	4.05	3.15	3.47	137.	40.	177.
	36.0	1.5	1.16	.034	7.7	.16	.09	-.90	.48	.37	.64	65.	41.	106.
	36.0	6.1	1.61	.034	7.7	.16	.34	-1.31	.68	1.12	.72	74.	40.	114.
	57.9	1.5	1.16	.034	4.5	.17	.05	-1.34	.56	.16	.88	16.	18.	34.
518	25.0	1.5	1.16	.034	25.4	.25	.48	-1.13	7.17	2.94	1.05	168.	139.	307.
	25.0	6.1	1.61	.034	25.9	.24	1.88	-1.24	8.23	6.91	4.46	149.	64.	213.
	76.2	1.5	1.16	.034	7.2	.32	.16	-1.13	.95	.61	.56	92.	40.	131.
	115.8	3.0	1.31	.034	4.5	.35	.21	-.76	1.24	.62	1.24	63.	61.	124.
	115.8	6.1	1.61	.034	4.5	.35	.43	-1.24	.95	1.26	.90	56.	69.	125.
519	25.0	1.5	1.16	.034	23.5	.25	.89	-1.13	7.48	4.26	1.04	163.	150.	313.
	25.0	6.1	1.61	.034	25.0	.25	3.51	-1.31	7.99	11.04	4.16	147.	70.	217.
	76.2	1.5	1.22	.034	7.2	.32	.45	-.83	2.00	1.51	1.44	89.	75.	164.
	115.8	3.0	1.31	.034	4.5	.35	.43	-1.28	1.40	1.17	.59	63.	51.	114.
	115.8	6.1	1.61	.034	4.5	.35	.85	-.97	1.34	2.04	1.47	56.	34.	90.
521	38.1	3.0	1.31	.034	26.3	.38	.95	-1.28	9.14	5.09	1.10	165.	148.	313.
	112.8	1.5	1.16	.034	7.7	.49	.16	-.55	1.80	.64	1.56	98.	65.	163.
	112.8	5.5	1.55	.034	7.8	.49	.59	-1.52	1.45	2.18	.59	84.	52.	136.
	206.7	3.0	1.31	.034	3.9	.56	.18	-.76	.68	.50	.85	60.	48.	108.
	38.1	3.0	1.31	.034	26.3	.38	.95	-1.28	9.44	6.03	1.21	165.	152.	317.
522	112.8	1.5	1.16	.034	7.7	.49	.16	-1.13	.64	.56	.53	97.	57.	154.
	112.8	5.5	1.55	.034	7.8	.49	.59	-1.24	2.10	2.00	1.30	84.	66.	150.
	176.8	3.0	1.31	.034	4.6	.54	.21	-.83	.70	.60	.84	67.	48.	115.
	213.4	3.0	1.31	.034	3.7	.57	.17	-.69	.60	.52	.89	59.	44.	103.
	38.1	3.0	1.31	.034	26.8	.38	.48	-1.28	7.45	2.67	.83	164.	136.	300.
523	112.8	1.5	1.16	.034	7.8	.49	.08	-.48	.62	.15	.63	21.	16.	37.
	112.8	1.5	1.16	.034	7.8	.49	.08	-.48	.62	.32	.85	70.	44.	114.
	112.8	5.5	1.55	.034	7.8	.49	.30	-.76	1.78	1.15	1.79	84.	39.	123.
	213.4	3.0	1.31	.034	3.7	.57	.09	-.41	.68	.24	.96	14.	27.	41.
	38.1	3.0	1.31	.034	25.0	.50	.93	-1.28	11.30	4.09	1.07	161.	147.	308.
524	152.4	3.0	1.31	.034	7.4	.64	.33	-.69	.91	.91	.84	89.	26.	115.
	152.4	4.9	1.49	.034	7.4	.64	.52	-1.45	1.05	1.56	.55	84.	38.	121.
	12.2	12.2	2.21	.034	7.4	.64	1.30	-1.45	2.03	3.20	1.58	66.	47.	114.
	237.7	3.0	1.31	.034	4.5	.71	.21	-1.28	.18	.51	.51	66.	42.	108.

TABLE 3.1.1 (CONTINUED)

APPLIED PRESSURE										BLADDER OSCILLATION RESPONSE				
FISH HOR. SHOT RANGE (M)	FISH DEPTH (M)	AMBIENT PRESS. (BARS)	VAPOR PRESS. (BARS)	PEAK PRESS. (BARS)	TIME CONST. (MSEC)	NEG.		POS. CYCLES	OSCILLATION PARAMETERS					
						DURATION (MSEC)	PRESS. (BARS)		NEG. CYCLES	X	Y	Z		
525	51.8	1.31	.034	23.7	.51	1.55	-1.28	4.85	1.09	157.	151.	308.		
	152.4	1.31	.034	7.4	.64	.57	-.55	1.42	1.76	89.	51.	139.		
	152.4	1.55	.034	7.4	.64	1.02	-1.52	2.32	.62	81.	49.	130.		
	237.7	2.21	.034	4.5	.71	2.26	-1.38	4.75	2.39	66.	44.	110.		
529	33.5	1.31	.034	4.5	.71	.36	-1.24	.78	.60	65.	36.	101.		
	57.9	2.21	.034	8.2	.15	2.75	-.90	4.56	2.93	61.	27.	88.		
	57.9	1.16	.034	4.5	.17	.21	-1.13	.45	.54	59.	38.	98.		
	79.9	1.91	.034	4.5	.17	1.27	-.83	1.94	.93	42.	15.	57.		
530	79.9	1.16	.034	3.1	.19	.16	-.48	.29	.82	25.	27.	53.		
	79.9	1.91	.034	3.1	.19	.93	-.76	1.41	1.08	31.	29.	60.		
	33.5	2.21	.034	8.4	.15	5.31	-.83	8.59	2.81	62.	21.	83.		
	57.9	1.16	.034	4.4	.17	.42	-.83	.71	.85	58.	45.	103.		
531	57.9	1.16	.034	4.4	.17	.42	-.83	.83	.95	60.	50.	110.		
	79.9	1.91	.034	4.5	.17	2.49	-.76	3.91	1.44	43.	17.	61.		
	79.9	1.16	.034	3.1	.19	.31	-.76	.50	.70	44.	30.	74.		
	79.9	1.91	.034	3.1	.19	1.84	-.90	3.03	.94	33.	22.	55.		
783	76.2	1.31	.034	7.2	.32	.64	-.90	1.56	1.34	84.	72.	156.		
	96.0	1.31	.034	5.5	.33	.51	-1.24	1.29	.66	72.	35.	107.		
	115.8	1.31	.034	4.5	.35	.43	-.76	.86	1.12	61.	40.	101.		
	164.6	1.31	.034	3.0	.38	.30	-.83	.63	.96	47.	60.	107.		
784	231.6	1.31	.034	2.1	.41	.21	-.41	.36	.97	27.	35.	62.		
	56.5	3.37	.017	19.4	.52	4.71	-1.30	14.16	19.47	93.	24.	117.		
	94.1	2.79	.018	11.2	.58	2.03	-1.43	5.20	4.26	75.	35.	110.		
	94.1	2.79	.018	11.2	.58	2.03	-1.43	4.64	4.01	74.	39.	113.		
786	13.0	1.14	.019	19.6	.14	.88	-.98	1.35	1.03	137.	99.	235.		
	13.0	1.14	.019	19.6	.14	.88	-.98	1.18	1.00	134.	74.	208.		
	7.7	3.00	.019	22.0	.13	11.28	-.68	13.61	7.06	92.	17.	108.		
	7.5	3.30	.019	18.2	.14	11.56	-.69	17.88	9.17	79.	14.	93.		
786	23.3	3.30	.019	18.2	.14	11.56	-.69	15.93	8.21	78.	15.	93.		
	23.3	3.30	.019	18.2	.14	11.56	-.69	14.21	7.38	77.	17.	94.		

TABLE 3.1.2 APPLIED PRESSURE PARAMETERS AND BLADDER OSCILLATION RESPONSE FOR WHITE PERCH  
(1 bar =  $10^5$  pascals = 14.50 psi)

SHOT	FISH HO. RANGE (m)	FISH DEPTH (m)	AMBIENT PRESS. (BARS)	VAPOR PRESS. (BARS)	PEAK PRESS. (BARS)	APPLIED PRESSURE			BLADDER OSCILLATION RESPONSE				
						TIME CONST. (MSEC)	POSITIVE NEG. DURATION (MSEC)	NEGATIVE DURATION (MSEC)	POS. CYCLES	NEG. CYCLES	A	Y	Z
517	12.8	1.5	1.16	.034	25.2	.12	.24	-1.13	.50	.54	144.	78.	222.
	12.8	6.1	1.61	.034	23.5	.12	.87	4.05	.99	1	121.	35.	156.
	36.0	1.5	1.16	.034	7.7	.16	.09	-.90	.12	.52	19.	15.	34.
	36.0	6.1	1.61	.034	7.7	.16	.34	-.131	.46	.58	63.	40.	103.
519	57.9	1.5	1.16	.034	4.5	.17	.05	-.34	.05	.65	-.0.	4.	4.
	25.0	1.5	1.16	.034	23.5	.25	.89	-1.13	1.18	.66	150.	50.	200.
	25.0	6.1	1.61	.034	25.0	.25	3.51	-1.38	2.99	1.37	136.	68.	204.
	76.2	2.1	1.22	.034	7.2	.32	.45	-.83	.49	.75	76.	61.	137.
521	115.8	3.0	1.31	.034	4.5	.35	.43	-1.28	.39	.53	40.	28.	68.
	115.8	6.1	1.61	.034	4.5	.35	.85	-.97	.68	.87	46.	34.	80.
	38.1	3.0	1.31	.034	26.3	.38	.95	-1.28	1.65	.68	157.	39.	196.
	112.8	1.5	1.16	.034	7.7	.49	.16	-.55	.22	.84	20.	29.	49.
522	112.8	5.5	1.55	.034	7.8	.49	.59	-1.52	.74	.54	76.	19.	95.
	206.7	3.0	1.31	.034	3.9	.56	.18	-.76	.18	.58	14.	11.	25.
	38.1	3.0	1.31	.034	26.3	.38	.95	-1.28	1.61	.68	157.	39.	196.
	112.8	1.5	1.16	.034	7.7	.49	.16	-.55	.22	.84	20.	29.	49.
523	112.8	5.5	1.55	.034	7.8	.49	.59	-1.52	.74	.54	76.	19.	95.
	213.4	3.0	1.31	.034	3.7	.57	.09	-.41	.10	.72	-.0.	9.	9.
	38.1	3.0	1.31	.034	26.3	.38	.95	-1.28	1.61	.68	157.	39.	196.
	112.8	1.5	1.16	.034	7.7	.49	.16	-.55	.22	.84	20.	29.	49.
524	152.4	4.9	1.49	.034	7.4	.64	.52	-1.45	.63	.52	77.	71.	148.
	152.4	12.2	2.21	.034	7.4	.64	1.30	-1.45	1.37	.95	61.	34.	111.
	237.7	3.0	1.31	.034	4.5	.71	.21	-1.28	.21	.50	15.	12.	27.
	51.8	3.0	1.31	.034	23.7	.51	1.55	-1.28	2.19	.78	152.	120.	272.
525	152.4	5.5	1.55	.034	7.4	.64	1.02	-1.52	1.05	.56	75.	9.	84.
	152.4	12.2	2.21	.034	7.4	.64	2.26	-1.38	2.14	1.18	61.	41.	102.
	237.7	3.0	1.31	.034	4.5	.71	.36	-1.24	.35	.53	46.	31.	77.
	33.5	12.2	2.21	.034	8.2	.15	2.75	-.90	2.18	1.43	54.	24.	78.
529	57.9	1.5	1.16	.034	4.5	.17	.21	-1.13	.20	.51	14.	11.	25.
	57.9	9.1	1.91	.034	4.5	.17	1.27	-.83	.98	1	38.	20.	58.
	79.9	1.5	1.16	.034	3.1	.19	.16	-.48	.13	.57	12.	10.	22.
	79.9	9.1	1.91	.034	3.1	.19	.93	-.76	.74	.96	29.	24.	53.
530	33.5	12.2	2.21	.034	8.4	.15	5.31	-.83	3.74	1.64	54.	25.	79.
	57.9	1.5	1.16	.034	4.4	.17	.42	-.83	.37	.61	40.	28.	68.
	57.9	9.1	1.91	.034	4.5	.17	2.49	-.76	1.64	.97	38.	29.	67.
	79.9	1.5	1.16	.034	3.1	.19	.31	-.76	.55	.95	11.	9.	19.
530	79.9	9.1	1.91	.034	3.1	.19	1.84	-.90	1.24	.51	29.	16.	45.



TABLE 3.1.2 (CONTINUED)

FISH MO. & SHOT	FISH DEPTH (m)	AMBIENT PRESS. (BARS)	VAPOR PRESS. (BARS)	APPLIED PRESSURE				BLADDER OSCILLATION RESPONSE			
				TIME (MSEC)	POSITIVE DURATION (MSEC)	NEG. DURATION (MSEC)	NEGATIVE DURATION (MSEC)	POS. CYCLES	NEG. CYCLES	OSCILLATION X	OSCILLATION Y
7431	76.2	1.31	.034	.32	.64	-.40	2.07	.72	.94	75.	59.
	96.0	1.31	.034	.33	.51	-1.24	1.54	.54	.56	62.	40.
	115.4	1.31	.034	.35	.43	-.76	1.08	.43	.71	54.	36.
	164.6	1.31	.034	.30	.30	-.43	.91	.26	.63	23.	18.
742	231.6	1.31	.034	.41	.21	-.41	.76	.16	.60	9.	8.
	91.4	1.16	.017	.58	.20	-.44	3.70	.41	1.46	81.	66.
	91.4	1.16	.017	.58	.20	-.44	3.70	.37	1.35	81.	66.
	91.4	1.16	.017	.58	.20	-.44	3.70	.31	1.25	54.	53.
743	13.7	1.16	.017	.58	1.68	-1.79	3.50	2.48	1.32	80.	74.
	13.7	1.16	.017	.58	1.68	-1.79	3.50	1.97	1.21	79.	53.
	60.7	1.16	.017	.52	.28	-.70	7.40	.73	2.00	145.	71.
	60.7	1.16	.017	.52	.28	-.70	7.40	.69	1.92	144.	71.
744	60.7	1.16	.017	.52	.28	-.70	7.40	.56	1.34	143.	108.
	56.5	1.16	.017	.52	.471	-1.30	14.50	6.98	10.20	90.	22.
	56.5	1.16	.017	.52	.471	-1.30	14.50	6.25	9.03	89.	22.
	56.5	1.16	.017	.52	.471	-1.30	14.50	5.59	8.29	88.	26.
745	55.8	1.16	.017	.52	5.76	-1.03	15.40	8.95	14.20	81.	14.
	55.8	1.16	.017	.52	5.76	-1.03	15.40	8.19	12.81	80.	14.
	55.8	1.16	.017	.52	5.76	-1.03	15.40	7.22	11.36	80.	14.
	94.0	1.16	.018	.58	1.80	-1.77	4.25	2.73	2.05	74.	53.
746	94.0	1.16	.018	.58	1.80	-1.77	4.25	2.53	1.83	74.	61.
	94.0	1.16	.018	.58	1.80	-1.77	4.25	2.29	1.68	73.	53.
	94.0	1.16	.018	.58	1.80	-1.77	4.25	2.12	1.54	72.	47.
	94.1	1.16	.018	.58	2.03	-1.43	4.42	3.01	2.78	72.	29.
747	94.1	1.16	.018	.58	2.03	-1.43	4.42	2.77	2.71	71.	33.
	94.4	1.16	.018	.59	3.59	-1.30	1.08	5.58	1.46	57.	21.
	94.4	1.16	.018	.59	3.59	-1.30	1.08	4.88	1.54	56.	18.
	94.4	1.16	.018	.59	3.59	-1.30	1.08	4.51	1.24	55.	23.
748	94.4	1.16	.018	.59	3.59	-1.30	1.08	4.24	1.02	55.	18.
	94.4	1.16	.018	.59	3.59	-1.30	1.08	3.67	1.21	54.	23.
	12.7	1.16	.018	.13	1.24	-.95	4.98	1.24	1.04	132.	62.
	12.7	1.16	.018	.13	1.24	-.95	4.98	1.03	.99	129.	43.
749	11.0	1.16	.018	.13	1.24	-.95	4.98	6.51	2.88	100.	30.
	10.3	1.16	.018	.14	9.63	-1.12	6.10	8.83	4.99	76.	26.
	10.3	1.16	.018	.14	10.97	-1.12	6.10	8.18	4.13	75.	28.
	10.4	1.16	.018	.14	11.19	-1.12	6.10	8.18	4.13	75.	28.
750	10.4	1.16	.018	.14	11.19	-1.12	6.10	8.18	4.13	75.	28.
	10.4	1.16	.018	.14	11.19	-1.12	6.10	8.18	4.13	75.	28.
	10.4	1.16	.018	.14	11.19	-1.12	6.10	8.18	4.13	75.	28.
	10.4	1.16	.018	.14	11.19	-1.12	6.10	8.18	4.13	75.	28.
751	14.2	1.16	.019	.12	10.09	-.77	6.29	6.60	3.34	117.	30.
	14.2	1.16	.019	.12	10.09	-.77	6.29	5.87	3.27	115.	33.
	14.2	1.16	.019	.12	10.09	-.77	6.29	5.15	2.41	113.	36.
	15.7	1.16	.019	.13	10.32	-.68	6.37	7.68	4.04	111.	27.
752	15.7	1.16	.019	.13	10.32	-.68	6.37	6.24	3.07	108.	33.
	15.7	1.16	.019	.13	10.32	-.68	6.37	6.24	3.07	108.	33.
	15.7	1.16	.019	.13	10.32	-.68	6.37	6.24	3.07	108.	33.
	15.7	1.16	.019	.13	10.32	-.68	6.37	6.24	3.07	108.	33.

TABLE 3.1.3 OBSERVED INJURIES FOR SPOT AND CALCULATED OSCILLATION PARAMETER Z

SHOT	CHARGE WEIGHT (KG)	CHARGE DEPTH (M)	FISH HCR. RANGE (M)	FISH DEPTH (M)	FISH LENGTH (CM)	BLADDER RADIUS (MM)	POSITIVE CYCLES	CALCULATED OSCILLATION PARAMETER, Z	SAMPLE SIZE	OBSERVED CUMULATIVE INJURIES AT LEVEL			
										1	2	3	4
517	.45	1.5	12.8	1.5	9.4	3.02	1.32	201.	10	10	10	9	0
			12.8	6.1	9.2	2.72	3.15	177.	10	10	10	10	0
			36.0	1.5	9.4	3.00	.37	106.	10	0	0	0	0
			36.0	6.1	9.1	2.69	1.12	114.	12	0	0	0	0
			57.9	1.5	9.9	3.15	.16	34.	13	0	0	0	0
518	3.63	6.1	25.0	1.5	8.7	2.79	2.94	307.	10	10	10	10	0
			25.0	6.1	9.3	2.77	6.91	213.	13	13	13	13	0
			76.2	1.5	9.8	3.12	.61	131.	22	22	22	16	0
			115.8	3.0	10.0	3.10	.62	124.	10	9	9	6	0
			115.8	6.1	9.3	2.77	1.26	125.	10	10	10	2	0
519	3.63	12.2	25.0	1.5	8.5	2.72	4.26	313.	9	9	9	9	0
			25.0	6.1	8.4	2.49	11.04	217.	10	10	10	10	0
			76.2	2.1	9.1	2.87	1.51	164.	11	11	11	8	0
			115.8	3.0	9.5	2.95	1.17	114.	10	10	10	3	0
			115.8	6.1	9.7	2.87	2.04	90.	10	0	0	0	0
521	14.06	9.1	38.1	3.0	9.8	3.02	5.09	313.	11	11	11	11	3
			112.8	1.5	10.1	3.25	.64	163.	20	20	20	16	0
			112.8	5.5	9.6	2.84	2.18	136.	10	10	10	7	0
			206.7	3.0	10.5	3.28	.50	108.	21	1	1	1	0
522	14.06	9.1	38.1	3.0	8.3	2.59	6.03	317.	12	12	12	12	2
			112.8	1.5	11.7	3.73	.56	154.	21	21	18	14	1
			112.8	5.5	10.4	3.10	2.00	150.	10	10	10	9	0
			176.8	3.0	10.9	3.40	.60	115.	22	14	15	13	0
			213.4	3.0	9.5	2.95	.52	103.	10	0	0	0	0
523	14.06	4.6	38.1	3.0	12.0	3.73	2.67	300.	10	10	10	10	5
			112.8	1.5	23.2	7.42	.15	37.	9	9	5	2	0
			112.8	5.5	10.5	3.35	.32	114.	12	12	11	5	0
			112.8	3.0	11.4	3.12	1.15	123.	11	11	11	7	0
			213.4	3.0		3.53	.24	41.	10	3	3	0	0
524	30.84	12.2	51.8	3.0	12.9	3.99	4.09	308.	10	10	10	10	3
			152.4	3.0	13.9	4.34	.91	115.	20	20	18	10	0
			152.4	4.9	12.4	3.73	1.56	121.	20	19	15	10	0
			152.4	12.2	13.5	3.71	3.20	114.	10	10	10	8	0
			237.7	3.0	13.1	4.06	.51	108.	10	9	8	5	0

TABLE 3.1.3 (CONTINUED)

SHOT	CHARGE WEIGHT (KG)	CHARGE DEPTH (M)	FISH HOR. RANGE (M)	FISH DEPTH (M)	FISH LENGTH (CM)	BLADDER RADIUS (MM)	POSITIVE CYCLES	CALCULATED OSCILLATION PARAMETER, Z	SAMPLE SIZE	OBSERVED CUMULATIVE INJURIES AT LEVEL			
										1	2	3	4
525	30.84	21.3	51.8	3.0	14.4	4.47	4.85	308.	10	10	10	10	10
			152.4	3.0	14.2	4.42	1.42	139.	20	20	20	20	0
			152.4	5.5	14.0	4.17	2.32	130.	10	10	10	8	0
			152.4	12.2	13.7	3.76	4.75	110.	10	10	10	1	0
			237.7	3.0	13.9	4.32	.78	101.	10	10	10	2	1
529	.45	6.1	33.5	12.2	12.8	3.53	4.56	88.	11	11	10	7	0
			57.9	1.5	12.5	3.99	.45	98.	21	3	0	0	0
			57.9	9.1	13.5	3.86	1.94	57.	11	5	1	1	0
			79.9	1.5	12.9	4.11	.29	53.	11	11	0	0	0
			79.9	9.1	13.5	3.84	1.41	60.	10	10	0	0	0
530	.45	12.2	33.5	12.2	12.1	3.33	8.59	83.	10	9	0	0	0
			57.9	1.5	12.9	4.14	.71	103.	10	5	2	2	0
			57.9	1.5	10.8	3.48	.83	110.	9	2	0	0	0
			57.9	9.1	11.8	3.35	3.91	61.	10	3	1	1	0
			79.9	1.5	13.4	4.29	.50	74.	10	0	0	0	0
531	3.63	12.2	79.9	9.1	11.3	3.20	3.03	55.	10	2	1	1	0
			76.2	3.0	11.7	3.63	1.56	156.	10	10	7	5	0
			96.0	3.0	10.8	3.38	1.29	107.	16	15	6	4	0
			115.8	3.0	13.3	4.14	.86	101.	10	8	6	1	0
			144.6	3.0	11.6	3.61	.63	107.	10	5	3	2	0
783	31.84	9.1	231.6	3.0	12.9	3.99	.36	62.	10	0	0	0	0
			56.5	24.0	12.8	3.18	14.16	117.	2	2	2	1	0
			94.1	18.1	14.3	3.73	5.20	110.	6	3	0	0	0
			94.1	18.1	16.0	4.17	4.64	113.	4	4	0	0	0
			94.1	18.1	18.8	4.88	3.96	105.	5	1	1	0	0
786	.57	9.0	13.0	1.3	19.3	6.20	1.35	235.	7	7	7	5	1
			13.0	1.3	22.0	7.09	1.18	208.	3	3	3	3	1
			7.7	20.3	19.8	5.05	13.61	108.	10	10	6	3	0
			7.5	23.3	16.3	4.06	17.88	93.	8	8	1	0	0
			7.5	23.3	18.3	4.57	15.93	93.	4	4	0	0	0
786	.57	9.0	7.5	23.3	20.5	5.11	14.21	94.	8	8	8	0	0
			7.5	23.3	20.5	5.11	14.21	94.	8	8	8	0	0



TABLE 3.1.4 OBSERVED INJURIES FOR WHITE PERCH AND CALCULATED OSCILLATION PARAMETER Z

SHOT	CHARGE WEIGHT (KG)	CHARGE DEPTH (M)	FISH HOB. RANGE (M)	FISH DEPTH (M)	FISH LENGTH (CM)	BLADDER RADIUS (MM)	POSITIVE CYCLES	CALCULATED OSCILLATION PARAMETER Z	SAMPLE SIZE	OBSERVED CUMULATIVE INJURIES AT LEVEL			
										NUMBER OF FISH			
										1	2	3	4
517	45	1.5	12.4	1.5	14.3	9.78	.50	222.	4	4	4	3	0
			12.4	6.1	17.9	8.86	.99	156.	3	3	3	3	0
			36.0	1.5	14.0	9.63	.12	34.	4	0	0	0	0
			57.9	6.1	14.4	7.80	.46	103.	3	0	0	0	0
				1.5	14.5	9.88	.05	4.	5	0	0	0	0
519	3.63	12.2	24.0	1.5	14.5	9.88	1.17	200.	10	10	10	10	0
			25.0	6.1	14.0	8.92	2.98	203.	10	10	10	9	0
			76.2	2.1	14.7	9.88	.49	137.	10	10	10	5	0
			115.8	3.0	14.0	9.35	.39	68.	10	0	0	0	0
			115.8	6.1	14.4	9.09	.68	80.	10	0	0	0	0
521	14.04	9.1	34.1	3.0	17.3	8.97	1.65	196.	10	10	10	10	0
			112.8	1.5	17.5	9.35	.22	49.	10	0	0	0	0
			112.8	5.5	16.9	8.43	.74	95.	11	11	10	8	0
			204.7	3.0	17.6	9.14	.18	25.	10	0	0	0	0
				3.0	17.8	9.25	1.60	196.	10	10	10	10	0
522	14.04	9.1	112.8	1.5	17.7	9.42	.22	36.	10	2	0	0	0
			112.8	5.5	17.2	8.59	.73	141.	10	10	10	10	0
			176.8	3.0	18.4	9.78	.21	27.	10	0	0	0	0
			213.4	3.0	17.1	8.86	.17	25.	10	0	0	0	0
				3.0	17.4	9.14	1.04	212.	10	10	10	10	0
523	14.04	4.6	34.1	3.0	17.4	9.14	1.04	212.	10	10	10	10	0
			112.8	1.5	17.3	9.25	.12	37.	10	0	0	0	0
			112.8	5.5	16.4	8.41	.44	148.	10	9	5	0	0
			213.4	3.0	16.9	8.79	.10	9.	9	0	0	0	0
				3.0	17.7	9.19	1.70	243.	10	10	10	10	10
524	30.84	12.2	51.8	3.0	14.5	9.60	.42	136.	6	0	0	0	0
			152.4	3.0	14.5	9.40	.63	111.	10	4	2	1	0
			152.4	4.9	14.6	9.40	.63	111.	10	6	2	1	0
			152.4	12.2	14.0	8.71	1.36	118.	10	8	8	2	0
			237.7	3.0	19.1	9.88	.21	27.	10	1	0	0	0
525	30.84	21.3	51.8	3.0	14.4	9.78	2.13	160.	10	10	10	10	10
			152.4	5.5	14.5	9.25	1.05	84.	10	10	7	5	0
			152.4	12.2	14.3	4.41	2.13	102.	10	10	6	2	0
			237.7	3.0	14.5	9.63	.35	77.	5	2	1	1	0
				3.0	14.3	7.47	2.17	78.	11	6	0	0	0
529	45	6.1	33.5	12.2	14.3	7.47	2.17	78.	11	6	0	0	0
			57.9	1.5	16.9	9.04	.20	25.	19	0	0	0	0
			57.9	9.1	17.1	8.13	.98	54.	10	1	0	0	0
			79.9	1.5	16.8	8.99	.13	22.	10	0	0	0	0
			79.9	9.1	16.7	7.90	.74	53.	10	4	0	0	0
530	45	12.2	33.5	12.2	14.8	7.70	3.72	79.	10	8	1	0	0
			57.9	1.5	17.0	9.07	.37	68.	21	1	0	0	0
			57.9	9.1	17.5	8.31	1.64	67.	10	0	0	0	0
			79.9	1.5	16.6	8.86	.24	19.	10	0	0	0	0
			79.9	9.1	17.4	8.26	1.23	45.	10	0	0	0	0

TABLE 3.1.4 (CONTINUED)

SHOT	CHARGE WEIGHT (KG)	CHARGE DEPTH (M)	FISH HOR. RANGE (M)	FISH DEPTH (M)	FISH LENGTH (CM)	BLADDER RADIUS (MM)	POSITIVE CYCLES	CALCULATED OSCILLATION PARAMETER, Z	SAMPLE SIZE	OBSERVED CUMULATIVE INJURIES AT LEVEL			
										1	2	3	4
531	3.63	12.2	76.2	3.0	15.8	8.23	.72	135.	10	10	10	10	0
			96.0	3.0	17.0	8.81	.54	102.	15	5	1	1	0
			115.8	3.0	16.8	8.71	.43	91.	10	1	0	0	0
			164.6	3.0	16.9	8.79	.26	41.	10	0	0	0	0
			231.6	3.0	17.2	8.94	.16	17.	10	0	0	0	0
782	31.93	9.1	91.4	1.5	14.8	7.87	.41	146.	10	6	2	2	0
			91.4	1.5	16.5	8.81	.37	146.	9	5	4	2	0
			91.4	1.5	19.8	10.59	.31	106.	9	3	1	0	0
			91.4	13.7	14.9	6.73	2.47	155.	9	9	9	8	0
			91.4	13.7	18.7	8.46	1.97	132.	8	7	7	4	0
783	31.84	9.1	60.7	1.5	14.3	7.62	.72	216.	11	11	11	11	5
			60.7	1.5	15.1	8.08	.69	215.	12	12	12	12	10
			60.7	1.5	18.6	9.96	.56	250.	6	6	6	6	5
			56.5	24.0	15.0	6.25	6.96	111.	6	6	6	6	0
			56.5	24.0	16.8	6.96	6.23	111.	24	24	24	22	0
			56.5	24.0	18.7	7.77	5.57	115.	13	13	13	13	0
			55.8	30.0	14.6	5.84	8.92	95.	9	9	9	8	0
			55.8	30.0	16.0	6.38	8.16	95.	16	16	16	12	0
			55.8	30.0	18.1	7.24	7.19	94.	4	4	4	3	0
			94.0	16.6	14.7	6.45	2.72	127.	9	9	9	3	0
			94.0	16.6	15.8	6.96	2.52	135.	15	15	15	9	0
			94.0	16.6	17.4	7.67	2.28	126.	4	4	4	1	0
			94.0	16.6	18.9	8.31	2.11	119.	19	19	19	2	0
784	32.48	9.1	94.1	18.1	14.8	6.43	2.99	100.	13	13	13	1	0
			94.1	18.1	16.1	6.99	2.76	104.	5	5	5	2	0
			94.4	30.3	14.5	5.77	5.56	79.	10	10	10	1	0
			94.4	30.3	16.6	6.60	4.86	74.	10	10	10	0	0
			94.4	30.3	17.9	7.14	4.50	79.	11	11	11	0	0
			94.4	30.3	19.0	7.57	4.23	73.	7	7	7	0	0
			94.4	30.3	22.0	8.76	3.66	77.	3	3	3	0	0
			12.7	1.5	15.3	8.15	1.24	194.	11	11	11	10	0
			12.7	1.5	19.0	10.16	1.02	172.	5	5	5	4	0
			11.0	15.1	18.9	8.41	6.49	130.	9	9	9	0	0
			10.3	21.2	18.0	7.62	8.80	102.	10	9	7	0	0
			10.3	21.2	19.4	8.20	8.15	102.	9	9	5	0	0
			10.4	24.2	17.8	7.37	9.60	88.	10	9	4	0	0
			10.4	24.2	20.1	8.33	8.51	88.	10	9	4	0	0
786	.57	9.0	8.6	14.2	19.3	8.69	6.57	147.	9	9	8	0	0
			8.6	14.2	21.6	9.70	5.85	148.	8	8	8	0	0
			8.6	14.2	24.6	11.05	5.13	149.	2	2	2	0	0
			8.4	15.7	17.6	7.80	7.65	138.	10	10	9	0	0
			8.4	15.7	21.5	9.53	6.21	141.	11	11	11	1	0

The positive duration TPOS (see sketch Figure 3.1.1) was calculated as described in Appendix C for the 1973 tests; for the 1975 tests measured values were used. The negative pressure PNEG and its duration DTNEG were measured from the pressure records.

The last five columns, Tables 3.1.1 and 3.1.2, list calculated parameters for the oscillatory response of the swim bladder. The number of positive cycles is the positive duration measured in complete cycles of oscillation starting from the initial "at rest" expansion. The number of negative cycles locates the final return to ambient pressure (end of negative phase — see Figure 3.1.1) in terms of the bladder oscillation. "Zero" is taken as the last expansion occurring before surface cut-off. See, e.g., Figure 2.3.1. Thus, unless the number of negative cycles is greater than 0.5, no final expansion takes place during the negative phase. The number of negative cycles,  $(\Delta t/T)_{NP}$ , is a measure of the contribution of the negative phase to the final bladder expansion. The relationship is roughly as follows:

$(\Delta t/T)_{NP} \leq 0.5$	No contribution
$0.5 < (\Delta t/T)_{NP} < 1.0$	Partial contribution
$1.0 \leq (\Delta t/T)_{NP}$	Full contribution

The reader is referred to Appendix B for a more complete description.

The bladder oscillation parameters X, Y, Z are defined as follows:

$$X = -100 \ln A_{MIN}/A_i \quad (3.1.3)$$

$$Y = 100 \ln A_{MAX}/A_i \quad (3.1.4)$$

$$Z = X + Y = 100 \ln A_{MAX}/A_{MIN} \quad (3.1.5)$$



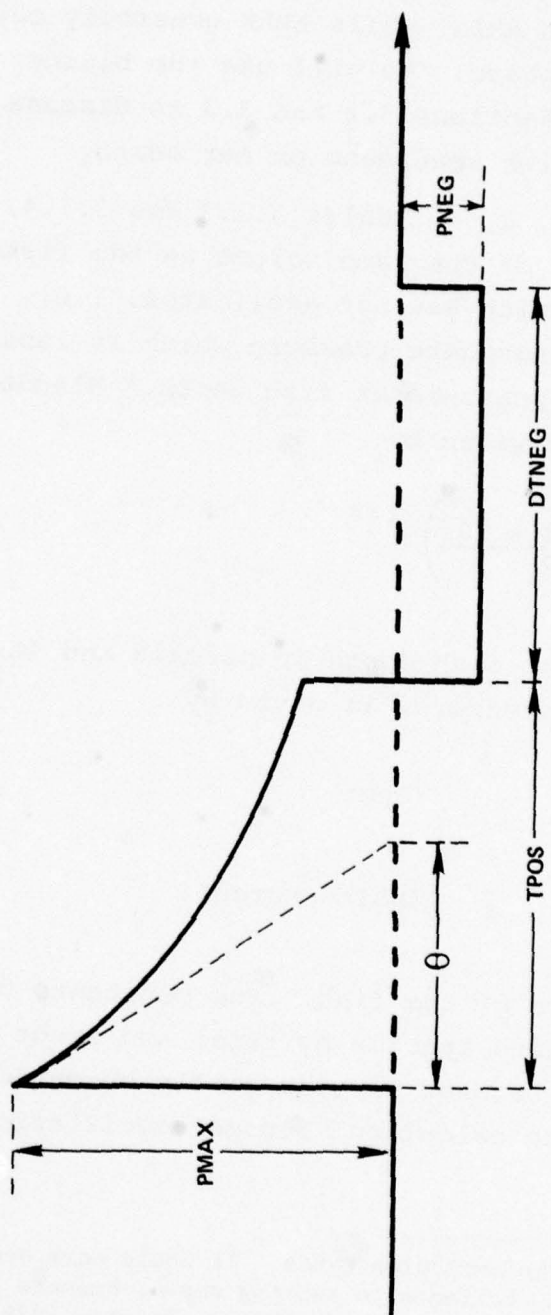


FIG. 3.1.1 SKETCH SHOWING CALCULATED PRESSURE-TIME SIGNATURE



where  $\ln$  is the natural logarithm,  $A_i$  is the initial at rest bladder radius, and AMIN and AMAX are the smallest and largest radii during the oscillatory response. In the cases studied so far, the first compression has always been AMIN, while AMAX generally occurs during or following the negative phase. We will use the bladder oscillation parameters X, Y, and Z in Sections 3.2 and 3.3 to discuss and correlate the observed injuries to fish specimens on our tests.

The bladder radius,  $A_i$  — Tables 3.1.3 and 3.1.4, column 7 — is the radius for a sphere of the same volume as the fishes' bladder at fish depth for a fish which has not acclimated, i.e., for a fish at equilibrium with one atmosphere pressure which is isothermally compressed to hydrostatic pressure at fish depth.\* Bladder radius  $A_i$  for non-acclimated fish is given by

$$A_i = (A_i)_0 \left( \frac{1.013 \times 10^5}{p_i} \right)^{1/3} \quad (3.1.6)**$$

where  $p_i$  is the pressure at fish depth in pascals and  $(A_i)_0$ , the radius at one atmosphere pressure, is given by

$$(A_i)_0/L = 0.033 \quad (\text{Spot}) \quad (3.1.7)$$

$$(A_i)_0/L = 0.055 \quad (\text{White Perch}) \quad (3.1.8)$$

where L is the fork length of the fish. The constants 0.033 and 0.055 were selected for each species by trial and error so as to optimize the correlation between experimentally observed injuries to the test specimens and the calculated bladder oscillation parameter Z (e.g., Figure 3.2.1).

---

\*This is how it was done on the explosion tests. It would have been prohibitively expensive to have let the fish acclimate to testing depth, because of the time required. This problem is discussed by Gaspin, Wiley, Peters, 1976.

\*\*For the calculations of this report the exponent,  $1/3\gamma$ , where  $\gamma = 1.4$  — for adiabatic compression — was inadvertently used. Since the computations reported here should be quite insensitive to this error, they were not redone.

The number of fish of a given average size at each test specimen location and summaries of the injuries evaluated upon post-shot dissection are listed in the last 5 columns of Tables 3.1.3 and 3.1.4.

Thus, e.g., on Shot 531 (Table 3.1.3) at the 76.2 meter range position there were 10 Spot, all 10 of which received injuries of level 1 or greater, 7 of which received injuries of level 2 or greater, 5 of which received injuries of level 3, and none of which received level 4 injuries. (There were no injuries of level 5 observed on either the 1973 or 1975 tests.)

Table 3.1.5 is a condensed version of the code used to evaluate the explosion damage to the fish upon post-shot dissection.<sup>3</sup> Successive injury levels are of increasing severity and each fish is classified to fall into one and only one level of injury. Figure 3.1.2 depicts this fundamental design of the injury code. Thus, the fundamental physical problem of this report is to estimate test conditions for the transitions from one injury level to the next. We will do this by estimating the probability of events such as "occurrence of injury level 3 or greater" as a function of the calculated damage parameter  $Z$  (Equation 3.1.5). It is convenient -- but not fundamental to the analysis -- that such "cumulative" injuries are also what is of practical interest in explosion testing. For example, the event "injury of level 3 or greater" has been found to correlate with the observed fish-kill\* on underwater explosion tests. And, the event "injury of level 2 or greater" has been considered to give the fish "little chance to survive predation."<sup>1</sup>

---

3. The injury evaluation code is due to: Hubbs, C. L., Schultz, E. P., and Wisner, R., Unpublished preliminary report on "Investigation of Effects on Caged Fishes from Underwater Nitro-Carbo-Nitrate Explosions," U. of California, Scripps Institute of Oceanography, 1960. The complete code is also listed in reference 1.

\* The term "observed fish-kill" refers to the dead and dying fish found on the surface and bottom following an underwater explosion.

TABLE 3.1.5

## CODE FOR EVALUATING VISIBLE FISH DAMAGE

Injury  
Level

0	No damage
1	Light hemorrhaging in tissues covering kidney
2	Light hemorrhaging throughout body cavity, some kidney damage, but gas bladder intact
3	Severe hemorrhaging throughout body cavity, gross kidney damage, and gas bladder burst
4	Partial break-thru of body wall, bleeding about anus
5	Ruptured body cavity, internal organs scrambled or lost



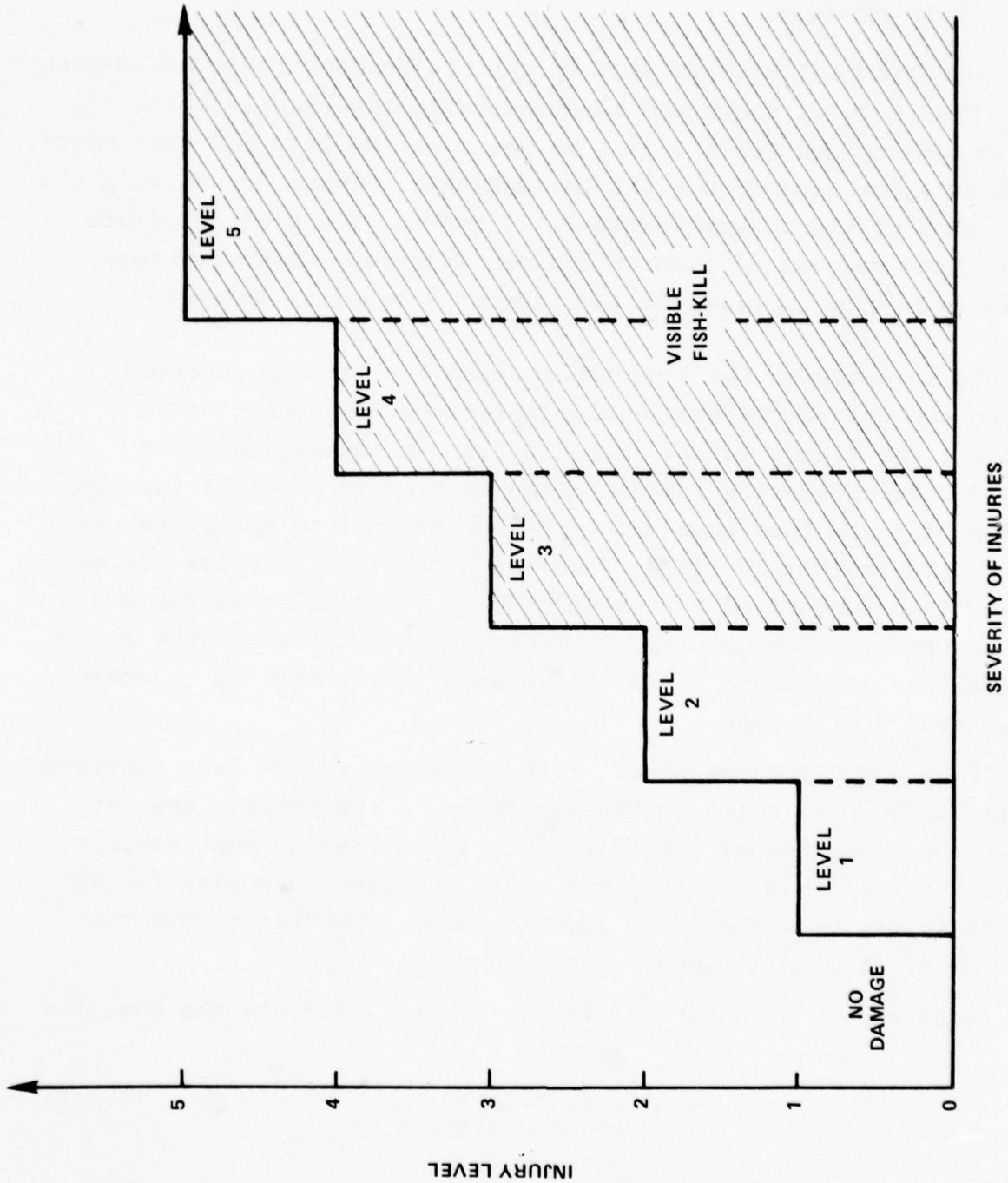


FIG. 3.1.2 SKETCH DEPICTING INJURY CODE FOR EVALUATING VISIBLE FISH DAMAGE



However, should the reader require for example the probability,  $P(\text{level 2 injury})$ , it is just the difference,  $P(\text{level 2 or greater}) - P(\text{level 3 or greater})$ .

### 3.2 OBSERVED INJURIES TO SPOT VS CALCULATED OSCILLATION PARAMETER

Figure 3.2.1 shows the experimentally observed injuries (as shown in each row of Table 3.1.3) to Spot on the 1973 and 1975 tests plotted as a function of  $Z = 100 \ln \text{AMAX/AMIN}$ . There are three plots, one for each of the injury levels 1, 2, and 3. The plotted points represent the percent of fish of a given size at a given specimen location receiving injuries of the indicated level or greater.

To investigate the functional dependence of the observed injury on the calculated oscillation parameter  $Z$  we constructed Table 3.2.1 and Figure 3.2.2. Table 3.2.1 was constructed from Table 3.1.3 by reordering (sorting) the entries in order of increasing value of  $Z$  and then separating the new table into groups representing approximately 100 fish. The total observed injuries for each group was then summarized by the successive row entries in Table 3.2.1. Thus, for the first group with a mid-range value for  $Z=54$ ; 41% of the fish received injuries of level 1 or greater; 11%, level 2 or greater; and 5%, level 3 or greater.

Figure 3.2.2 shows plots of the averaged injury data tabulated in Table 3.2.1. The solid curves are drawn by eye through the data points. The experimental data for level 3 injuries to Spot exhibit less scatter than that for levels 1 or 2; and also less than for all levels of injury to White Perch (Section 3.3). Whether or not this has any physical significance is not known.

Also shown, as a dashed line in Figure 3.2.2, is the equation

$$p = \frac{1}{1 + \text{EXP}[-0.055(Z-125)]} \quad (3.2.1)$$

where  $p$  is the probability of observing injury of level 3 or greater. Equation 3.2.1 is the Cumulative Logistic Probability Function with

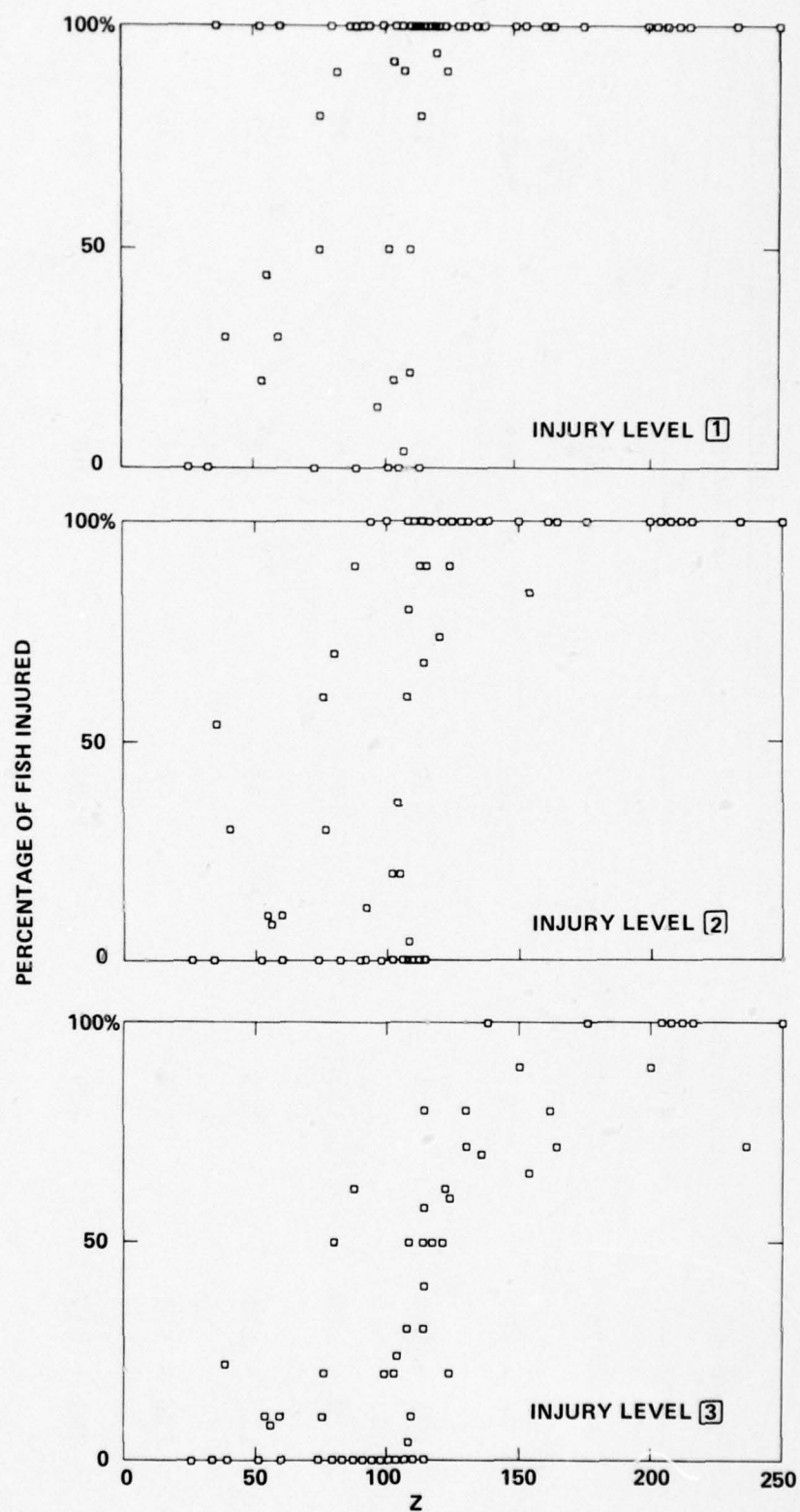


FIG. 3.2.1 OBSERVED INJURIES TO SPOT AS A FUNCTION OF Z

TABLE 3.2.1. AVERAGED OBSERVED INJURY PROBABILITY FOR SPOT AS A FUNCTION OF CALCULATED OSCILLATION PARAMETER Z

Range of Z	Mid-point of Range	Observed Cumulative Injury Probability, $\hat{P}(Z)$ at Level		
		1	2	3
34 - 74	54	.41	.11	.05
76 - 98	87	.65	.34	.15
101 - 108	104	.50	.33	.17
110 - 115	112	.73	.59	.32
115 - 131	123	.98	.92	.57
136 - 177	156	1.00	.97	.82
201 - 317	259	1.00	1.00	.97

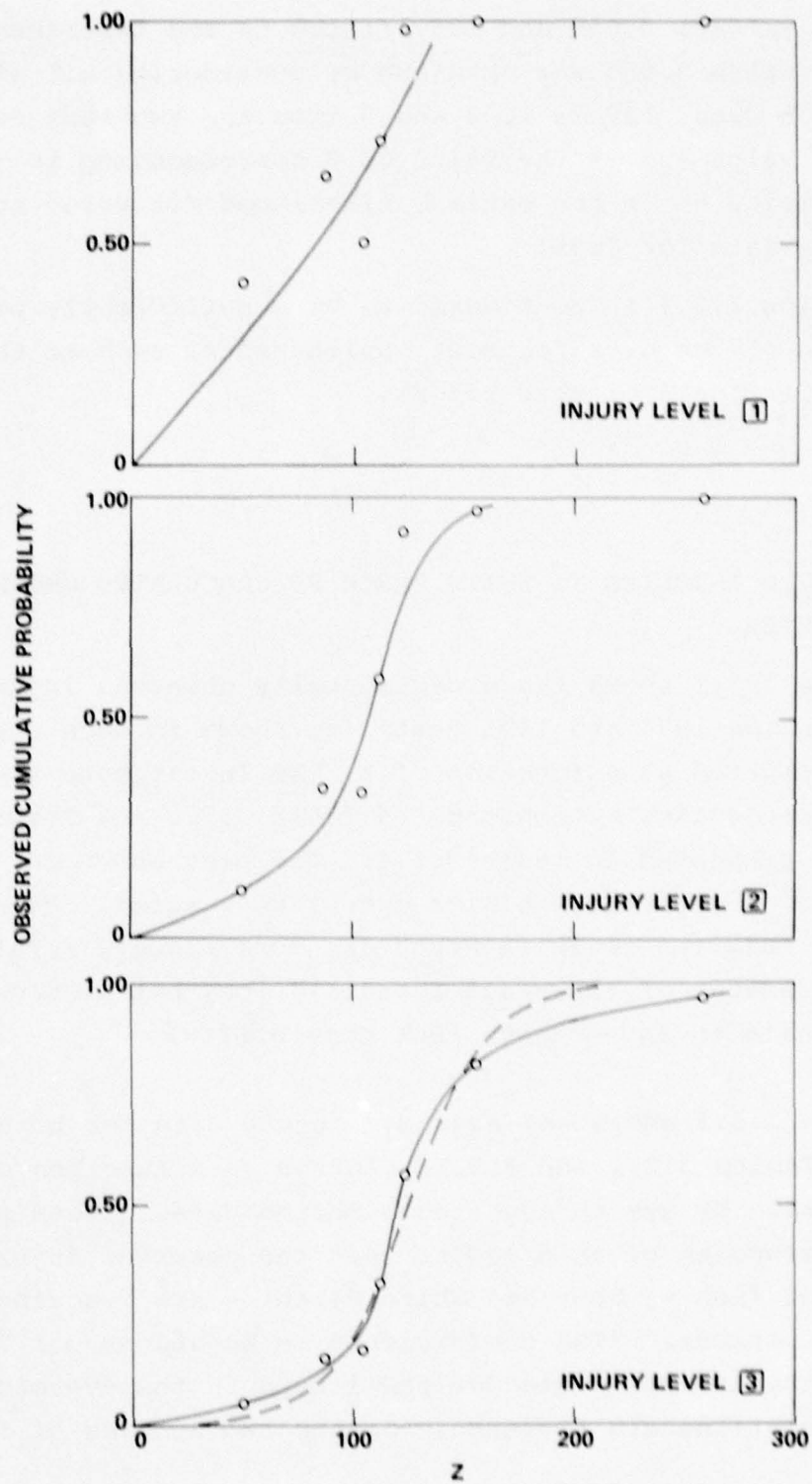


FIG. 3.2.2 OBSERVED CUMULATIVE INJURY TO SPOT AS A FUNCTION OF Z



the parameter values, 0.055 and 125, fitted to the experimental data. The parameter value 0.055 was obtained by considering all of the Spot and White Perch data, levels 1, 2 and 3 from the two test series. The parameter value 125 -- the value of  $Z$  corresponding to 50% injury probability -- is the maximum likelihood fit value to the level 3 injury data for Spot.

Equation 3.2.1 is considered to be a sufficiently precise representation of the data for most applications, such as those described in Section 4 of this report.

### 3.3 OBSERVED INJURIES TO WHITE PERCH VS CALCULATED OSCILLATION PARAMETER

Figure 3.3.1 shows the experimentally observed injuries to White Perch on the 1973 and 1975 tests (as shown in each row of Table 3.1.4) plotted as a function of  $Z$ . To investigate the functional dependencies we constructed Table 3.3.1 and Figure 3.3.2 from the data presented in Table 3.1.4. The plot shown in Figure 3.3.2 for level 3 injuries exhibits excessive scatter. Perhaps these level 3 injuries to White Perch are more closely related to some other parameter of the bladder oscillation, but it did not appear worthwhile to investigate that possibility.

Figure 3.3.3 shows the averaged injury data for both Spot and White Perch (Tables 3.2.1 and 3.3.1) plotted as a function of  $Z$ . The curves were drawn by eye through the combined data. These plots support the viewpoint of this report that the observed injuries to both species of fish -- Spot and White Perch -- are described by the same damage functions. (The coefficients -- Equations 3.1.7 and 3.1.8 -- for the effective bladder radii used in the dynamical response calculations are different for the two species of fish, however.)

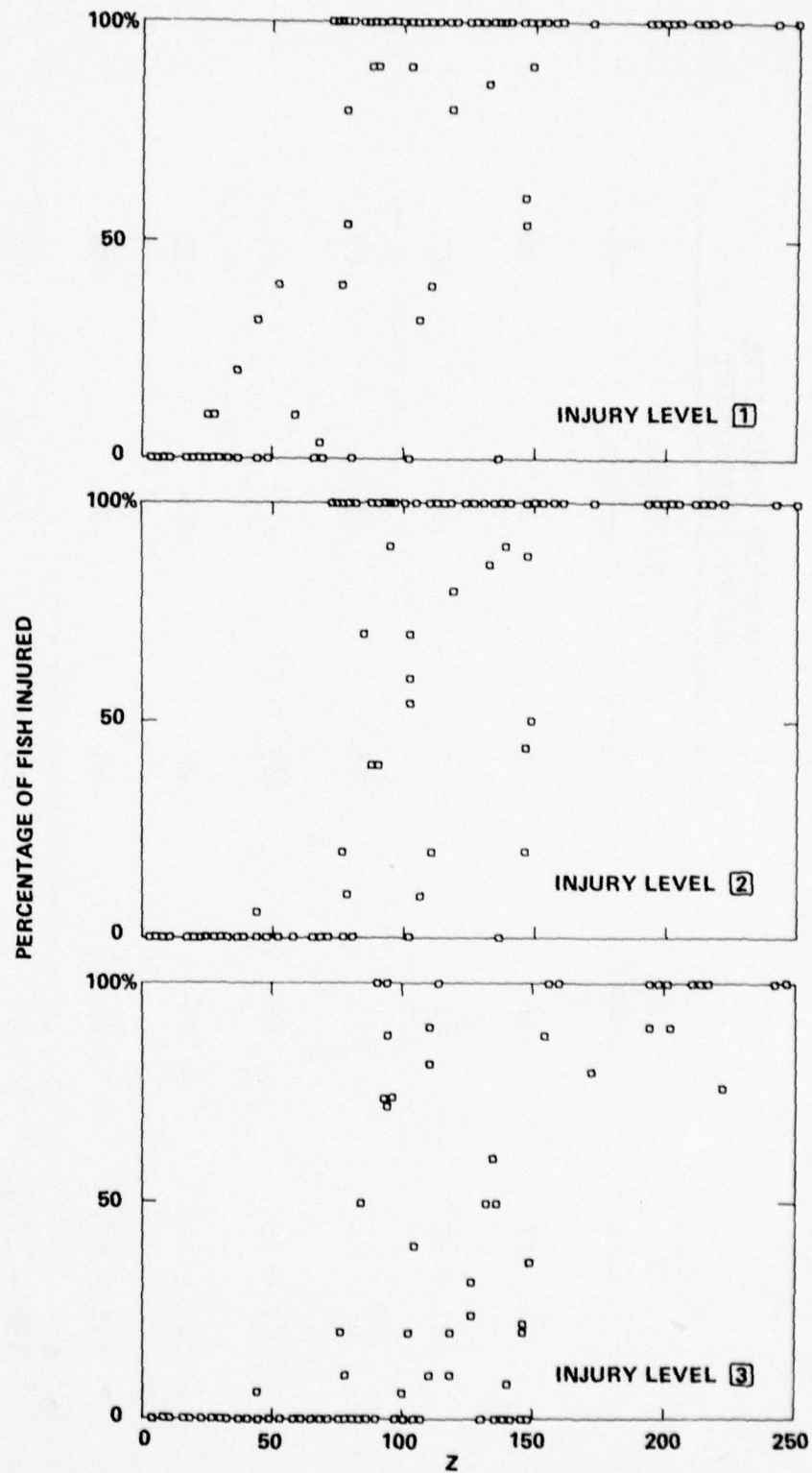


FIG. 3.3.1 OBSERVED INJURIES TO WHITE PERCH AS A FUNCTION OF Z

TABLE 3.3.1 AVERAGED OBSERVED INJURY PROBABILITY FOR WHITE PERCH AS A FUNCTION OF CALCULATED OSCILLATION PARAMETER Z

RANGE OF Z	MID-POINT OF RANGE	OBSERVED CUMULATIVE INJURY PROBABILITY		
		1	AT LEVEL 2	3
4 - 27	16	.00	.00	.00
27 - 58	42	.14	.01	.01
67 - 79	73	.48	.33	.02
79 - 95	87	.89	.77	.50
100 - 111	106	.84	.70	.33
115 - 137	126	.91	.91	.38
138 - 172	155	.91	.79	.34
194 - 250	222	1.00	1.00	.97



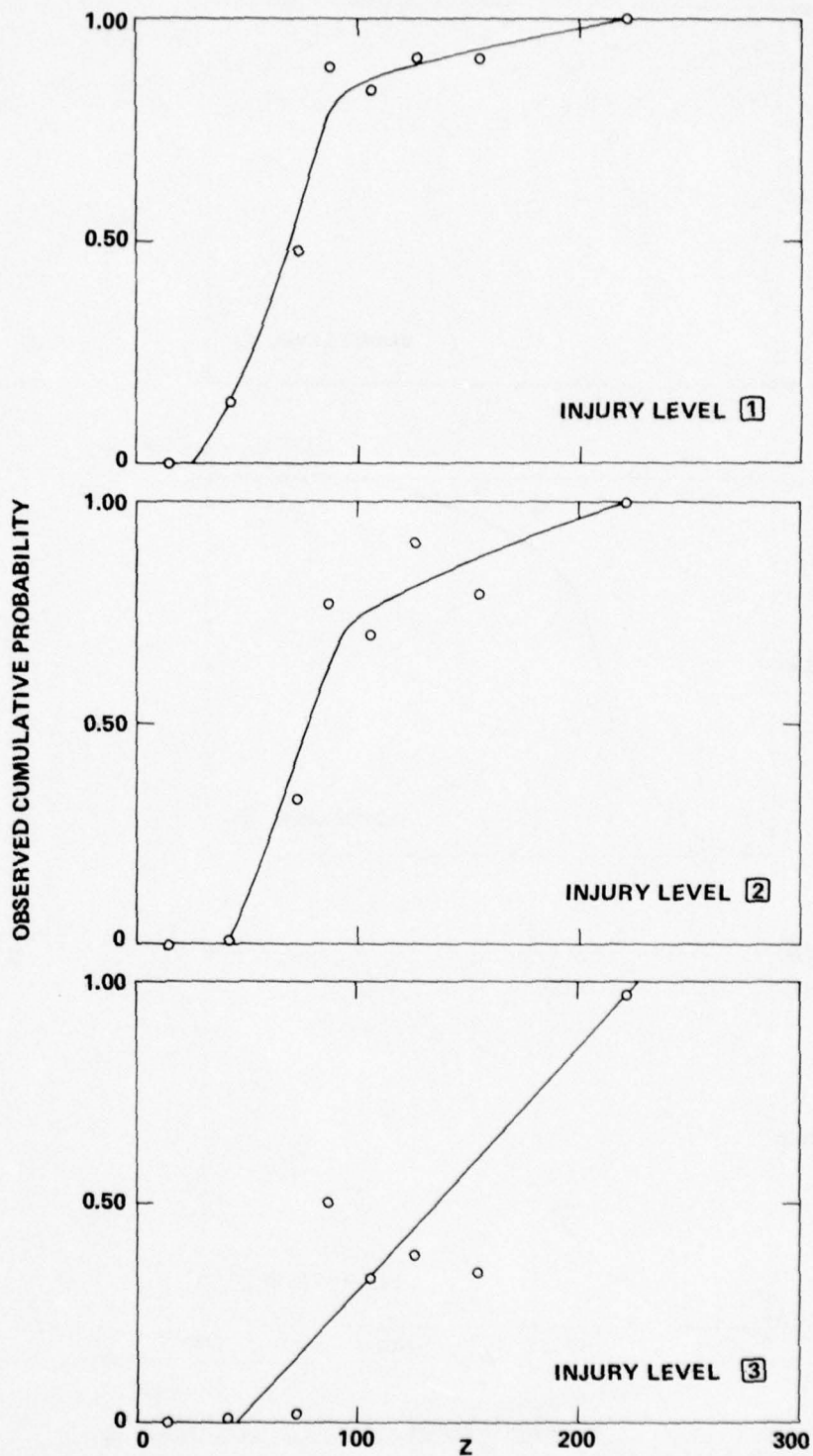


FIG. 3.3.2 OBSERVED CUMULATIVE INJURY TO WHITE PERCH AS A FUNCTION OF Z

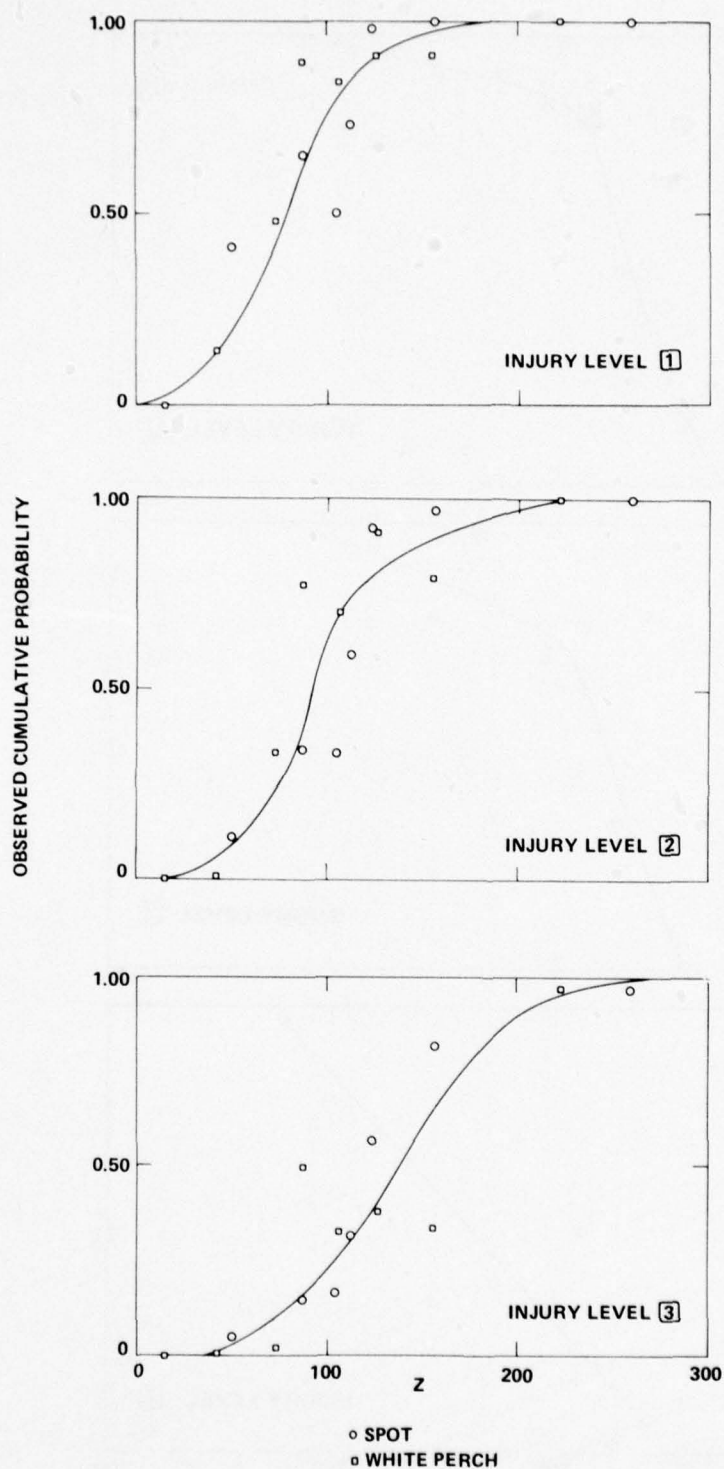


FIG. 3.3.3 OBSERVED CUMULATIVE INJURY AS A FUNCTION OF Z--  
SPOT AND WHITE PERCH COMBINED DATA

### 3.4 COMPARISON OF SHOCKWAVE IMPULSE AND CALCULATED BLADDER OSCILLATION AS DAMAGE PARAMETERS

Yelverton et al<sup>4</sup> at the Lovelace Foundation working in a test pond with eight species of bladder fish at depths down to 10 feet obtained fish-kill results describable by an Impulse Damage Parameter,

$$Z_I = 80 \ln [I/M^{1/3}] \quad (3.4.1)$$

where  $\ln$  is the natural logarithm,  $I$  is the impulse of the positive portion of the pressure wave in psi-msec and  $M$  is the mass of the fish in grams. [The arbitrary constant, 80, was calculated by the author to correspond to the value, 100, in the Bladder Oscillation Parameter (Equation 3.1.5).]

The results reported by Yelverton et al<sup>4</sup> give a kill-probability

$$p = \frac{1}{1 + \text{EXP}[-0.083(Z_I - 132)]} \quad (3.4.2)$$

where  $Z_I$  is the Impulse Parameter. Equation 3.4.2 is derived from Figure 6 of Yelverton et al by fitting the cumulative logistic probability distribution to their results for observed mortality upon holding the fish for 24 hours after the explosion test.

Figure 3.4.1a shows the level 3 injury results for Spot and White Perch (Tables 3.1.3 and 3.1.4) plotted as a function of the Impulse Damage Parameter. Note that the Impulse Damage Parameter does not describe these results.

Figure 3.4.1b shows a subset of the level 3 injury results for Spot and White Perch plotted as a function of the Impulse Damage

---

4. Yelverton, J. T., et al, "The Relationship between Fish Size and their Response to Underwater Blast," DNA Report 3677T, Lovelace Foundation, 1975.



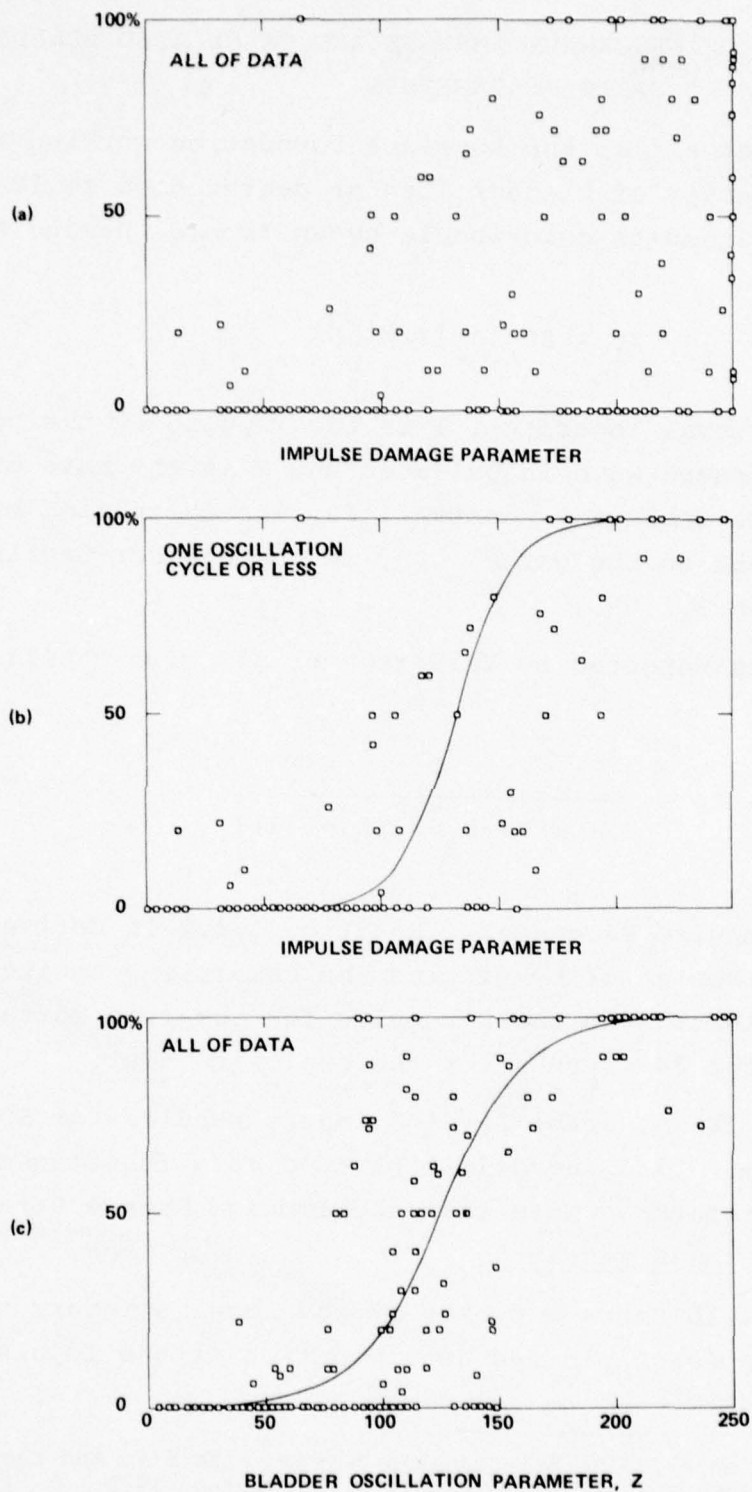


FIG. 3.4.1 CORRELATIONS OF LEVEL 3 INJURIES FOR SPOT AND WHITE PERCH WITH IMPULSE DAMAGE PARAMETER AND WITH BLADDER OSCILLATION PARAMETER

Parameter. In Figure 3.4.1b those data points where the bladder response calculation showed more than ~~one~~ oscillation during the positive phase (Tables 3.1.3 and 3.1.4) have been removed. The curve is Equation 3.4.2, the kill-probability result from Yelverton et al (1975). Thus, their 24-hr mortality is approximately equivalent to our level 3 dissection injuries;\* and, perhaps more important, the Impulse Damage Parameter is shown to describe only those explosion geometries where the charge and/or the fish are at shallow enough depth that approximately one or less cycles of bladder oscillation occur before surface reflection terminates the positive pressure phase.

Figure 3.4.1c shows for comparison all of the level 3 injury results plotted as a function of the Bladder Oscillation Parameter. The curve is Equation 3.2.1 derived from the Spot level 3 injury data.

### 3.5 DISCUSSION OF INJURY CORRELATIONS

It is not accidental that both the bladder oscillation parameter and the impulse damage parameter can be used to describe the fish-kill for shallow explosion geometries. To see how this comes about we examine the response of an air bubble to impulsive pressure loading.

"Let the pressure be applied suddenly and let it disappear again before the bubble has had time to change appreciably in size. Then, the bubble will begin contracting inward at a certain radial velocity  $v_i$  given by

$$v_i = - \frac{I}{\rho A_i} \quad (3.5.1)$$

---

\*In examining dead and disabled fish which have been collected from the water surface following underwater explosions Martin Wiley and Greig Peters (Chesapeake Biological Laboratory, Solomons, Md.) have found only fish having injuries of level 3 or greater. This indicates that fish having received lesser injuries do not show up in the visible fish kill although they may later fall victim to predation.

where  $\rho$  is the density of the water and  $I = \int p \, dt$ , the applied impulse."<sup>5</sup> By the methods of Appendix A we can now calculate the radius ratio  $AMAX/AMIN$  for the oscillating bubble. See Figure 3.5.1.

The solution -- by means of a tabulated function -- is of the form

$$\frac{AMAX}{AMIN} = \text{FUNCTION} \left[ \frac{I}{A_i \sqrt{\rho p_i}} \right] \quad (3.5.2)$$

where  $p_i$  is the initial value of the ambient water pressure.

Since  $\sqrt{p_i}$  does not vary greatly for shallow explosion geometries and since in most bladder fish the swim bladder comprises a roughly constant fraction of the total volume (about 6%), Equation 3.5.2 can be written

$$\frac{AMAX}{AMIN} = \text{FUNCTION} \left[ \frac{I}{M^{1/3}} \right] \quad (\text{approximately}) \quad (3.5.3)$$

where we have substituted  $M$ , the mass of the fish, for the volume, since all fish are approximately neutrally buoyant. Equation 3.5.3 shows that the Bladder Oscillation Parameter and the Impulse Damage Parameter are for practical purposes equivalent, for the special condition of shallow fish depth and impulsive pressure loading.

Taken together, the results of the Lovelace Foundation for fish-kill as a function of the impulse and the present results described in terms of the bladder oscillation parameter (and, in part by the impulse damage parameter) give us confidence that we have achieved a correct approximate solution to the problem of

---

5. Kennard, E. H., "Radial Motion of Water Surrounding a Sphere of Gas in Relation to Pressure Waves," 1943, published in Vol. II of "Underwater Explosion Research," Office of Naval Research, 1950.



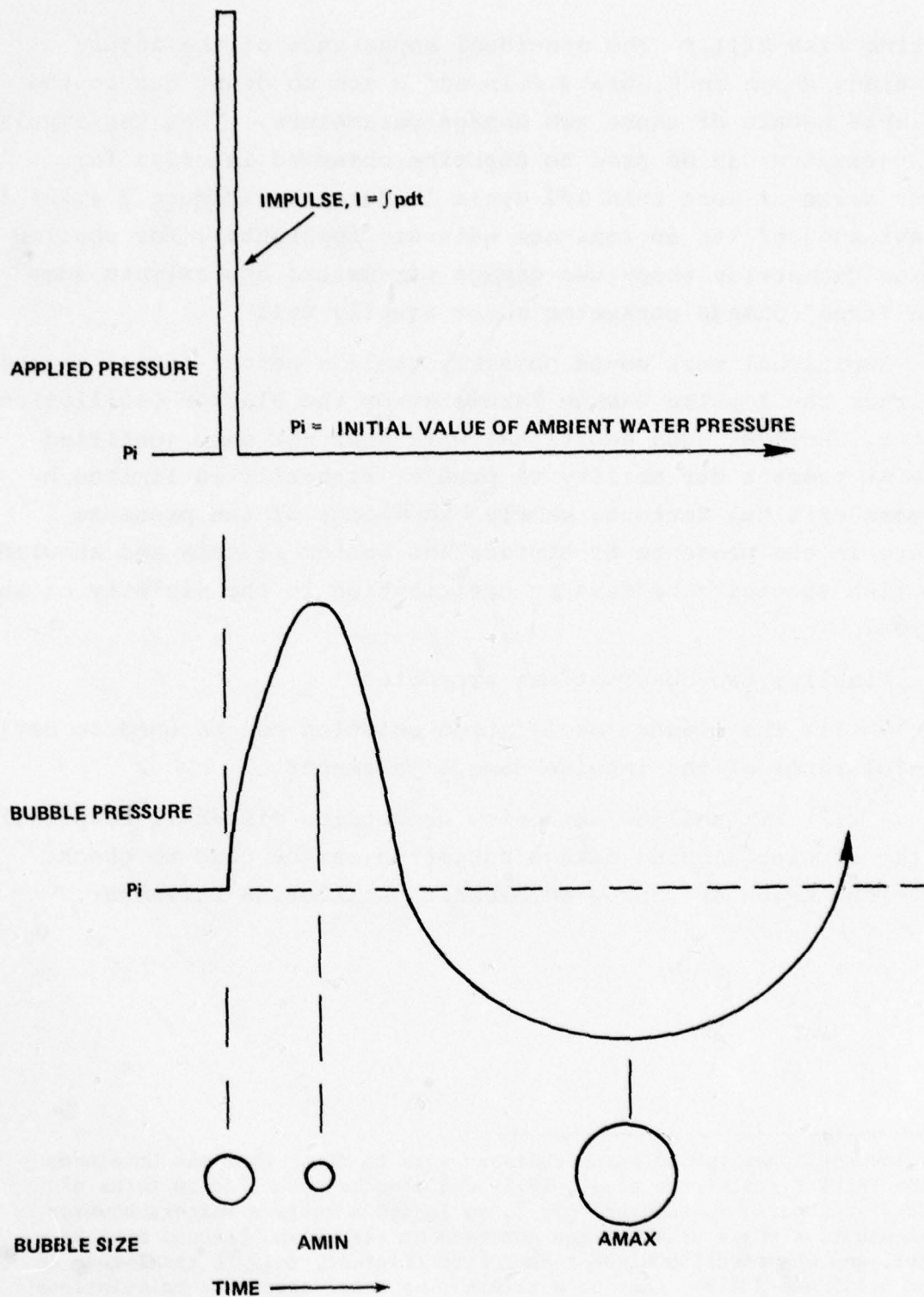


FIGURE 3.5.1 SKETCH ILLUSTRATING BUBBLE RESPONSE TO A PRESSURE WAVE OF VERY SHORT DURATION

predicting fish-kill.\* The non-ideal appearance of the injury correlations shown in Figure 3.4.1b and c are no doubt due to the approximate nature of these two damage parameters. That the impulse damage parameter can be used to describe observed injuries for pressure waves of more than 1/2-cycle in duration (Figure 3.4.1b) is clear evidence of its approximate nature. Apparently, for shallow explosion geometries these two damage parameters approximate some unknown "true" damage parameter about equally well.

Additional work could possibly yield a better damage parameter than either the Impulse Damage Parameter or the Bladder Oscillation Parameter. However such additional work does not seem justified because at present our ability to predict fish-kill is limited by other more critical factors, namely, knowledge of the pressure signature in the presence of surface and bottom effects and knowledge of the fish species/size/density distribution in the vicinity of the explosion.

Finally, two observations are noted:

- (1) The bladder oscillation solution can be used to define the useful range of the impulse damage parameter.
- (2) For shallow explosion geometries fish-kill computations using the simpler impulse damage parameter can be used to check computations using the computed bladder oscillation parameter.

---

\*We are also confident (based on unpublished work to date) that the Lovelace Foundation results (Yelverton et al, 1975) can also be described in terms of the bladder oscillation parameter. To do so is not a routine matter, however, since the negative phase pressure and duration at each fish location must be calculated, and an effective bladder radius coefficient,  $(A_1)_0/L$  (analogous to Equations 3.1.7 and 3.1.8), must be determined by trial-and-error calculations for each fish.

## 4 APPLICATIONS

### 4.1 FISH-KILL CONTOURS

Figure 4.1.1 shows the region of greater than 50% kill predicted for 18-cm long Spot in the vicinity of a 32 kilogram pentolite explosion at 9 meter depth. The procedure for making Figure 4.1.1 is as follows. First, we calculate the bladder oscillation parameter  $Z$  for an array of horizontal ranges,  $x$ , and depths,  $y$ ; i.e.,  $Z = f(x,y)$ . These values,  $Z = 100 \ln(AMAX/AMIN)$ , are tabulated in Table 4.1.1. Next, assuming that injury of level 3 constitutes kill, we read from Figure 3.2.2 the value,  $Z_{50\%} = 120$ , for 50% kill probability. Finally, we plot in Figure 4.1.1 the regions of Table 4.1.1 having  $Z$  greater than  $Z_{50\%}$ .

To calculate  $Z$  in Table 4.1.1 we first calculated an approximate pressure-time signature by the method described in Appendix C. Then, we calculated the response to this signature as described in Section 2 and in Appendix B, except that these computations were for undamped oscillatory bladder response.\*

Figure 4.1.2 shows predicted regions of greater than 10%, 50% and 90% kill for 21.5-cm long White Perch for 32 KG pentolite at 9 meter depth. The procedure for making Figure 4.1.2 was the same as described for Figure 4.1.1. Values of  $Z_{10\%} = 77$  and  $Z_{90\%} = 190$  read from Figure 3.2.2 were used to obtain the 10% and 90% kill contours in Figure 4.1.2. In Figure 4.1.2 contour details such as shown in Figure 4.1.1 have been smoothed out.

Note two important features of our solution to the fish-kill problem which are evident in Figure 4.1.2:

- (1) The fish-kill is strongly dependent on the depth of the fish.

---

\*Due to "no damping" and because of discrepancies between the negative pressures and durations calculated by Appendix C and results from the 1975 test series these calculations are considered approximate -- but quite adequate for the purposes of this report.



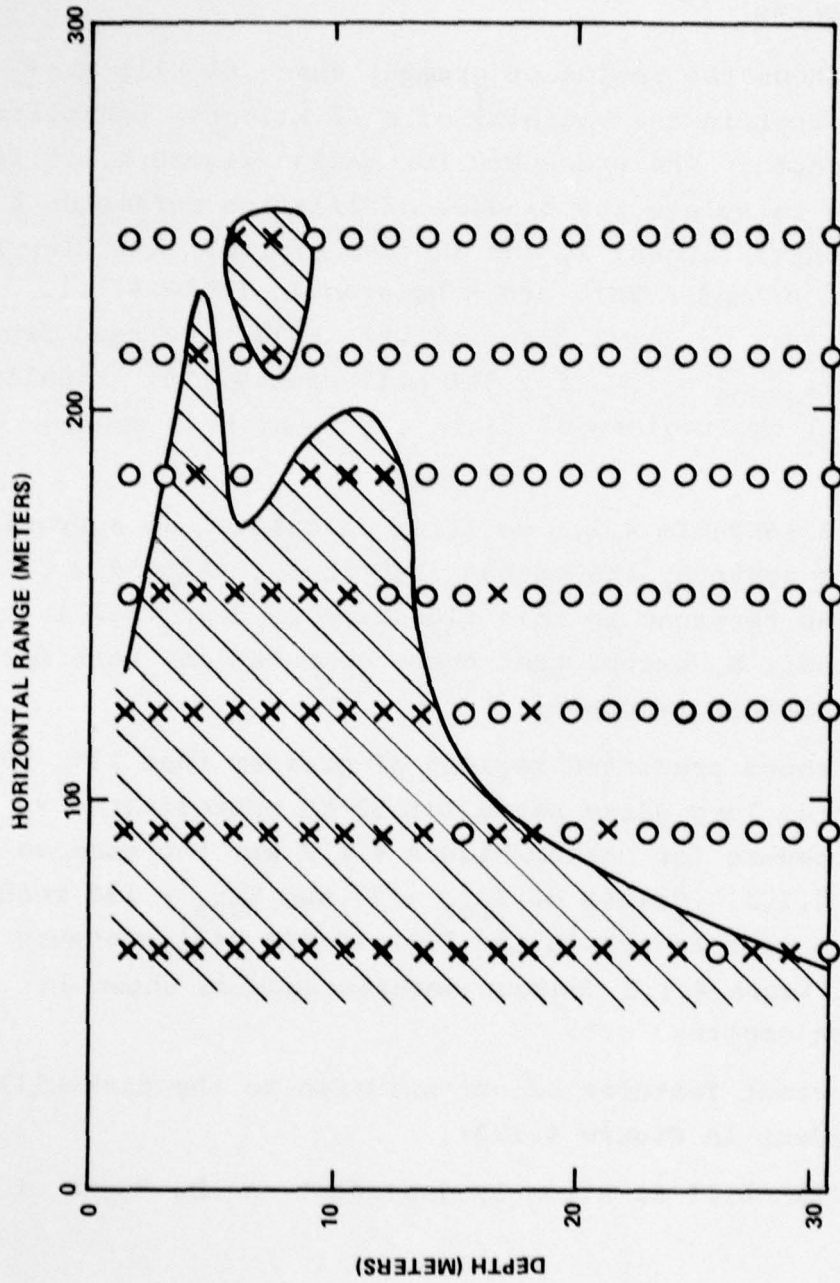


FIG. 4.1.1 REGION OF GREATER THAN 50% KILL FOR 18 CM SPOT -- 32 KG PENTOLITE AT 9 M DEPTH

TABLE 4.1.1

BLADDER OSCILLATION PARAMETER Z AS A FUNCTION OF FISHES' DEPTH  
AND HORIZONTAL RANGE\*

Charge: 32 KG Pentolite at 9 M Depth

Fish: Spot, 18 cm Fork Length

	HORIZONTAL RANGE (METERS)						
	61	91	122	152	183	213	244
FISH DEPTH (METERS)							
0	-	-	-	-	-	-	-
1.5	299	333	131	94	52	44	39
3.0	302	291	139	153	111	112	72
4.6	310	288	111	96	131	143	98
6.1	228	217	194	139	102	98	122
7.6	244	185	193	158	-	124	128
9.1	174	207	150	171	131	104	119
10.7	228	151	135	147	137	103	98
12.2	156	140	149	115	136	111	89
13.7	205	159	140	94	109	111	90
15.2	149	116	95	110	92	112	99
16.8	188	131	102	123	75	90	100
18.3	142	138	132	98	90	66	87
19.8	175	107	91	74	103	62	67
21.3	136	140	86	78	90	76	55
22.9	163	95	106	104	68	87	60
24.4	133	91	92	82	59	76	65
25.9	110	114	80	67	71	58	75
27.4	128	96	95	76	85	50	66
29.0	125	119	82	91	57	53	50
30.5	118	92	74	60	54	73	42

\*These values for Z were calculated using approximate predicted pressure-time inputs and no damping of the calculated bladder motion.

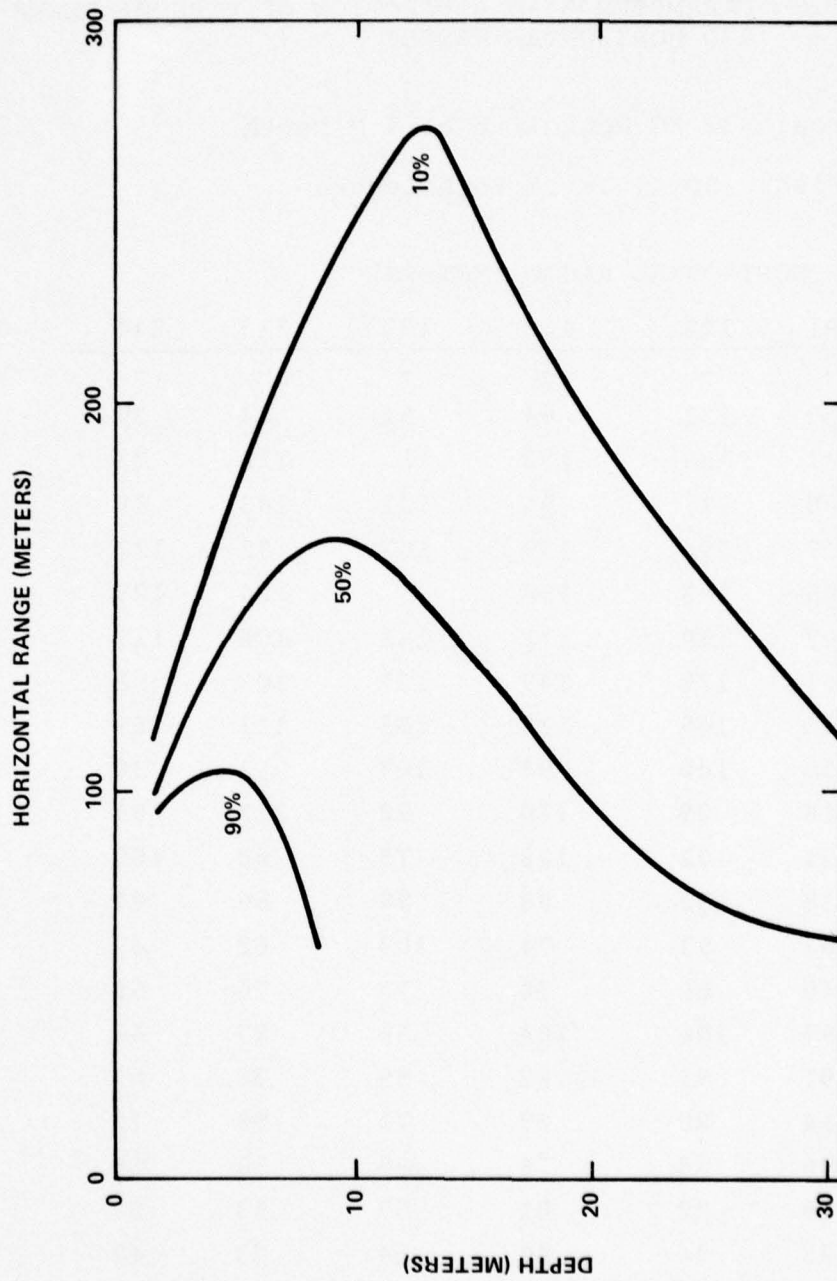


FIG. 4.1.2 REGIONS OF GREATER THAN 10%, 50%, AND 90% KILL FOR 21.5 CM WHITE PERCH --  
32 KG PENTOLITE AT 9 M DEPTH



(2) Regions of less than 50% kill -- since they encompass a tremendous volume of water -- make a major contribution to the total number of fish killed by an underwater explosion.

These two features are examined further in Sections 4.2 and 4.3.

#### 4.2 KILL PROBABILITIES AS A FUNCTION OF DEPTH FOR DIFFERENT SIZED FISH

Figure 4.2.1 shows the variation of predicted kill-probability with fishes' depth at a fixed horizontal range for different fish corresponding to three different sized swim bladders. The predicted kill-probability is obtained from calculated Z-values, e.g., Table 4.1.1, using Equation 3.2.1 (dashed line in Figure 3.2.2). The approximate length of Striped Bass corresponding to the equivalent bladder radii of the bladder oscillation calculations was calculated from

$$\frac{\text{Bladder Radius}}{\text{Fish Length}} = .042 \quad (4.2.1)^*$$

For the two larger sized fish in Figure 4.2.1 the maxima occurring at about 7 and 11 meters depth, respectively, are caused by surface cut-off occurring at the first half-cycle of bladder oscillation. At shallower depths the bladder does not have time to respond fully to the positive portion of the explosion wave; while coincidence of the first half-cycle and surface cut-off amounts to a resonance between the oscillatory response and the driving pressure field outside. Thus, at shallow depth the larger fish are in effect protected from harm by their swim bladders; while at the resonance depth their swim bladders "do them in."

---

\*The value .042 is 80% of that experimentally measured from a sample of 3 Stripped Bass. The value 80% represents a guess at the correction to go from measured radius to equivalent computation radius for this fish.

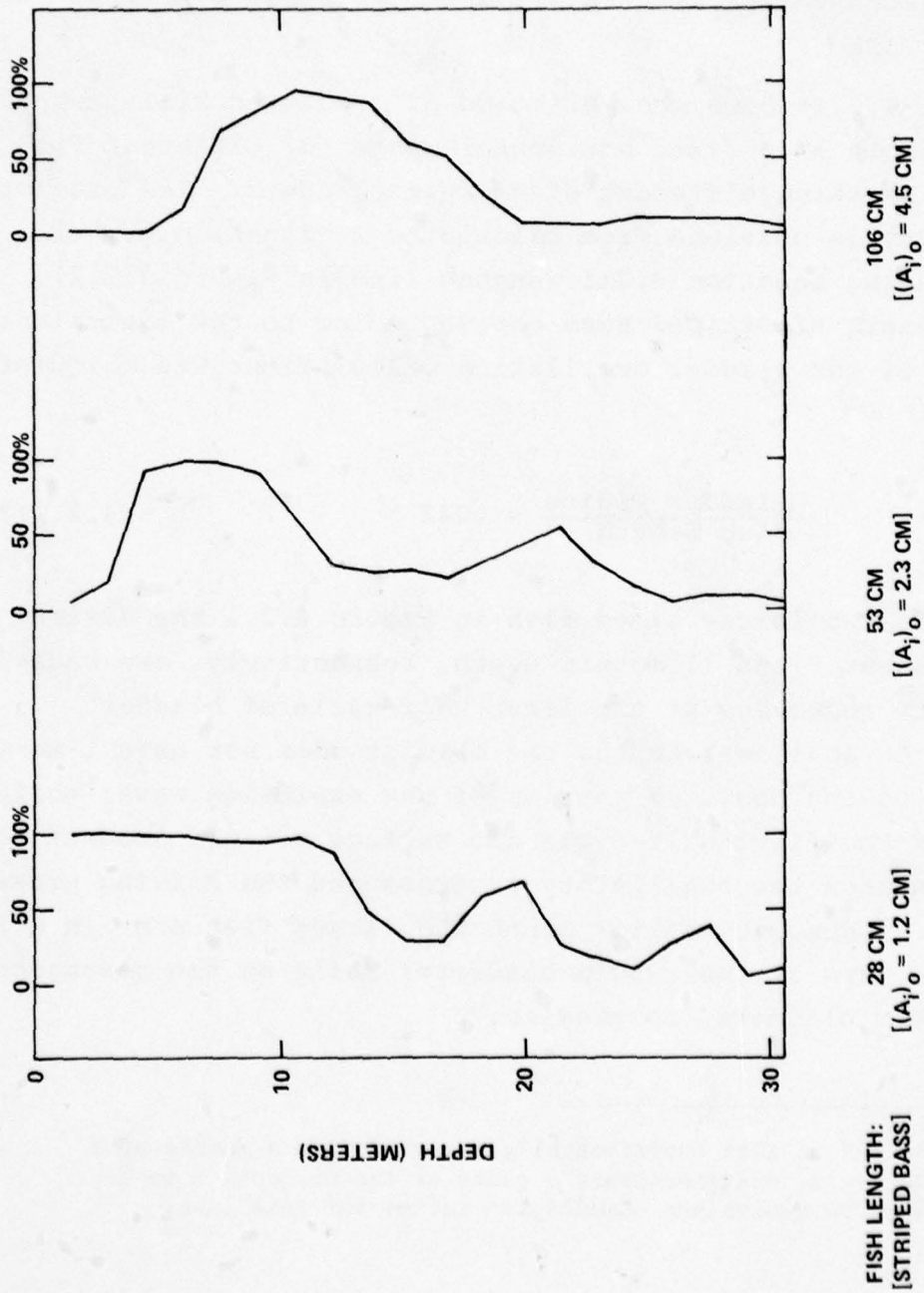


FIG. 4.2.1 PREDICTED KILL PROBABILITIES AS A FUNCTION OF DEPTH FOR DIFFERENT SIZE FISH --  
32 KG CHARGE AT 9 M DEPTH  
HORIZONTAL RANGE: 91 METERS

#### 4.3 TOTAL FISH-KILL AND ITS SPATIAL DISTRIBUTION

In this section we calculate the total fish-kill from an underwater explosion and its distribution as a function of horizontal range and depth, assuming a uniform spatial distribution of a single size class of one species of fish.

Table 4.3.1 (top) lists the bladder oscillation parameter  $Z$  for 21.5 cm White Perch calculated over a cylindrical grid surrounding a 32 kilogram charge fired at 9 meter depth. Table 4.3.1 (bottom) lists the corresponding kill probabilities from Equation 3.2.1.

To calculate the fish-kill we must know which fish are where; and, in general, this is impossible. Nevertheless, to gain insight as to the potential of a given explosion geometry for killing fish it is useful to assume a fictitious fish density distribution. For this purpose we will assume a nominal uniform density distribution of 1 fish per thousand cubic meters of water.

To calculate the fish-kill we must integrate the product, fish density  $\times$  kill probability, over the region surrounding the explosion. Thus, for this example we compute the products of "fish present" and "kill probability" (Tables 4.3.2 and 4.3.1) to get the "fish killed" in each mesh volume, Table 4.3.2 (bottom) -- each mesh consisting of a **cylindrical** annulus 100 feet thick and 5 feet in depth. Summing the distribution of "fish killed" shown at the bottom of Table 4.3.2 results in a total kill of 1245 fish out of 6228 fish present. Note that we have neglected 200 fish present in the 150-ft radius cylinder of water containing the charge as well as all fish present beyond a horizontal range of 850 feet. Nevertheless, we have described the most significant portion of the distribution of fish killed by this underwater explosion.

It is apparent, for example that if fish were present only at depths greater than 70 or 80 feet relatively few fish would be killed. Likewise, if fish (of this particular size) were present only within some 10 feet of the surface the kill would be relatively



TABLE 4.3.1 BLADDER OSCILLATION PARAMETER AND KILL PROBABILITY AS A FUNCTION OF FISHES' DEPTH AND HORIZONTAL RANGE

Charge: 32 KG Pentolite at 9 M Depth

Fish: White Perch, 21.5 cm Fork Length

		Horizontal Range (feet)						
		200	300	400	500	600	700	800
Fish Depth (feet)	5	251	208	41	41	35	10	7
	10	220	211	119	73	32	30	28
	15	206	215	156	100	62	31	26
	20	287	197	131	129	86	79	58
	25	206	180	147	114	109	74	69
	30	168	175	130	146	94	93	64
	35	172	187	117	120	113	88	81
	40	211	163	120	97	102	97	96
	45	168	125	135	89	94	99	84
	50	144	110	139	94	76	82	87
	55	133	111	121	99	70	77	73
	60	177	133	91	104	76	62	68
	65	139	141	83	108	72	58	55
	70	132	110	81	94	86	63	51
	75	128	98	79	70	91	60	49
	80	154	86	98	67	87	66	54
	85	107	110	105	63	76	70	52
	90	120	119	81	61	56	75	57
	95	125	76	66	69	54	65	61
	100	122	88	71	84	51	56	65

BLADDER  
OSCILLATION  
PARAMETER

		200	300	400	500	600	700	800
Fish Depth (feet)	5	1.00	.99	.01	.01	.01	.00	.00
	10	.99	.99	.42	.05	.01	.01	.00
	15	.99	.99	.85	.20	.03	.01	.00
	20	1.00	.98	.58	.55	.10	.07	.02
	25	.99	.95	.77	.35	.29	.06	.04
	30	.91	.94	.57	.76	.15	.15	.03
	35	.93	.97	.39	.43	.34	.12	.08
	40	.99	.89	.43	.18	.22	.18	.17
	45	.91	.50	.63	.12	.15	.19	.09
	50	.74	.30	.68	.15	.06	.09	.11
	55	.61	.32	.45	.19	.05	.07	.05
	60	.95	.61	.13	.24	.06	.03	.04
	65	.68	.71	.09	.28	.05	.02	.02
	70	.60	.30	.08	.15	.10	.03	.02
	75	.54	.18	.07	.05	.13	.03	.02
	80	.83	.10	.18	.04	.11	.04	.02
	85	.27	.30	.25	.03	.06	.05	.02
	90	.43	.42	.08	.03	.02	.06	.02
	95	.50	.06	.04	.04	.02	.04	.03
	100	.46	.12	.05	.09	.02	.02	.04

KILL  
PROBABILITY

**TABLE 4.3.2 FISH PRESENT AND NUMBER KILLED AS A FUNCTION OF WATER DEPTH AND HORIZONTAL RANGE**

Charge: 32 KG Pentolite at 9 M Depth

Fish: White Perch, 21.5 cm Fork Length

Fish Density

Distribution: Uniform Density =  $1 \times 10^{-3}$  Fish/Meter<sup>3</sup>

		Horizontal Range (feet)						
		200	300	400	500	600	700	800
Fish Depth (feet)	5 -	18	27	36	44	53	62	71
	10 -	18	27	36	44	53	62	71
	15 -	18	27	36	44	53	62	71
	20 -	18	27	36	44	53	62	71
	25 -	18	27	36	44	53	62	71
	30 -	18	27	36	44	53	62	71
	35 -	18	27	36	44	53	62	71
	40 -	18	27	36	44	53	62	71
	45 -	18	27	36	44	53	62	71
	50 -	18	27	36	44	53	62	71
	55 -	18	27	36	44	53	62	71
	60 -	18	27	36	44	53	62	71
	65 -	18	27	36	44	53	62	71
	70 -	18	27	36	44	53	62	71
	75 -	18	27	36	44	53	62	71
	80 -	18	27	36	44	53	62	71
	85 -	18	27	36	44	53	62	71
	90 -	18	27	36	44	53	62	71
	95 -	18	27	36	44	53	62	71
	100 -	18	27	36	44	53	62	71

FISH  
PRESENT

		200	300	400	500	600	700	800
Fish Depth (feet)	5 -	18	26	0	0	0	0	0
	10 -	18	26	15	2	0	0	0
	15 -	18	27	30	9	2	0	0
	20 -	18	26	21	25	6	5	2
	25 -	18	25	27	16	16	4	3
	30 -	16	25	20	34	8	9	2
	35 -	17	26	14	19	18	7	6
	40 -	18	24	15	8	12	11	12
	45 -	16	13	23	5	8	12	7
	50 -	13	8	24	7	3	5	8
	55 -	11	8	16	9	2	4	4
	60 -	17	16	5	11	3	2	3
	65 -	12	19	3	13	3	2	1
	70 -	11	8	3	7	6	2	1
	75 -	10	5	3	2	7	2	1
	80 -	15	3	7	2	6	2	1
	85 -	5	8	9	1	3	3	1
	90 -	8	11	3	1	1	4	2
	95 -	9	2	1	2	1	2	2
	100 -	8	3	2	4	1	1	3

FISH  
KILLED

light. However, for fish of this size between depths of 20 and 60 feet the kill will be extensive out to a range of about 800 feet; and if a large school several hundred feet in diameter with a density say, of one fish per cubic meter were within this region, a disastrous fish-kill would result. (Such an occurrence is unlikely, however, as it is Navy policy to delay operations if a school of fish is observed in the vicinity of the test site.)



REFERENCES

1. Gaspin, Joel B., 1975, "Experimental Investigations of the Effects of Underwater Explosions on Swimbladder Fish, I: 1973 Chesapeake Bay Tests," NSWC/WOL/TR 75-58.
2. Gaspin, J.B., M. L. Wiley, and G. B. Peters, 1976, "Experimental Investigation of the Effects of Underwater Explosions on Swimbladder Fish, II: 1975 Chesapeake Bay Tests," NSWC/WOL/TR 76-61.
3. Hubbs, C. L., E. P. Schultz, and R. Wisner, 1960, Unpublished preliminary report on investigation of effects on caged fishes from underwater Nitro-Carbo-Nitrate explosions, U. of Calif. Scripps Institute of Oceanography.
4. Yelverton, J. T., et al, 1975, "The Relationship between Fish Size and their Response to Underwater Blast", Lovelace Foundation, DNA Report 3677T.
5. Kennard, E. H., 1943, "Radial Motion of Water Surrounding a Sphere of Gas in Relation to Pressure Waves", published in Vol. II of "Underwater Explosion Research", Office of Naval Research, 1950.
6. Goertner, J. F., 1974, "Response of Air Bubbles to Underwater Explosion Pressures: Square Step Approximation with Application to Fish-bladder-cavity response", Unpublished internal technical note NOLTN 10205.
7. Cole, R. H., 1948, "Underwater Explosions", Princeton University Press.

8. Snay, H. G., and E. A. Christian, 1952, "Underwater Explosion Phenomena: The Parameters of a Non-Migrating Bubble Oscillating in an Incompressible Medium", NAVORD Report 2437
9. Weston, D. E., 1966 "Sound Propagation in the Presence of Bladder Fish", published in Vol. II of "Underwater Acoustics", edited by V. M. Albers, 1967, Plenum Press
10. Lippson, A. J., 1973, "The Chesapeake Bay in Maryland—an Atlas of Natural Resources", John Hopkins University Press
11. Walker, R. R., and J. D. Gordon, 1966, "A Study of the Bulk Cavitation Caused by Underwater Explosions", David Taylor Model Basin Report 1896
12. Sternberg, H. M., and W. A. Walker, 1971, "Calculated Flow and Energy Distribution Following Underwater Detonation of a Pentolite Sphere", Physics of Fluids, September 1971
13. Del Grosso, V. A., "New Equation for the Speed of Sound in Natural Waters (with Comparisons to Other Equations)", J. Acoust. Soc. Am., October 1974

APPENDIX A

RESPONSE OF GAS BLADDER TO UNDERWATER EXPLOSION PRESSURES:  
SQUARE STEP APPROXIMATION<sup>6</sup>

ABSTRACT

This appendix presents the theory of the radial motion of a gas-filled spherical bubble responding to step changes in the water pressure.

The theory is used to estimate the motion of a fish-bladder sized bubble subjected to the pressure signature from an underwater explosion. Some important qualitative results as well as some crude quantitative results are readily obtained. For example:

(1) For a simple positive step which returns to ambient pressure, the maximum bladder extension depends on both the magnitude and duration of the pressure pulse. If cut-off occurs when the bladder (undamped oscillation) is at maximum size, no extension beyond its initial at-rest size occurs. If cut-off occurs at any other time, some over-extension of the bladder occurs.

(2) A sudden decrease in the ambient pressure will always result in some over-extension of the bladder. If this negative pressure (below ambient) follows a positive step with cut-off occurring at maximum size, the over-extension is due solely to the negative portion of the pressure signature; if not, the over-extension is due to both the positive step and the negative pressure following cut-off. The effects are additive in a non-linear manner described in this appendix.

---

6. Appendix A was formerly given internal distribution as NOLTN 10205, Goertner, 1974, "Response of Air Bubbles to Underwater Explosion Pressures: Square Step Approximation with Application to Fish-bladder-cavity Response".



# I. ON THE MOTION OF AN AIR BUBBLE SUBJECTED TO A SERIES OF STEP CHANGES IN THE OUTSIDE WATER PRESSURE

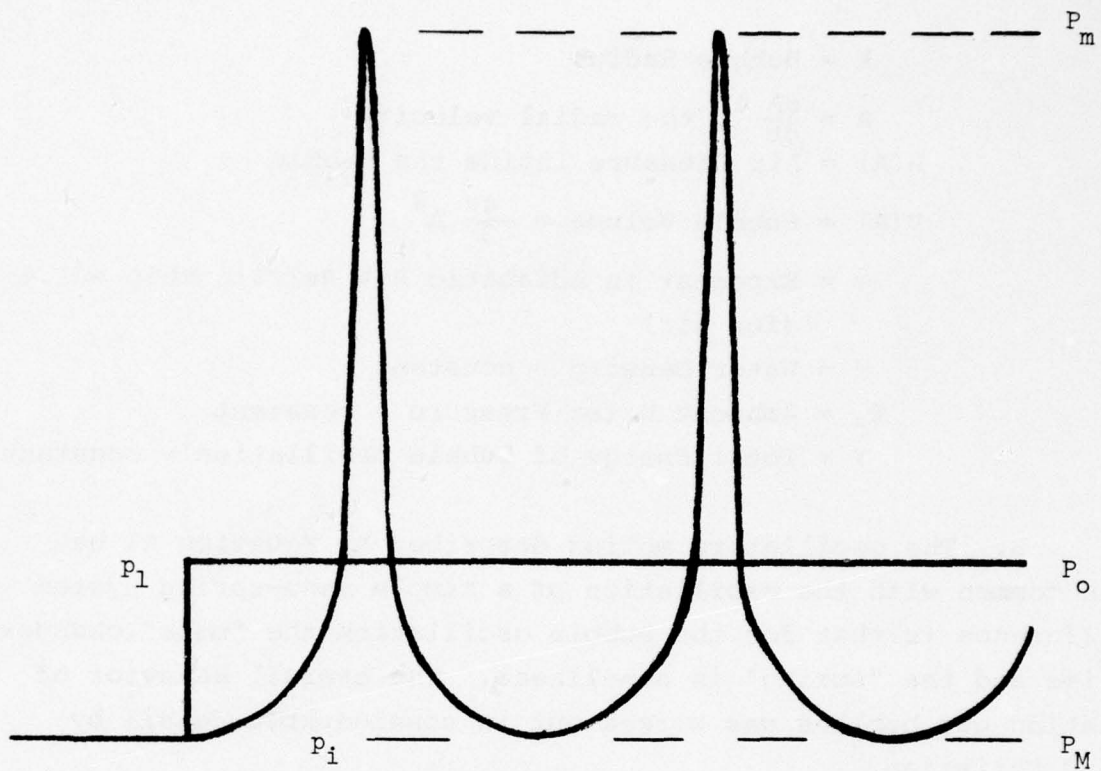
1. Consider a spherical bubble at rest in water at the initial value  $p_i$  of the ambient pressure. Let  $A_i$  be its initial radius when at rest. Its internal air pressure is the initial ambient pressure  $p_i$ . At  $t = 0$ , the ambient pressure jumps to a new value  $p_1$ ; and the bubble is then oscillating. The situation for the air pressure inside the bubble, trying to adjust to the new outside pressure, is sketched in Figure A-1.

2. In this Appendix we concern ourselves with the motion of a bubble subjected to a succession of jumps to new ambient pressures  $p_n$ . At each ambient pressure the bubble motion is described by the following differential equation.<sup>7</sup>

$$\underbrace{\frac{3}{2} \left( \frac{4\pi}{3} \rho A^3 \right) \dot{A}^2}_{\text{Kinetic Energy of Surrounding Water}} + \underbrace{\frac{4\pi}{3} p_o A^3}_{\text{Potential Energy of Pushed-back Water}} + \underbrace{E(A)}_{\substack{\text{Internal Energy of Air} \\ \text{Inside Bubble}}} = Y \quad (A1)$$

Total Energy

7. Cole, R. H., 1948, "Underwater Explosions", Princeton University Press.



$p_i$  = Initial outside water pressure  
 $p_l$  = New value of outside water pressure  
 $P_M$  = Bubble air pressure at maximum size  
 $P_o$  = Bubble air pressure at "Equilibrium"  
 $\quad = p_l$   
 $P_m$  = Bubble air pressure at minimum size

FIG. A-1 BUBBLE AIR PRESSURE AND OUTSIDE WATER PRESSURE AS A FUNCTION OF TIME (SKETCH)

where

$$E(A) = \frac{P(A) \times V(A)}{\gamma - 1} \quad (A2)$$

$A$  = Bubble Radius

$\dot{A} = \frac{dA}{dt}$  , the radial velocity

$P(A)$  = Air Pressure Inside the Bubble

$V(A)$  = Bubble Volume =  $\frac{4\pi}{3} A^3$

$\gamma$  = Exponent in Adiabatic P-V Relationship = 1.4  
(for air)

$\rho$  = Water Density = constant

$P_o$  = Ambient Water Pressure = constant

$Y$  = Total Energy of Bubble Oscillation = constant

3. The oscillatory motion described by Equation A1 has much in common with the oscillation of a simple mass-spring system — the difference is that for the bubble oscillation the "mass" changes with time and the "spring" is non-linear. The overall behavior of oscillating gas bubbles was worked out in considerable detail by Snay and Christian.<sup>8</sup>

They rewrote Equation A1 in the non-dimensional form

$$a^3 \dot{a}^2 + a^3 + k a^{-3(\gamma-1)} = 1 \quad (A3)$$

where  $a$  is the non-dimensional radius  $a = A/L$  and  $\dot{a}$  is the derivative of " $a$ " with respect to the non-dimensional time  $t' = t/C$ . The parameters  $k$  and  $\gamma$  characterize the bubble motion. " $k$ " can be expressed by

$$k = \frac{P_{Mm}}{P_o(\gamma-1)} \left[ 1 + \frac{P_{Mm}}{P_o(\gamma-1)} \right]^{-\gamma} \quad (A4)$$

where  $P_{Mm}$  is the internal pressure at either extremum of the bubble oscillation —  $M$  refers to the maximum bubble volume ( $P_M$  = minimum pressure),  $m$  refers to the minimum bubble volume ( $P_m$  = maximum pressure) — and  $P_o$  is the ambient hydrostatic pressure.

<sup>8</sup> Snay, H. G., and E. A. Christian, 1952, "Underwater Explosion Phenomena: The Parameters of a Non-Migrating Bubble Oscillating in an Incompressible Medium", NAVORD Report 2437



4. The length scale factor  $L$  and the time scale factor  $C$  are defined by

$$L = \left( \frac{3 Y}{4 \pi P_o} \right)^{1/3} \quad (A5)$$

$$C = L \left( \frac{3 \rho}{2 P_o} \right)^{1/2} \quad (A6)$$

where  $Y$  is the total energy (Equation A1) and  $\rho$  is the density of the water.

5. Snay and Christian in their report have determined the overall behavior of the oscillatory solutions to Equation A3 for  $\gamma$  in the range,  $1.0 \leq \gamma \leq 1.5$ . Table A1 (below) list some of their results for  $\gamma = 1.4$ . The dimensionless quantities --  $a_M$ ,  $a_m$  and  $T'$  -- are the maximum radius, the minimum radius and the period of oscillation of the bubble, respectively.

TABLE A-1  
Bubble Parameters for  $\gamma = 1.4$

$k$	$a_M$	$a_m/a_M$	$T'$	$T'$ Calculated From Equation A32
0.0	1.000	0.0	1.492	1.476
0.05	0.982	0.085	1.505	1.496
0.10	0.963	0.152	1.522	1.516
0.15	0.942	0.220	1.538	1.536
0.20	0.920	0.288	1.557	1.556
0.25	0.893	0.364	1.577	1.576
0.30	0.863	0.447	1.596	1.596
0.35	0.823	0.548	1.616	1.616
0.40	0.768	0.699	1.636	1.636
0.432	0.659	1.000	1.650	1.649

6. In what follows, we will use both Equations A1 and A3. Transitions from one outside pressure level,  $p_n$ , to another,  $p_{n+1}$ , are simply described using Equation A1. And, Snay and Christian's results, e.g., those listed in Table I, which were computed from Equation A3, are convenient for computing the bubble behavior within a given state.

7. Boundary Conditions at Pressure Jumps. We now consider a step change in outside pressure from  $p_n$  to  $p_{n+1}$ . Let  $V_{c_n}$  be the bubble volume at the instant of change, and  $y_n$  and  $y_{n+1}$  be the old and new total energies. For the  $n^{\text{th}}$  state we rewrite Equation A1 as

$$\frac{3}{2} \left( \frac{4\pi}{3} \rho A^3 \right) \dot{A}^2 + \frac{4\pi p_n}{3} A^3 + E(A) = y_n \quad (\text{A7})$$

Now, since the oscillating system described by (A7) has finite mass, neither  $A$  nor  $\dot{A}$  can change impulsively, i.e.,

$$\Delta A \approx 0 \quad (\text{A8})$$

$$\Delta \dot{A} \approx 0 \quad (\text{A9})$$

at each pressure jump. Thus, the first and third terms of (A7) do not change at the jump, and the change in the total energy is given by

$$y_{n+1} = y_n + (p_{n+1} - p_n) V_{c_n} \quad (\text{A10})$$

where  $V_{c_n}$  is the bubble volume at the time of the jump.

8. Equations (A7), (A8), (A10) completely specify the motion in the  $n^{\text{th}}$  state given suitable initial conditions. In the present case the initial or zeroth state is specified by

$$A = \text{constant} = A_i \quad (\text{A11})$$

$$P(A_i) = \text{constant} = p_i \quad (\text{A12})$$

In particular, the total energy  $Y_n$  and the outside pressure  $p_n$  are sufficient to specify the amplitude of the oscillation. And, if the radius function  $A(t)$  is known, the phase will then be determined by the jump conditions,  $\Delta A = 0$  and  $\Delta \dot{A} = 0$ .

9. Some General Equations for the  $n^{\text{th}}$  State. We now list some further equations that can be used to calculate the parameters of the bubble oscillation in the  $n^{\text{th}}$  state.

$$k_n = \frac{(p_n/p_i)^{\gamma-1}}{(\gamma-1) \left( \frac{Y_n}{p_i v_i} \right)^{\gamma}} \quad (\text{A13})$$

$$L_n = \left( \frac{3Y_n}{4\pi p_n} \right)^{1/3} \quad (\text{A14})$$

$$C_n = L_n \left( \frac{3\rho}{2p_n} \right)^{1/2} \quad (\text{A15})$$

$$\left( \text{AMAX} \right)_n = a(k_n) \times L_n \quad (\text{A16})$$

$$\frac{\text{AMIX}}{\text{AMAX}_n} = \text{Tabulated Function}(k_n) \quad (\text{A17})$$

$$P(A) = p_i \left( \frac{A_i}{A} \right)^{3\gamma} \quad (\text{A18})$$

$$\bar{A}_n = A_i \left( \frac{p_i}{p_n} \right)^{1/3\gamma} \quad (\text{A19})$$

$$T_n = t(k_n) \times C_n \quad (\text{A20})$$



Equation A19 gives the equilibrium radius  $\bar{A}$  (radius after the oscillation has damped out) for the bubble in the  $n^{\text{th}}$  state. Equation A19 is derived from (A18) by setting  $P(A)$  equal to  $p_n$ .

10. Bubble Motion in State 1. Consider the step change in outside pressure from  $p_i$  to  $p_1$ . In accordance with the jump conditions (A8) and (A9) and the initial conditions (A11) and (A12) we set  $\dot{A} = 0$  and  $A = A_i$  in (A7) to obtain the total energy

$$Y_1 = (p_1 + \frac{p_i}{\gamma-1}) V_i \quad (\text{A21})$$

where we have also used Equation A2 to evaluate the internal energy  $E(A_i)$ .

11. Since  $A = 0$ , the oscillation in state 1 starts at an extremum. Whether this extremum is a maximum volume  $V_M$  or minimum  $V_m$  is determined by  $p_1$  being "greater than" or "less than"  $p_i$ .

If  $p_1 > p_i$ , then

$$A_{M_1} = A_i \quad (\text{A22})$$

$$P_{M_1} = p_i \quad (\text{A23})$$

IF  $p_1 < p_i$ , then

$$A_{m_1} = A_i \quad (\text{A24})$$

$$P_{m_1} = p_i \quad (\text{A25})$$

12. Since the oscillation in state 1 starts at an extremum, the bubble parameter  $k$  can easily be computed from Equation A4. From (A4) together with (A23) and A25 we get

$$k_1 = X_1 (1 + X_1)^{-\gamma} \quad (\text{A26})$$

where

$$X_1 = \frac{p_i}{(\gamma - 1) p_1} \quad (\text{A27})$$

13. Calculation of the Subsequent Extremum. The bubble radius at the next extremum (1/2 period later in time) is calculated from the initial value  $A_{Mm} = A_i$  by either dividing or multiplying by the ratio  $\left(\frac{a_M}{a_m}\right)_1$  obtained from Table I (by linear interpolation for the calculations done here). The corresponding air pressure  $P_{Mm}$  inside the bubble is then calculated using Equation A18, i.e.,

$$P_{Mm_1} = p_i \left( \frac{A_{Mm_1}}{A_i} \right)^{3\gamma} \quad (\text{A28})$$

14. Calculation of the Bubble Period. The bubble period of oscillation  $T$  is the product of the dimensionless period,  $t = F(\gamma, k)$ , given in Table I and the time scale factor  $C$  (Equations A15 and A14)

$$T_1 = T'_1 \times C_1 \quad (\text{A29})$$

Combining (A14), (A21) and (A27), we write for the length scale factor

$$L_1 = A_i (1 + X_1)^{1/3} \quad (\text{A30})$$

And, combining (A15), (A27) and (A30), we write the time scale factor as

$$C_1 = \left( \frac{0.6 \rho}{P_i} x_1 \right)^{1/2} (1 + x_1)^{1/3} A_i \quad (A31)$$

where  $\rho$  is the water density.

15. For our purposes the dimensionless period  $T'$ , is conveniently approximated by the linear function

$$T' = 1.476 + 0.4 k \quad (A32)$$

Values of  $T'$  calculated by Equation A32 are listed in Table 1 alongside the tabulated function. The approximation, Equation A32, is good to better than 0.5% for values of  $k \geq 0.1$ .

16. Finally, combining (A26), (A27), (A29), (A31) and (A32) we write for the period of oscillation

$$T_1 = \left( \frac{0.6 \rho}{P_i} x_1 \right)^{1/2} (1 + x_1)^{1/3} (1.476 + 0.4k_1) A_i \quad (A33)$$

The physical quantities in Equation A33 may be expressed in any consistent set of units. For English Engineering Units we have

- $T_1$  = Bubble Period (SECONDS)
- $\rho$  = Density of the Water (SLUGS/FT<sup>3</sup>)
- $P_i$  = Initial Value of Ambient Water Pressure (LBS/FT<sup>2</sup>)  
[pressure in LBS/FT<sup>2</sup> = (pressure in PSI) x 144]
- $A_i$  = Initial Radius of Bubble (FT)



17. Simplifying Assumption. To proceed further with the general case we would now need the bubble radius as a function of time in order to apply the jump equations (A8), (A9) and (A10) at the instant the outside pressure changes to its new value,  $p_2$ . Although not particularly difficult, such computations are beyond the limited scope of this study. Consequently, at this point we introduce the simplifying assumption that all pressure changes occur at an instant when  $\dot{A} = 0$ , i.e., either at an extremum or at equilibrium bubble radius after the oscillation has completely damped out. Pressure jumps,  $p_n$  to  $p_{n+1}$ , which happen to occur at bubble extrema give the greatest and also the least amplitudes of oscillation in the  $n+1^{\text{th}}$  state ( $V_c = V_{Mm}$  in Equation A10). Thus, even when the pressure jumps occur at other times than the extrema, we can place exact upper and lower limits on the amplitude of oscillation in each state.

18. Bubble Motion in State 2. In accordance with our simplifying assumption we will assume the pressure jump,  $p_1$  to  $p_2$ , occurs at a time  $t_{c_1}$  such that

$$t_{c_1} = N \times \frac{1}{2} T_1 \quad (\text{A34})$$

where  $N$  is any positive integer. Alternatively,  $t_{c_1}$  may be taken large enough that the bubble oscillation has damped out, i.e.,  $A_{c_1} = \bar{A}_1 = A_i (p_1/p_i)^{1/3\gamma}$ , the equilibrium radius.

19. Let  $V_{c_1}$ ,  $A_{c_1}$ ,  $P_{c_1}$  be the volume, radius and air pressure, respectively, of the bubble at time,  $t_{c_1}$ . If the new outside pressure  $p_2$  is higher than  $P_{c_1}$ , the air pressure inside the bubble, the new oscillation begins at maximum volume; and if  $p_2$  is lower than  $P_{c_1}$ , the oscillation begins at minimum volume. Or, restated we have

$$\text{If } p_2 > p_{c1}, \text{ then } A_{M2} = A_{c1} \quad (\text{A35})$$

$$p_{M2} = p_{c1} \quad (\text{A36})$$

$$\text{If } p_2 < p_{c1}, \text{ then } A_{m2} = A_{c1} \quad (\text{A37})$$

$$p_{m2} = p_{c1} \quad (\text{A38})$$

20. Next, for the bubble parameter  $k$  we have

$$k_2 = x_2 (1 + x_2)^{-\gamma} \quad (\text{A39})$$

where

$$x_2 = \frac{p_{c1}}{(\gamma-1) p_2} \quad (\text{A40})$$

With this value for  $k_2$  the bubble radius at the subsequent extremum can now be calculated by either dividing or multiplying the starting value  $A_{c1}$  by the ratio  $(a_m/a_M)_2$  obtained from Table I. The corresponding air pressure  $p_{Mm}$  inside the bubble can then be calculated by Equation A18. And finally the period of oscillation can be calculated from

$$T_2 = \left( \frac{0.6\rho}{p_i} x_2 \right)^{1/2} (1 + x_2)^{1/3} (1.476 + 0.4 k_2) A_{c1} \quad (\text{A41})$$

21. Bubble Motion in State n. The corresponding equations for the  $n^{\text{th}}$  state can easily be obtained from those for state 2 by substituting "n's" for "2's" and "n-1's" for "1's". The only apparent exception is that the equivalent equation for (A34) should read

$$T_{c_n} = T_{c_{n-1}} + N \times \frac{1}{2} T_n \quad (\text{A42})$$



## II. ON THE MOTION OF A SWIM-BLADDER-SIZE AIR BUBBLE SUBJECTED TO AN EXPLOSION GENERATED PRESSURE WAVE

22. At the present time we ask such questions as: "Can a nearby explosion kill or seriously damage fish by extending their swim bladders?" Prodded by this, let us calculate the behavior of a bladder-sized air bubble subjected to an explosion pressure signature--one which kills many, but not all, of the fish present. The pressure signature shown in Figure A-2 is derived from a experimental test condition (Shot 525, Chesapeake Bay Tests, July-Aug 73) and appears to meet this criterion. It corresponds to a fish cage location where, upon subsequent dissection, all ten of ten 5.4" long Spot and six of ten 7.2" long White Perch were judged to have received lethal damage. For this calculation we will further approximate the outside pressure signature with the square-stepped one which is also shown in Figure A-2.

23. To get a better feel for physical phenomena, we will do the calculation in three stages. First, we will calculate the response to the positive portion, a square-step which returns to the initial ambient pressure level; then, the response to a simple step decrease in outside pressure to the level of the explosion induced underpressure; and finally, the combined response to the square-stepped signature sketched in Figure A-2.

24. We will take our bladder-sized air bubble from a 5.4" long Spot, and start the calculation with an initial (at rest) bubble radius given by\*

$$A_i = 0.0395 \text{ L}$$

(A43)

---

\*Footnote on page A-16

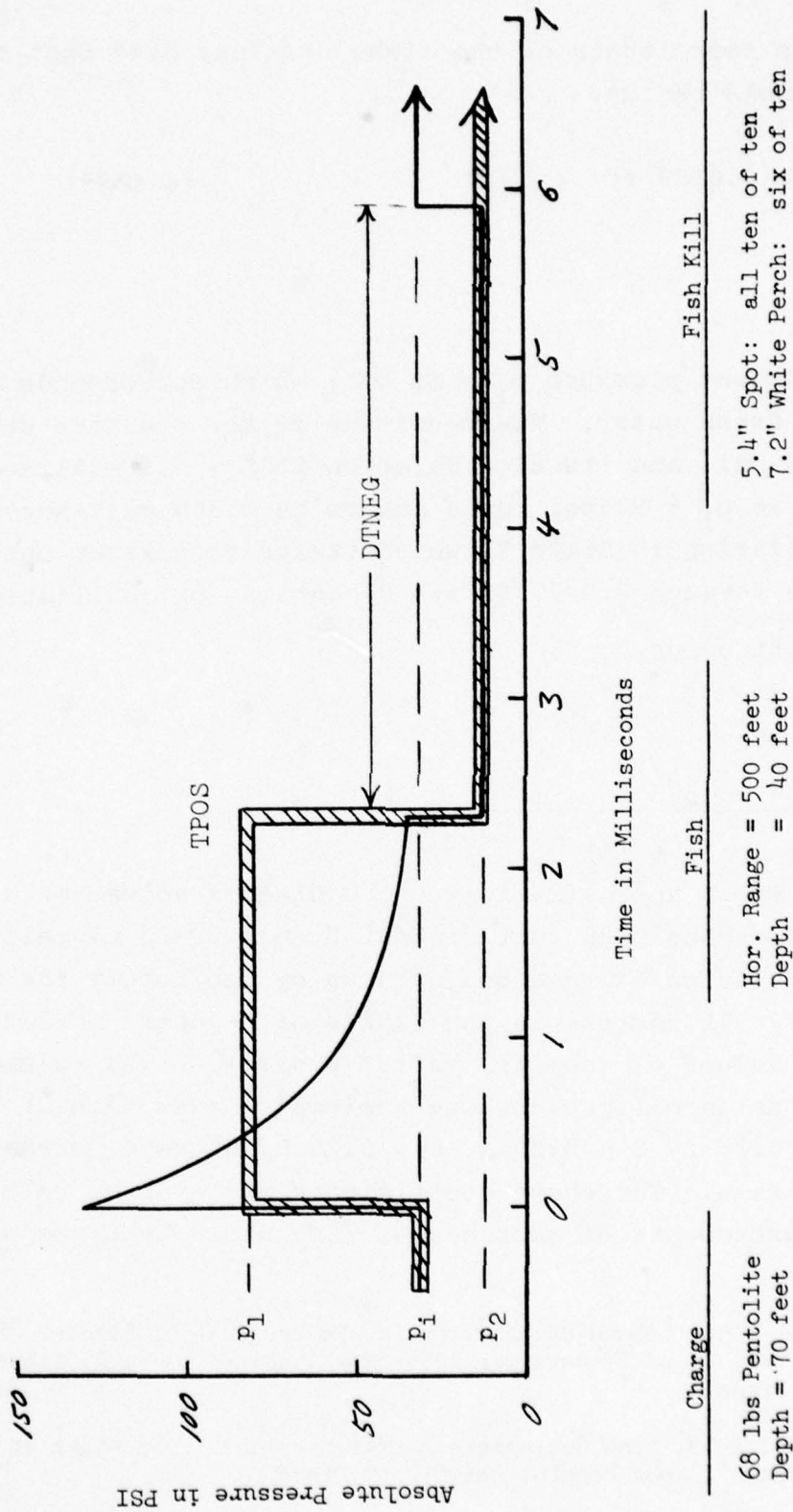


FIG. A-2 EXPONENTIAL AND SQUARE WAVE APPROXIMATIONS TO PRESSURE-TIME SIGNATURE

where  $L$  is the fork length of the fish. For our 5.4" Spot this gives an initial bubble radius

$$A_i = 0.0178 \text{ ft} \quad (\text{A44})$$

The initial ambient pressure  $p_i = 32$  psi, which corresponds to a depth of 40 feet in fresh water. The magnitude of the pressure step,  $p_1 - p_i$ , is 50 psi; and its time duration  $T_{POS} = 2.3$  milliseconds. The period  $T_1$  at  $p_1 = 82$  psi turns out to be 0.569 milliseconds, so that the oscillation in State 1, which starts at maximum bubble size  $A_{M_1} = A_i$ , goes through  $2.3/0.569 = 4.04$  periods of oscillation by the time cut off occurs.

---

(Footnote from page A-14)

\*This gives a rough approximation to the bladder volume of a 5.4" long fish at 40ft-depth and 500 feet distant from a 68-lb pentolite charge (Shot 525). Equation A43 was conjured up by the author for a "nominal fish". It represents the radius of a sphere of  $1/20^{\text{th}}$  of the estimated volume of the fish (after Weston).<sup>9</sup> The volume of the fish is taken as an ellipsoid whose semi-major axes (A,B,C) bear the relation,  $A = 0.38 L$ ,  $B = 0.30 A$ ,  $C = 0.25 B$ , where  $L$  is the overall length of the fish. The above coefficients are average values taken from crude measurements of sketches of fish shown by Lippson.<sup>10</sup>

9. Weston, D. E., 1966, "Sound Propagation in the Presence of Bladder Fish", published in Vol. II of "Underwater Acoustics", edited by V. M. Albers, 1967, Plenum Press

10. Lippson, A. J., 1973, "The Chesapeake Bay in Maryland — an Atlas of Natural Resources", John Hopkins University Press



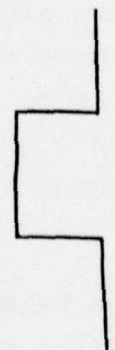


25. At cut-off time, TPOS, the measured outside water pressure drops to about 13 psi (Figure A2). Table A2 lists limiting case results for the final maximum radius (in State 2) which were calculated from the above parameter values by assuming cut-off times TPOS occurring at  $A_M$ ,  $A_m$ , and also sufficiently late that the oscillation has damped-out (so that  $A = \text{constant} = \bar{A}$ ).

26. Two sets of values for  $A_{M2}/A_i$  are given in Table A2, one for a final outside pressure  $p_2 = p_i = 32$  psi, the other for the measured value of  $p_2 = 13$  psi. The results listed in the top row of Table A2 (cut-off at bubble maximum) are the same as if the positive outside overpressure,  $p_1 - p_i$ , had never occurred. In other words, the upper right hand value of  $A_{M2}/A_i$  also applies to a simple step decrease in the ambient pressure  $p_i$  to a new value,  $p_2 = 13$  psi.

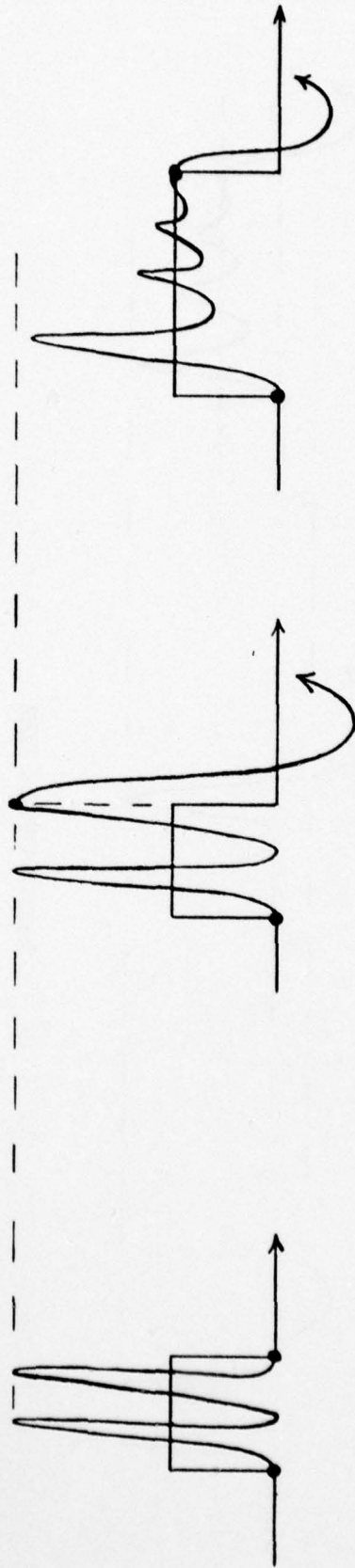
27. It is apparent from these crude results that both positive and negative excursions of the outside pressure significantly influence the final overshoot; and that time-of-occurrence of cut-off relative to the phase of the bubble oscillation cycle is of critical importance for positive excursions. It also looks like a good bet that underwater explosions do kill or cause serious damage to nearby fish by extending their swim bladders.

28. Figures A3 and A4 sketch the qualitative behavior of the inside air pressure and the bubble radius as functions of time for the six cases listed in Table A2.

TABLE A-2 DEPENDENCE OF RADIUS OVERSHOOT  $A_{M2}/A_i$  ON CUT-OFF

	Square Wave Followed by Negative Pressure	$\frac{A_{M_2}}{A_i}$	$\frac{A_{M_2}}{A_i}$
Cut-off occurs at Maximum Volume (minimum pressure)		1.00	1.48
Cut-off occurs at Minimum Volume (maximum pressure)		1.44	2.04
Oscillation Damps-out Before Cut-off		1.21	1.75

PRESSURE VERSUS TIME



CUT-OFF OCCURS AT  
BUBBLE MAXIMUM

CUT-OFF OCCURS AT  
BUBBLE MINIMUM

OSCILLATION DAMPS OUT  
BEFORE CUT-OFF

A-19

RADIUS VERSUS TIME

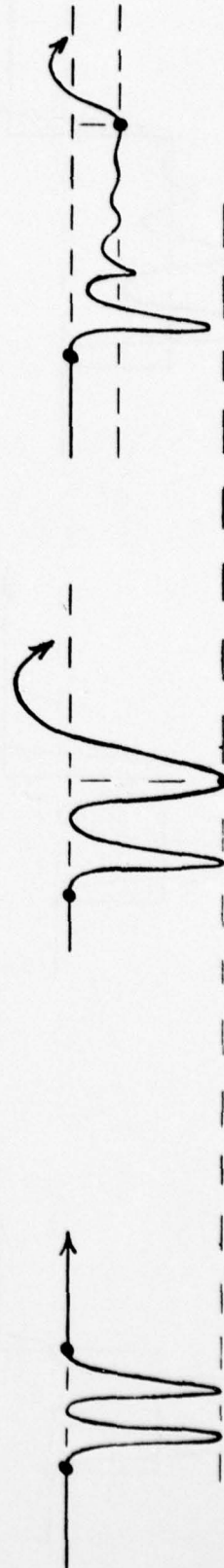
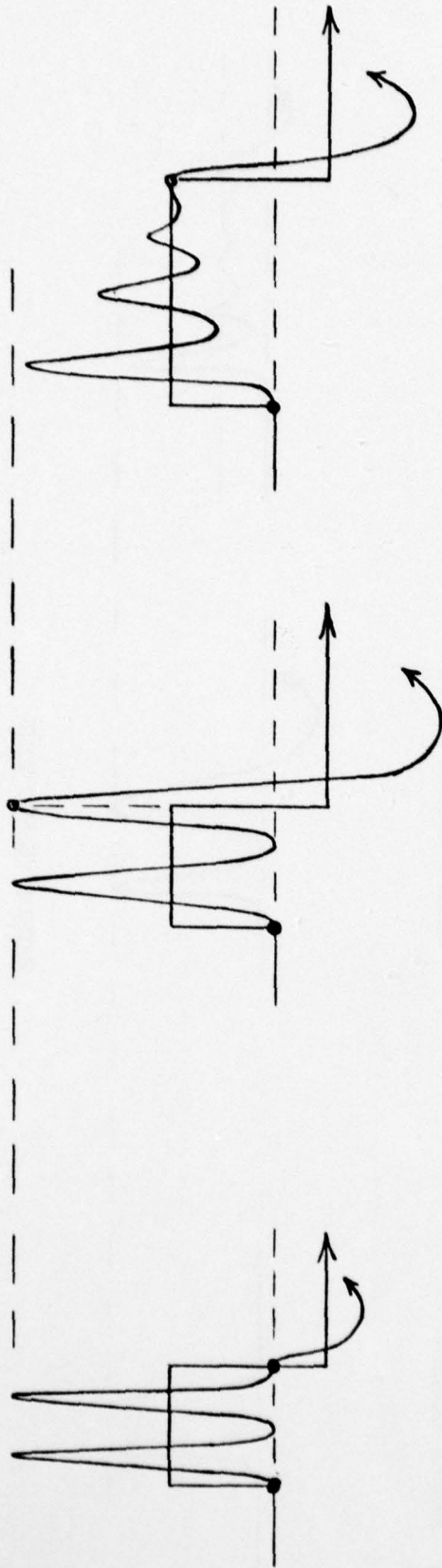


FIG. A-3 AIR BUBBLE RESPONSE TO A SQUARE WAVE



PRESSURE VERSUS TIME



A-20

NSWC/WOL TR 76-155

CUT-OFF OCCURS AT  
BUBBLE MAXIMUM

CUT-OFF OCCURS AT  
BUBBLE MINIMUM

OSCILLATION DAMPS OUT  
BEFORE CUT-OFF



RADIUS VERSUS TIME

FIG. A-4 AIR BUBBLE RESPONSE TO A SQUARE WAVE FOLLOWED BY AN UNDERPRESSURE

### III. DISCUSSION

29. After the above analysis was completed, George Young brought to my attention a similar analysis done in 1943 by E. H. Kennard (in connection with the proposed use of screens of bubbles as a protective device against explosion shock waves).<sup>5</sup> His development and presentation of the incompressible bubble theory (pp. 190-191, Ref. 5) is very convenient for calculating bubble motions such as the example used in this note, i.e., response to jumps in constant outside pressure states restricted to those instants when the radial velocity,  $\dot{A} = 0$ . I redid the calculations summarized in Table A2 using Kennard's "bubble theory" and the bubble radii and periods of oscillation were in all cases within 1% of my previous values calculated using the equations presented in this Appendix.

## IV. CONCLUSIONS

30. I hope that the analysis presented here (or some further development of it) will prove useful in correlating observed fish injury and kill with incident explosion pressure signatures. The present analysis is but a crude first cut, however; and if this approach to understanding fish damage should appear fruitful, considerable further development will probably be desirable and perhaps essential to achieving a useful correlation. Nevertheless, some things are already clear. For example:

(1) By itself, a step increase in the ambient pressure cannot extend the bubble/bladder beyond its original size, since the bubble oscillates between its original volume and some minimum volume which depends on the magnitude of the incident shock pressure. Extensions beyond the initial at-rest volume can only occur after return to ambient pressure or below.

(2) For a simple positive step pressure which returns to the ambient level, the maximum bubble/bladder extension depends on both the magnitude and duration of the pressure pulse. If cut-off occurs at the instant of maximum bubble volume, the bubble is returned to its initial at-rest state, having undergone no extension beyond this initial at-rest state. If cut-off occurs at any other time, some extension beyond the initial at-rest volume occurs. For a given incident pressure level, the greatest bubble/bladder extensions occur when cut-off is at the instant of minimum bubble volume.\*

---

\* Footnote next page



(3) A step decrease in the ambient pressure always results in an extension of the bubble/bladder. If such a drop follows a positive step where cut-off occurs at maximum bubble volume, the extension beyond initial at-rest volume is due solely to the negative portion of the pressure signature; if not, the over-extension is due to both the positive step and the underpressure following cut-off. The effects are additive in the non-linear manner described in this appendix.

---

(Footnote from preceding page)

\*For a simple step pressure pulse of level  $p_1$ , the energy of the residual bubble oscillation is given by

$$Y'_2 = Y_2 - Y_i = (p_1 - p_i) \times (V_i - V_{c_1})$$

where  $V_{c_1}$  is the bubble volume at the instant of cut-off. Thus, the energy of the residual oscillation and, consequently, extension of the bubble/bladder beyond initial at-rest volume take on greatest values for  $V_{c_1} = V_m$  and tend to zero as  $V_{c_1}$  approaches  $V_m$ .

## APPENDIX B

METHOD FOR CALCULATING GAS BLADDER RESPONSE  
TO EXPLOSION PRESSURE WAVE

Figure 2.3.2 sketched the way we approximated the explosion pressure signature by a sequence of pressure steps in order to calculate the bladder response by means of the equations developed in Appendix A. Appendix B gives the details of the procedure.

Boundary Condition at Pressure Jumps. Step changes in the outside water pressure from  $p_n$  to  $p_{n+1}$  occurring at half-period intervals change the equilibrium pressure  $P_o$  of the oscillating bubble flow (equal to the outside pressure  $p_n$ ). Since the oscillatory system described by Equation A1 has finite mass, neither  $A$  nor  $\dot{A}$  can change impulsively, i.e.,

$$\Delta A = 0 \quad (B1)$$

and

$$\Delta \dot{A} = 0 \quad (B2)$$

for all pressure jumps. And, thus for pressure jumps occurring at extrema where  $\dot{A}=0$ , only the equilibrium pressure  $P_o$  can change.

Let  $A_{c_n}$  be the ~~maximum~~ or minimum bubble radius at the time of the pressure jump  $p_n$  to  $p_{n+1}$ . If  $A_{c_n}$  is greater than the new equilibrium radius\*  $\bar{A}_{n+1}$ , the new oscillation begins at maximum

---

\*The equilibrium radius  $\bar{A}$  is the at-rest radius which corresponds to the equilibrium pressure  $P_o$  ( $= p_n$ , the outside pressure).  $\bar{A}_n$  is calculated from  $p_n$  using Equation B6, below.

size; and if  $A_{c_n}$  is smaller than  $\bar{A}_{n+1}$  the new oscillation begins at minimum size. Or, restated we have

$$\text{If } A_{c_n} > \bar{A}_{n+1}, \text{ then } AMAX_{n+1} = A_{c_n} \quad (B3)$$

$$\text{If } A_{c_n} < \bar{A}_{n+1}, \text{ then } AMIN_{n+1} = A_{c_n} \quad (B4)$$

Equilibrium Bubble Radius. At any time during the motion the internal gas pressure  $p$  is related to the bubble radius by

$$P(A) = p_i \left( \frac{A_i}{A} \right)^{3\gamma} \quad (B5)$$

Setting  $P(A)$  equal to  $p_n$  in (B5) yields the equilibrium bubble radius,

$$\bar{A}_n = A_i \left( \frac{p_i}{p_n} \right)^{1/3\gamma} \quad (B6)$$

where  $\gamma$  is the adiabatic exponent for air ( $= 1.40$ ) and the subscript "i" refers to the initial ambient "at rest" state.

Equilibrium Bubble Period. The equilibrium bubble period  $\bar{T}_n$  (for vanishingly small oscillations about the equilibrium radius) was given by Kennard.<sup>5</sup>

$$\bar{T}_n = 2\pi \bar{A}_n \sqrt{\rho / 3\gamma p_n} \quad (B7)$$

where  $\rho$  is the water density  $= 1.940 \text{ slugs/ft}^3$ .



Inserting the values for the water density and adiabatic exponent, equation B7 becomes

$$\bar{T}_n = 29.7 \frac{\bar{A}_n}{\sqrt{p_n}} \text{ milliseconds} \quad (\text{B7a})$$

where  $\bar{A}_n$  is in inches and  $p_n$  is pounds per square inch.

Maximum and Minimum Radius, and Period of Oscillation.

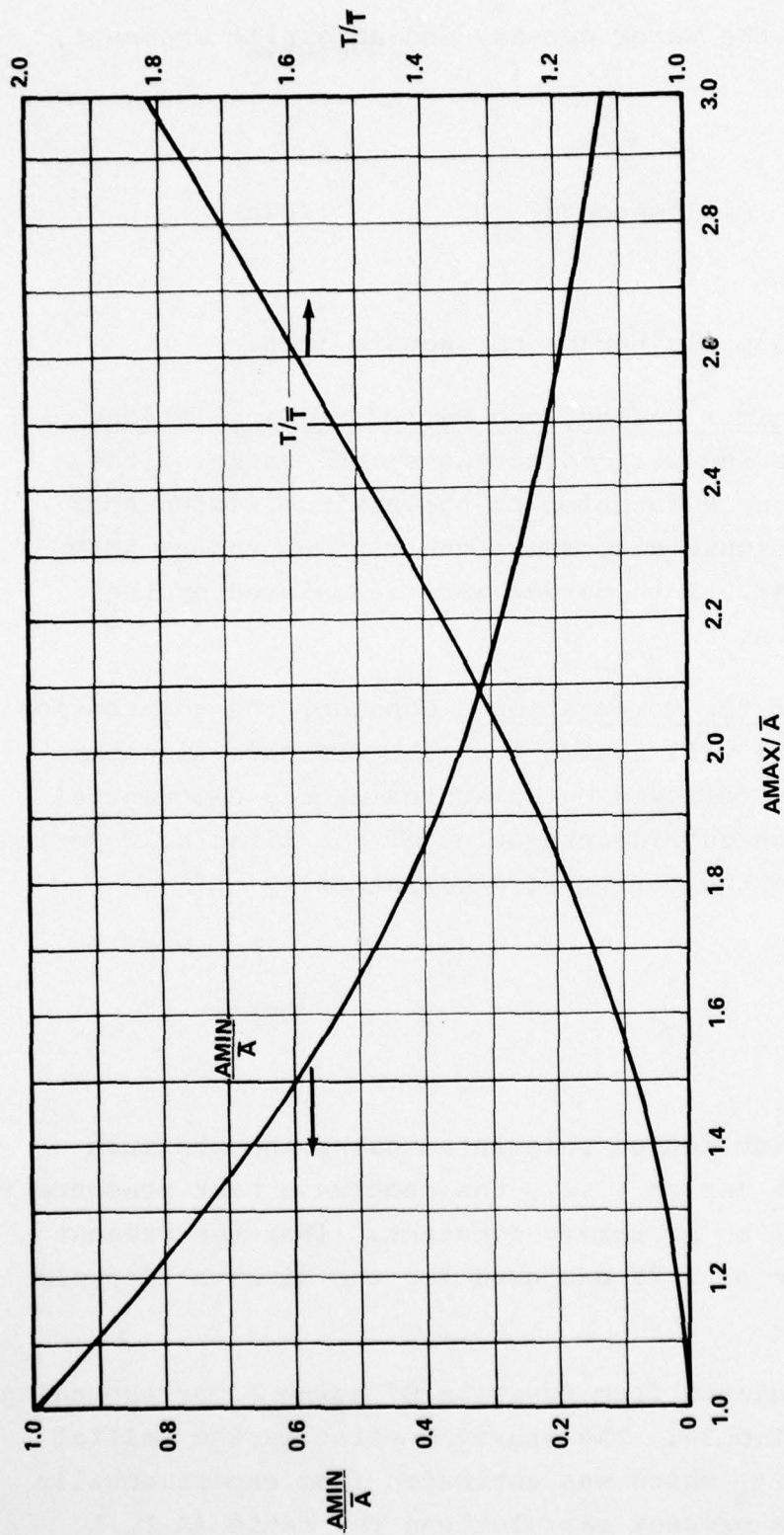
With increasing amplitude the period increases; the ratio of the periods,  $T/\bar{T}$ , is plotted as a function of the maximum radius AMAX in Figure B1. The same figure also shows the minimum radius AMIN plotted as a function AMAX. Both curves were calculated by the method given in Appendix A.

Some Details of the Computation. Consider the computation shown in Figure 2.3.2. We will assume that the pressure signature begins with a shock front followed by an approximately exponential decay. To get the average outside pressure for the first half-period of the motion we estimate the period of oscillation by

$$T = \alpha \times \bar{T}^* \quad (\text{B8})$$

where  $\bar{T}^*$  is the equilibrium period calculated using the pressure value at the start of the motion (i.e., the shockwave peak pressure + initial ambient) and  $\alpha$  is an arbitrary constant. (For the present computations an  $\alpha$ -value of 1.25 was used for the first half-cycle of oscillation.)

The parameter  $\bar{T}^*$  is calculated from Equation B7 using a corresponding  $\bar{A}^*$  calculated from Equation B6. The starting point is the initial bubble or bladder radius  $A_i$  which was estimated from experimentally measured values. For the present calculations the ratio  $(A_i)_0/L$



$\bar{A}$  = RADIUS WHEN AIR PRESSURE EQUALS HYDROSTATIC PRESSURE

$A_{MAX}$  = MAXIMUM RADIUS

$A_{MIN}$  = MINIMUM RADIUS

$T_o$  = PERIOD OF VERY SMALL OSCILLATIONS

$T$  = PERIOD OF OSCILLATION HAVING GIVEN VALUE OF  $A_{MAX}/\bar{A}$

FIG. B-1 CURVES REFERRING TO UNDAMPED OSCILLATIONS OF AN AIR BUBBLE IN WATER

(Equations 3.1.7 and 3.1.8) was then varied to obtain the best possible correlation between the calculated and experimentally observed injuries--Section 3.2 and 3.3.

Next, we read or calculate the outside pressure at the end of the first half-cycle of motion using the period estimate calculated by (B8); and then calculate  $p_1$ , the constant outside pressure for this approximate solution, as the average of the pressures at the beginning and end of the half-cycle. Using  $p_1$  we can then calculate the parameters for the first half-cycle of motion; and, in particular, obtain a considerably improved value for  $T$ . Using the improved value for  $T$  we then calculate from Equation B8 a better value for  $\alpha$  which we use to calculate the next half-cycle of motion.\*

Surface Cut-off. Upon arrival of the reflected wave from the water surface the outside water pressure suddenly drops to below the initial ambient level. This phenomenon is known as "surface cut-off". When cut-off occurred near an extremum--i.e., within 0.10 cycles of a maximum size, or within 0.08 cycles of a minimum--we calculated the final motion at the lowered outside pressure as starting from rest from the nearby extremum. Intermediate cases were calculated as starting from rest using an intermediate initial bubble size--based on the parameter  $(\Delta t/T)_{PC}$  which was calculated as follows:

$$\text{If } A_{c_{n-1}} + A_{MAX_n}, \text{ then } (\Delta t/T)_{PC} = (T_{POS} - t_{c_{n-1}})/T_n \quad (B9)$$

---

\*If necessary, we can use this improved value for  $T$  to get a better value of the average pressure  $p_1$ . So far this has not been necessary.



$$\text{If } A_{c_{n-1}} = \text{AMIN}_n, \text{ then } (\Delta t/T)_{PC} = (T_{POS} - t_{c_{n-1}})/T_n + 1/2 \quad (\text{B10})$$

The parameter  $(\Delta t/T)_{PC}$  locates positive phase cut-off in terms of bubble oscillation cycles. "Zero" is taken as the last expansion occurring during the positive phase. Using  $(\Delta t/T)_{PC}$ , the starting radius for the final oscillation at lowered pressure was then selected from the approximate values listed in Table B-1.

Phase Shift Correction. The effect of the negative pressure phase is often limited by its short duration relative to the bladder period of oscillation. Thus, it is also necessary to account for the phase shift which occurs upon surface cut-off. This was done by adding a time correction to the duration,  $\Delta t_{neg}$ , of the negative pressure phase. Using the parameter  $(\Delta t/T)_{PC}$  computed from Equation 11 or 12, this correction was approximated as follows:

$$\text{If } 0 \leq (\Delta t/T)_{PC} \leq 0.1, \text{ then Phase Corr} = 0 \quad (\text{B11})$$

$$\text{If } 0.1 \leq (\Delta t/T)_{PC} \leq 0.5, \text{ then Phase Corr} = -(t_{c_n} - T_{POS}) \quad (\text{B12})$$

$$\text{If } 0.5 \leq (\Delta t/T)_{PC} \leq 1.0, \text{ then Phase Corr} = T_{POS} - t_{c_{n-1}} \quad (\text{B13})$$

where  $t_{c_n}$  is the time at which  $\text{AMIN}_n$  would have occurred had not surface cut-off intervened. (Since this subsequent minimum depends

TABLE B-1

APPROXIMATE BOUNDARY CONDITION FOR USE WHEN PRESSURE JUMPS  
OCCUR BETWEEN EXTREMA

		START NEXT HALF-CYCLE WITH:
If $\left(\frac{\Delta t}{T}\right)_{PC}$	$\leq 0.10$	AMAX
	$< 0.25$	$(AMAX + \bar{A})/2$
	$\leq 0.32$	$\bar{A}$
	$< 0.42$	$(\bar{A} + AMIN)/2$
	$\leq 0.58$	AMIN
	$< 0.68$	$(AMIN + \bar{A})/2$
	$\leq 0.75$	$\bar{A}$
	$< 0.90$	$(\bar{A} + AMAX)/2$
	$\leq 1.00$	AMAX

primarily on the kinetic energy at cut-off and not on the outside pressure, this  $t_c$ -value calculated using the higher pressure should still be a good approximation to the time of occurrence of this minimum.)

Final Oscillation at Negative Pressure. In calculating the final bubble expansion achieved during the negative pressure phase we only consider those cases in which the final oscillation starts with a minimum radius--only they are of interest. In order to estimate this final expansion we calculate the parameter

$$(\Delta t/T)_{NP} = (DTNEG + \text{Phase Corr}) / T_{neg} + 1/2 \quad (B14)$$

where DTNEG is the duration of the negative phase--and again refer to Table B-1.

The parameter  $(\Delta t/T)_{NP}$  locates the end of the negative phase in terms of bubble oscillation cycles. "Zero" is taken as the last expansion occurring during the positive phase. If  $(\Delta t/T)_{NP} \leq 0.58$ , we conclude the negative phase is too short for any significant expansion to take place. Otherwise, we calculate the maximum size as indicated in the table. And, if  $(\Delta t/T)_{NP} \geq 0.90$ , the maximum bubble size is taken equal to AMAX. In any event, if  $(\Delta t/T)_{NP} < 0.90$ , we also calculate the final oscillation that would occur if surface cut-off had returned the outside pressure directly to ambient. If this results in a greater maximum expansion, we take this value as the maximum size achieved during final expansion.

Damping. Equation A1 describes undamped radial pulsation of an ideal frictionless fluid. While it seems unnecessary to make a detailed study of energy dissipation in the fishes' oscillating swim bladder, it does seem prudent to at least approximately account



AD-A075 809 NAVAL SURFACE WEAPONS CENTER WHITE OAK LAB SILVER SP--ETC F/G 19/4

DYNAMICAL MODEL FOR EXPLOSION INJURY TO FISH.(U)

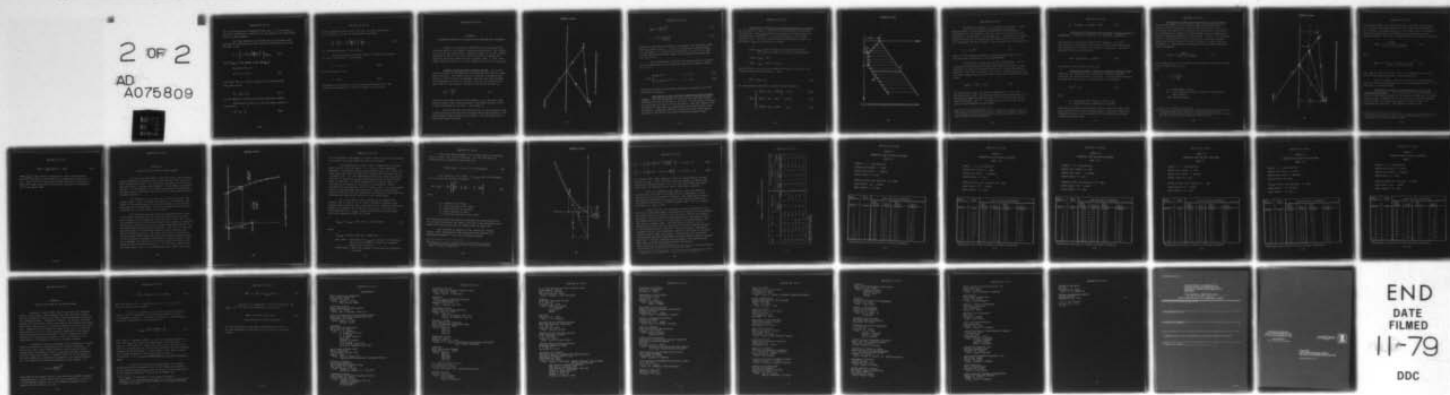
DEC 78 J F GOERTNER

UNCLASSIFIED NSWC/WOL/TR-76-155

NL

2 OF 2

AD  
A075809



for the fact that such dissipation must occur. In this study we did so by withdrawing a fraction  $\beta$  of the energy of the oscillatory motion at each extremum.

The total energy at an extremum can be calculated from Equation A1 by dropping the first term and substituting from (A2) and (B5) to get

$$Y_n = \left[ p_n + \frac{p_i}{\gamma-1} \left( \frac{(V_{Mm})_n}{V_i} \right)^{-\gamma} \right] (V_{Mm})_n \quad (B15)$$

where  $(V_{Mm})_n$  is the bubble volume,  $\frac{4}{3}\pi (A_{Mm})_n^3$

Rewriting (B5) as

$$p(V) = p_i (V/V_i)^{-\gamma} \quad (B16)$$

and noting that  $p_n = p(\bar{V}_n) = p_i (\bar{V}_n/V_i)^{-\gamma}$  and substituting into (B15) we get

$$\bar{Y}_n = \frac{\gamma}{\gamma-1} p_n \bar{V}_n \quad (B17)$$

for the energy of the non-oscillating equilibrium bubble.

Subtracting  $\bar{Y}_n$  from  $Y_n$  we get the bubble energy of oscillation,

$$Y'_n = Y_n - \bar{Y}_n \quad (B18)$$

Finally combining (B15), (B17) and (B18) and again noting that  $p_n = p_i (\bar{V}/V_i)^{-\gamma}$  we get the dimensionless equation,

$$\frac{Y'}{\bar{V}} = \left[ \frac{\gamma-1}{\gamma} + \frac{1}{\gamma} \left( \frac{V_{Mm}}{\bar{V}} \right)^{-\gamma} \right] \frac{V_{Mm}}{\bar{V}} - 1 \quad (B19)$$

for the bubble energy of oscillation.

At each extremum the bubble volume (or radius) was changed to yield a new energy of oscillation,

$$Y'' = (1 - \beta) Y' \quad (B20)$$

For this study we took

$$\beta = 0.30 \quad (B21)$$

Considering the precision of our present experimental data, the precise value chosen for  $\beta$  does not appear to be critical.



## APPENDIX C

## APPROXIMATE METHOD FOR CALCULATING THE PRESSURE-TIME SIGNATURE

Figure 3.1.1 shows the idealized form of pressure-time signature used for the bladder response computations of this report. For planning the 1975 series of explosion tests and for the examples presented in Section 4 of this report we needed to predict for arbitrary explosion geometries the variables, P<sub>MAX</sub>,  $\theta$ , T<sub>POS</sub>, P<sub>NEG</sub>, DT<sub>NEG</sub>, shown in Figure 3.1.1. This Appendix tells how this was done.

PRESSURE SIGNATURE BEFORE SURFACE CUT-OFF. The initial positive portion of the signature is the direct wave from the underwater explosion. The sudden negative excursion is caused by the arrival of the reflected rarefaction wave from the water surface. This phenomenon is known as "surface cut-off". We calculate the time, T<sub>POS</sub>, of this arrival relative to the direct arrival by

$$T_{POS} = \frac{R_1 - R}{c_o} \quad (C1)$$

where R is the slant range from the charge, R<sub>1</sub> is the slant range from the image of the charge mirrored in the water surface, and c<sub>o</sub> is the sound speed in the water. See Figure C1.

We calculate the free-field portion of the signature using a modification of the empirical Shockwave Similitude Equations. The peak pressure P<sub>MAX</sub> and the decay constant  $\theta$  are calculated by the usual similitude relations

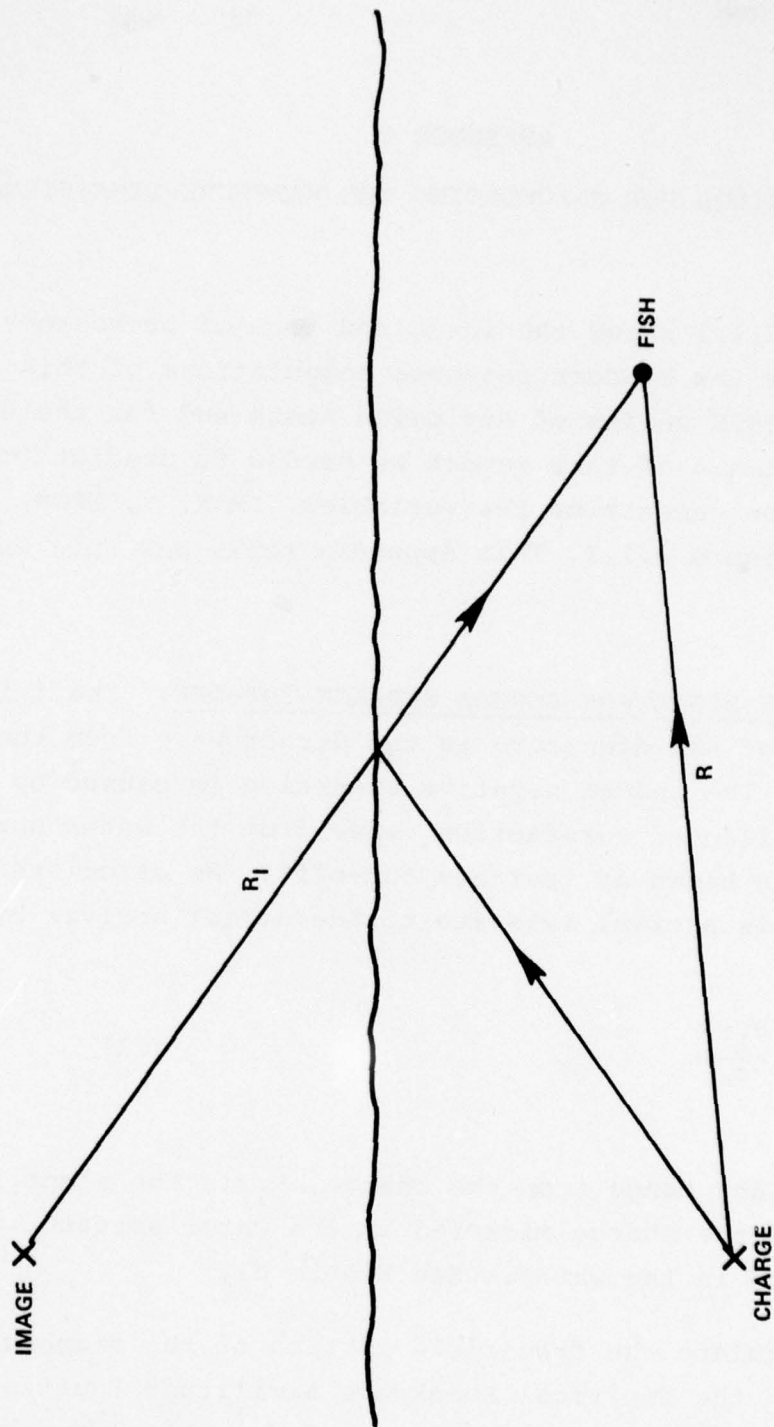


FIG. C-1 SKETCH SHOWING GEOMETRY OF SURFACE CUTOFF

$$P_{MAX} = k \left( \frac{W^{1/3}}{R} \right)^{\alpha} \quad (C2)$$

$$\theta = \ell W^{1/3} \left( \frac{R}{W^{1/3}} \right)^{\beta} \quad (C3)$$

where W is the explosive weight of the charge, R is the slant range from the charge, and k,  $\alpha$ ,  $\ell$ , and  $\beta$  are empirical constants (see, e.g., Reference 7). Values for the constants, k, and  $\ell$  and  $\beta$  used for the calculations of this report can be obtained from Equations 3.1.1 and 3.1.3.

The instantaneous free-field (or direct arrival) pressure,  $p_D$ , was calculated using two separate exponential segments joined at  $t = 1.8 \theta$

$$p_D(t) = \begin{cases} P_{MAX} e^{-t/\theta} & (t \leq 1.8 \theta) \\ 0.25 P_{MAX} e^{-t/4.3 \theta} & (t > 1.8 \theta) \end{cases} \quad (C4a)$$

$$(C4b)$$

which were fitted to the pressure signatures recorded on the 1973 explosion test series.

CALCULATION OF PNEG, NEGATIVE PRESSURE FOLLOWING SURFACE CUT-OFF. PNEG was determined by a calculation along the surface reflected ray from the charge to the fish. If the surface reflected ray went thru the region of bulk cavitation, PNEG was computed from the depths at which the ray intersected the top and bottom of the cavitation. Otherwise, PNEG was computed from the linear superposition of the direct and surface-reflected pressure waves.



Calculation of PNEG Above/Inside/Under Region of Cavitation.

Let the depths,  $y_t$  and  $y_c$ , locate the top and bottom of the region of cavitation. Let  $p_{ABS} = p_i + PNEG$  be the absolute pressure under the influence of cavitation, i.e., following arrival of the surface reflected wave. For fish located above/inside/under the region of cavitation,  $p_{ABS}$  is determined as follows:

Above:  $p_{ABS}$  changes linearly with depth from  $P_{ATM}$  at the surface to  $PVAP$  at the top of the cavitation.

Inside:  $p_{ABS} = PVAP$

Under:  $p_{ABS} = PVAP + \rho g(y - y_c)$

where  $PVAP$  and  $\rho$  are the vapor pressure and density of water, and  $g$  is the acceleration of gravity. Since

$$PNEG = p_{ABS} - p_i \quad (C5)$$

the corresponding equations for PNEG are (see Figure C2)

$$PNEG = \begin{cases} -[P_{ATM} + \rho g y_t - PVAP] \frac{y}{y_t} & 0 < y \leq y_t \end{cases} \quad (C6a)$$

$$PNEG = \begin{cases} -[P_{ATM} + \rho g y - PVAP] & y_t < y \leq y_c \end{cases} \quad (C6b)$$

$$PNEG = \begin{cases} -[P_{ATM} + \rho g y_c - PVAP] & y > y_c \end{cases} \quad (C6c)$$

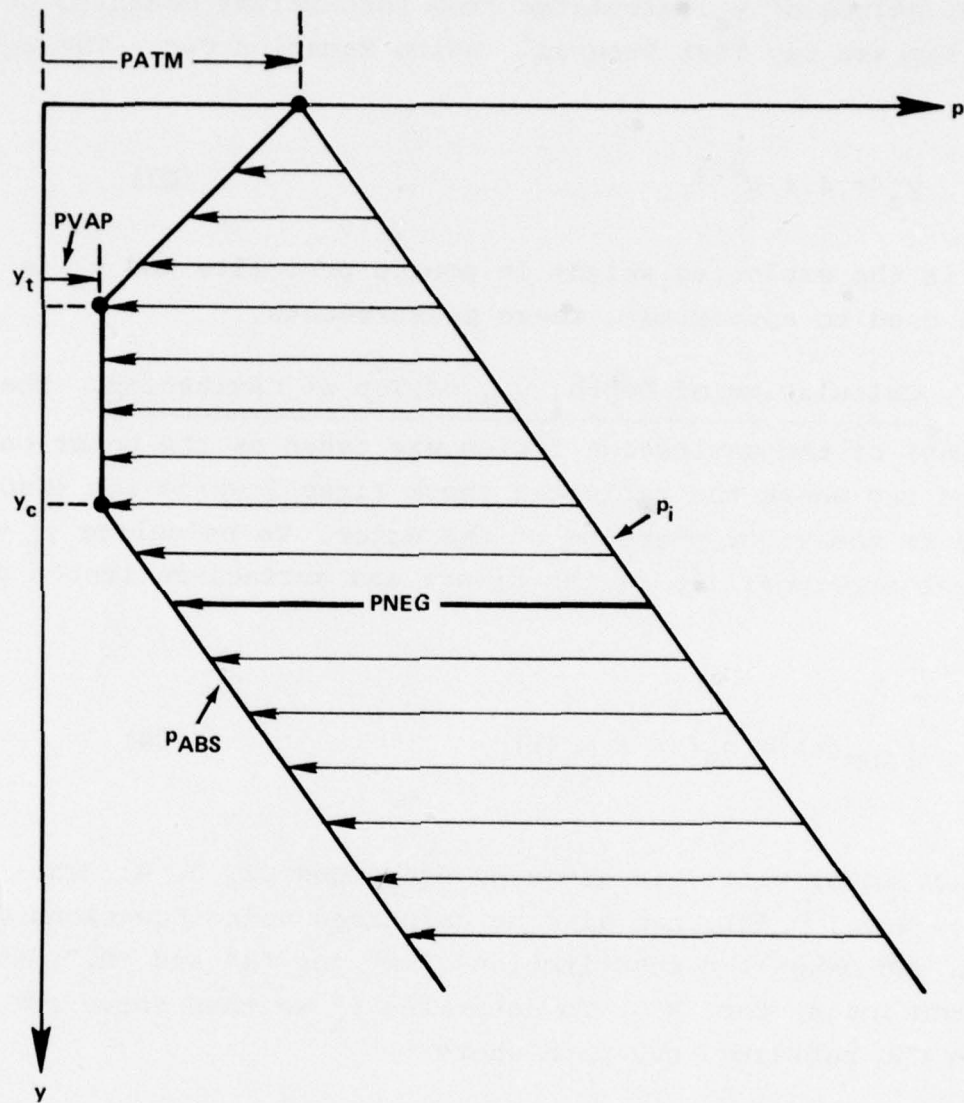


FIG. C-2 VARIATION OF PNEG ABOVE/INSIDE/UNDER REGION OF BULK CAVITATION

Calculation of Depth,  $y_c$ , of Bottom of Cavitation. Given

Equations C6a, b, c the problem of determining PNEG reduces to determination of the depths  $y_t$  and  $y_c$  of the top and bottom of the cavitation. To determine  $y_c$  we plotted, as a function of the charge weight  $W$ , values of  $y_c$  calculated from PNEG-values measured on the 1973 Chesapeake Bay Test Program<sup>1</sup> using Equation C6c. The equation.\*

$$y_c = 4.4 W^{0.3} \quad (C7)$$

where  $W$  is the explosive weight in pounds pentolite and  $y_c$  is in feet was used to approximate these measurements.

Calculation of Depth,  $y_t$ , of Top of Cavitation. The top

(beginning) of the cavitation region was taken as the point on the reflected ray where the reflected shock first lowered the absolute pressure to the vapor pressure of the water. To calculate  $y_t$  we use the linear superposition of the direct and surface-reflected pressure waves,

$$p_{SUM}(t) = p_D(t) + p_R(t) \quad (C8)$$

The direct wave,  $p_D(t)$ , is given by equations C2, 3, 4. The reflected wave,  $p_R(t)$ , can also be calculated using Equations C2, 3, 4 provided one makes the substitutions "-k" for "k" and " $R_1$ " (slant range from image) for "R". To determine  $y_t$  we then solve for the point on the reflected ray path where

---

\*Equation C7 gives a crude empirical fit to the PNEG-values measured on the 1973 test program. It was used out of necessity to make kill probability calculations used to design the 1975 test program but has not been re-evaluated using those and other available PNEG-measurements.



$$p_i + p_D(\text{TPOS}) + p_R(\text{TPOS}) = \text{PVAP} \quad (\text{C9})$$

Calculation of PNEG when Reflected Ray is Beyond Region of Cavitation. If the total pressure,  $p_i + p_D(\text{TPOS}) + p_R(\text{TPOS})$ ,

upon arrival of the surface reflection at depth,  $y_c = 4.4 W^{0.3}$  (Equation C7), was greater than or equal to PVAP, the reflected ray was considered to lie beyond the region of cavitation. When this happened PNEG was approximated by

$$\text{PNEG} = \frac{1}{2}[p_D(\text{TPOS}) + p_R(\text{TPOS})] \quad (\text{C10})$$

calculated at the location of the fish.

CALCULATION OF DTNEG, DURATION OF NEGATIVE PRESSURE, PNEG.

DTNEG was also determined by a calculation along the surface-reflected ray from the charge to the fish. If the surface-reflected ray went thru the region of cavitation and the condition,

$$R/W^{1/3} \leq 80 \quad (\text{C11})$$

where

R = slant range from charge to fish in feet

W = explosive weight (pentolite) in pounds

was true, then DTNEG was calculated from the time-of-flight of the water layer on top of the cavitating region. Otherwise, DTNEG was computed from the linear superposition of the direct and surface-reflected pressure waves.

Calculation of DTNEG from Time-of-Flight of Water Layer.

The duration, DTNEG, of the negative phase corresponds to the duration of bulk cavitation in the neighborhood of the fish. For this study the duration of cavitation was calculated at the point on the reflected ray at depth  $y_c$  (closure depth) given by Equation C7. Figure C3 shows the geometry of the problem. To get a first approximation to the duration of bulk cavitation at this point we used Walker and Gordon's result for time of flight of a water layer of thickness,  $y_c$ , decelerating (falling back) due to gravity and atmospheric pressure<sup>11</sup>

$$TFLIGHT = \frac{2 \cdot PMAX_c \cdot \theta_c}{\rho g (y_c + k) + PATM} \quad (C12)$$

where  $PMAX_c$  and  $\theta_c$  are the shockwave peak pressure and decay constant at the closure point  $(x_c, y_c)$ ,  
and

$$k = \frac{c_o \theta_c R_z}{2 \cdot DOB}$$

and

$c_o$  = sound speed in water

$R_z$  = slant range from charge to point of reflection at  
water surface

DOB = depth of burst.

<sup>11/</sup> Walker, R. R., and J. D. Gordon, 1966, "A Study of the Bulk Cavitation Caused by Underwater Explosions", David Taylor Model Basin Report 1896, pl8, Equation 5. Note, however, that we used an empirical equation (C7) to calculate the closure depth rather than Walker and Gordon's result.

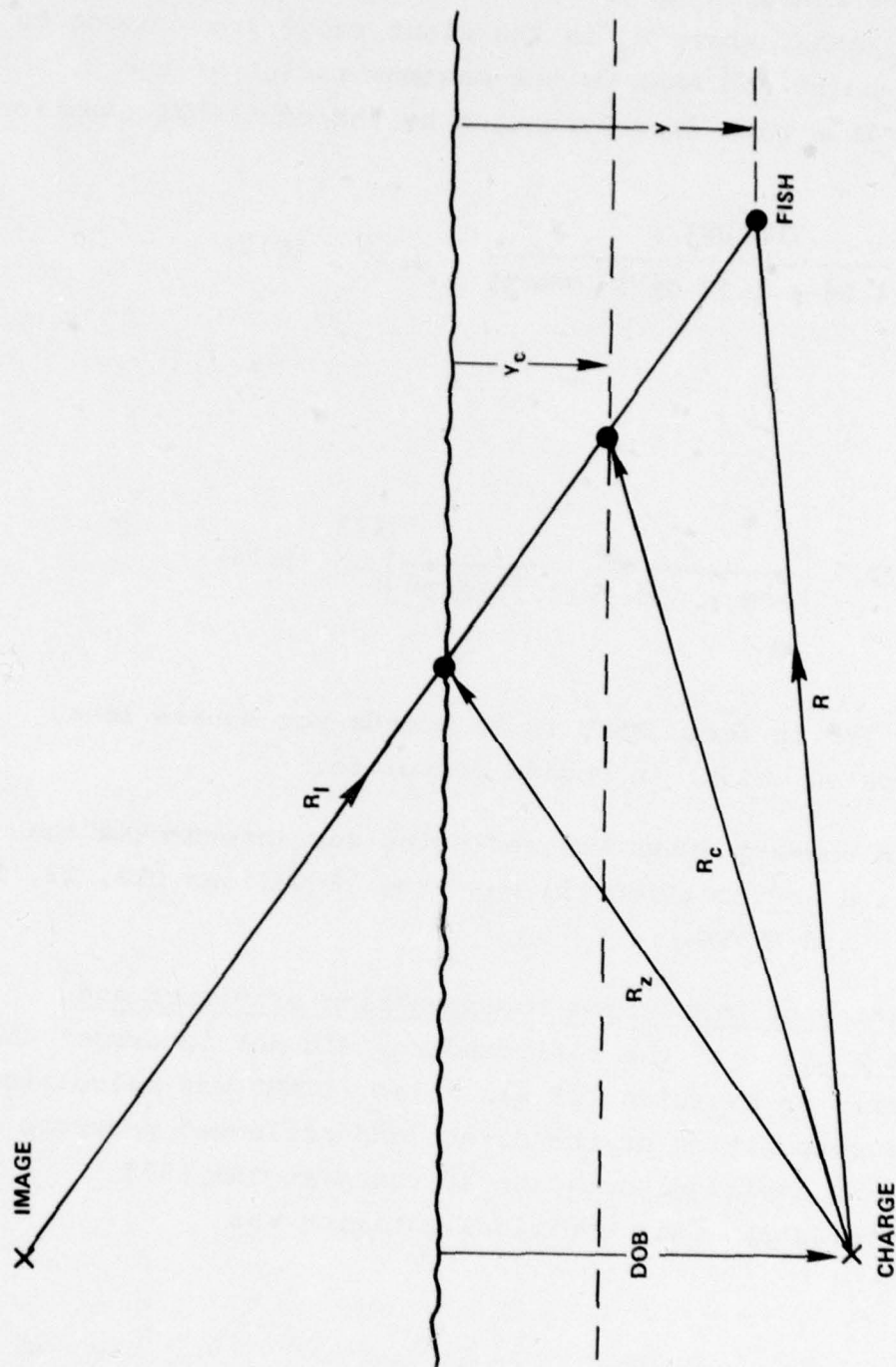


FIG. C-3 SKETCH SHOWING GEOMETRY OF CAVITATION CALCULATIONS



To determine DTNEG, we plotted the ratio of TFLIGHT (calculated by C12) to DTNEG-values measured on the 1973 Chesapeake Bay Program<sup>1</sup>, as a function of  $R_c/AMAX$ , where  $R_c$  is the slant range from charge to cavitation closure point and AMAX is the maximum radius of the explosion bubble. This plot is represented by the empirical equation\*

$$DTNEG = \frac{TFLIGHT}{4.04 - 1.13 \ln(R_c/AMAX)} \quad (C13)$$

where

$$AMAX = 12.7 \left[ \frac{W}{DOB + (33.9/14.7) \cdot PATM} \right]^{1/3} \quad (C14)$$

and, AMAX and DOB are in feet, PATM is in pounds per square inch, and W is the explosive weight in pounds pentolite.

Thus, in summary, when the reflected ray intersected the region of cavitation and Equation C11 was true, Equations C12, 13, 14 were used to calculate DTNEG.

Calculation of DTNEG from Superposition of Direct and Surface-Reflected Waves. If the reflected ray did not intersect the region of cavitation or Equation C11 was false, DTNEG was calculated from the linear superposition of the direct and reflected pressure waves by means of an empirical equation adjusted to the 1973 Chesapeake Bay Test data. This empirical equation was

---

\*This empirical fit was used to make the kill probability calculations for designing the 1975 test program. It has not been re-evaluated using the 1975 test program and other available DTNEG-measurements.

$$DTNEG = p_{SUM}^{-1}(PNEG/10) - TPOS \quad (C15)$$

where  $p_{SUM}^{-1}$  is the inverse of Equation C8, TPOS is the positive duration, and PNEG is calculated by the appropriate equation, C6 or C10. Thus, the end of the negative phase was taken as the point where the negative pressure calculated by Equation C8 returned to 10% of the value, PNEG.

## APPENDIX D

## LOCATION OF FISH CAGES BY SOUND RANGING

On four of the six shots of the 1975 tests, water currents caused significant deviation of the charge and the fish cages from their intended positions. The charge was suspended on one line and the cages--with a pressure gage attached to each--were suspended on another. In this appendix, we consider the problem of determining the deviations of the charge and the string of fish cages from their intended locations.

The separation,  $x_0$ , of the two lines at the surface was assumed known. Figure D1 shows the geometry of the problem. The length of the charge support line and the lengths of line between gages were also assumed known. We further assumed that the charge and gages lie in the same vertical plane.

We solved this problem using the measured arrival times of the direct shockwave and its reflected tension wave from the water surface at the respective gage locations. Step 1 was to use the relative arrivals of the direct shock to determine an orientation for the gage line giving a set of constant differences between the calculated arrivals and the measured ones. Step 2 was to use these gage positions to calculate the surface cut-off time--the time interval between arrival of the direct shock and its reflection--and to compare these values with the corresponding measured values. If there existed a systematic discrepancy in surface cut-off times not accountable to variations in the sound speed over the two ray paths, we then adjusted the angle,  $\theta_c$ , of the charge support line and redid steps 1 and 2. The calculations were redone until there



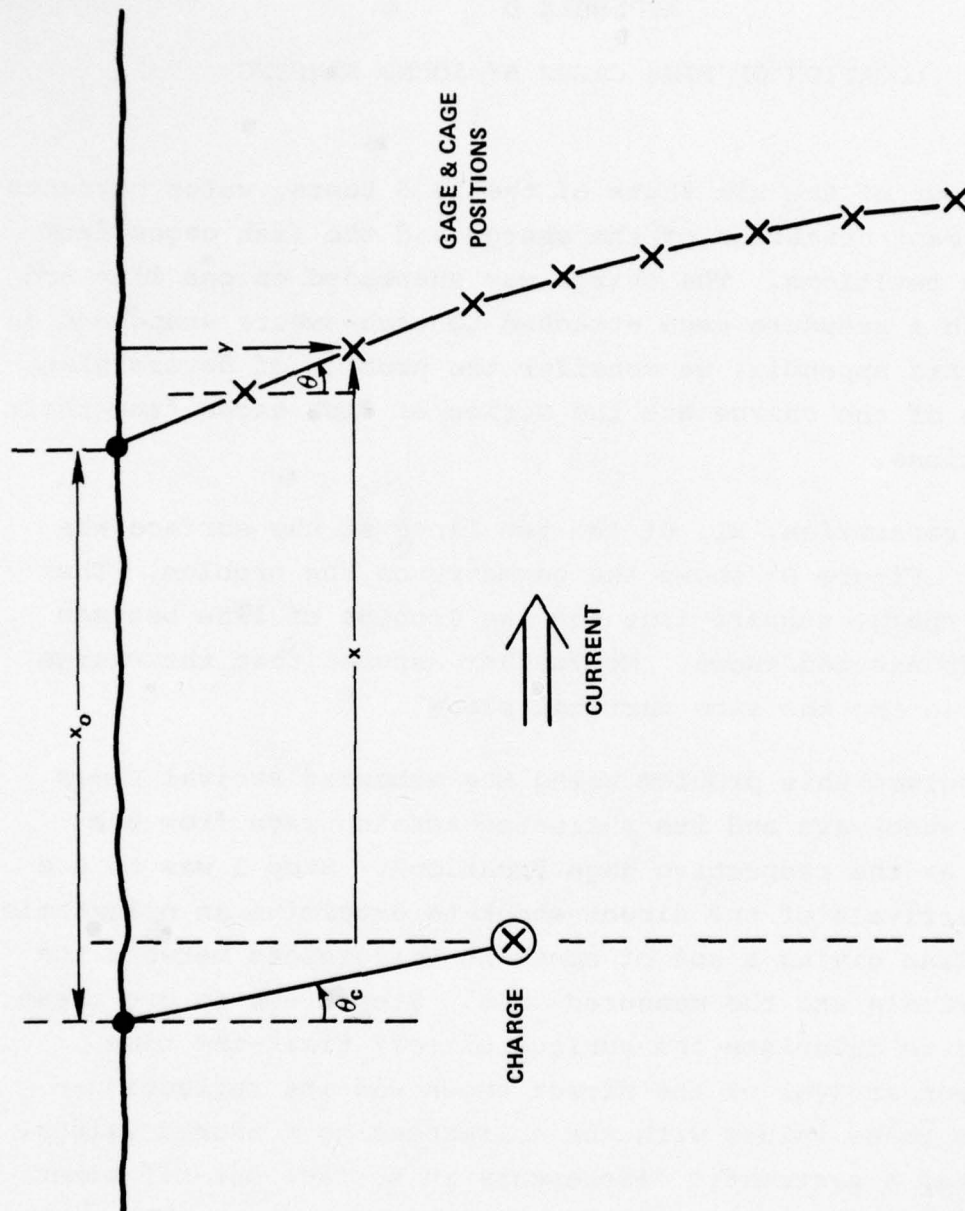


FIG. D-1 GEOMETRY FOR SOUND RANGING CALCULATIONS

was no systematic discrepancy in surface shut-off time not accountable to variation in sound speed over the two ray paths.

The computations of steps 1 and 2 assumed that the sound speed did not vary with depth. R. S. Price of this center has developed a high-speed computer program which takes into account the sound speed variation with depth--but assumes that the gages are in a straight line. For the computations done here, these two effects--curvature of the gage line and sound speed variation--are the same order of magnitude. In these computations, errors of about 0.4 milliseconds are caused by variations in sound speed. These correspond to gage position errors of about 2 feet. For our purposes errors of this magnitude were acceptable, however, significantly improved precision could be obtained by accounting for both gage line curvature and sound speed variation in the calculations.

As a final check on the computations we compared the absolute time of arrival of the direct shockwave measured on the pressure gage records to that calculated for the shockwave travelling between our computed charge and gage locations. To do this we calculated the time,  $\Delta t_{\text{meas}}$ , between the electrical firing pulse and direct shockwave arrival as follows

$$\Delta t_{\text{meas}} = \Delta t_{\text{sound}} + \text{VEL. CORR.} + \text{FIRING DELAY} \quad (\text{D1})$$

where

$\Delta t_{\text{sound}}$  = transit time for a sound wave

VEL. CORR. = correction to  $\Delta t_{\text{sound}}$  to account for detonation wave velocity inside the charge and shockwave velocity in the water

FIRING DELAY = dwell time between firing pulse and initiation of charge

The firing delay depends on the firing circuit, length and type of firing line, and the detonator. For the 1975 tests we estimated from a comparable test setup that

$$\text{FIRING DELAY} = +0.31 \pm 0.05 \text{ milliseconds} \quad (\text{D2})$$

The correction, VEL. CORR., to  $\Delta t_{\text{sound}}$  must be calculated. It is given by the following equation

$$\text{VEL. CORR.} = - \frac{R_o}{c_o} \left[ \int_1^{R/R_o} \left( \frac{U}{c_o} - 1 \right) d \frac{R}{R_o} + \left( 1 - \frac{c_o}{D} \right) \right] \quad (\text{D3})$$

where

$R_o$  = radius of the charge

$c_o$  = sound velocity in the water

$U$  = shock velocity in the water

$R$  = radial distance to gage

$D$  = detonation velocity in the charge

The first term inside the brackets represents the contribution due to the water shock while the second, that due to the detonation wave. Equation D3 was derived from the sketch shown in Figure D-2.

The integrand in Equation D3 was obtained by fitting results from a hydrodynamic code calculation for pentolite by Sternberg and Walker<sup>12</sup> with the following equations

---

<sup>12/</sup> Sternberg, H. M., and W. A. Walker, 1971, "Calculated Flow and Energy Distribution Following Underwater Detonation of a Pentolite Sphere", Physics of Fluids, September 1971



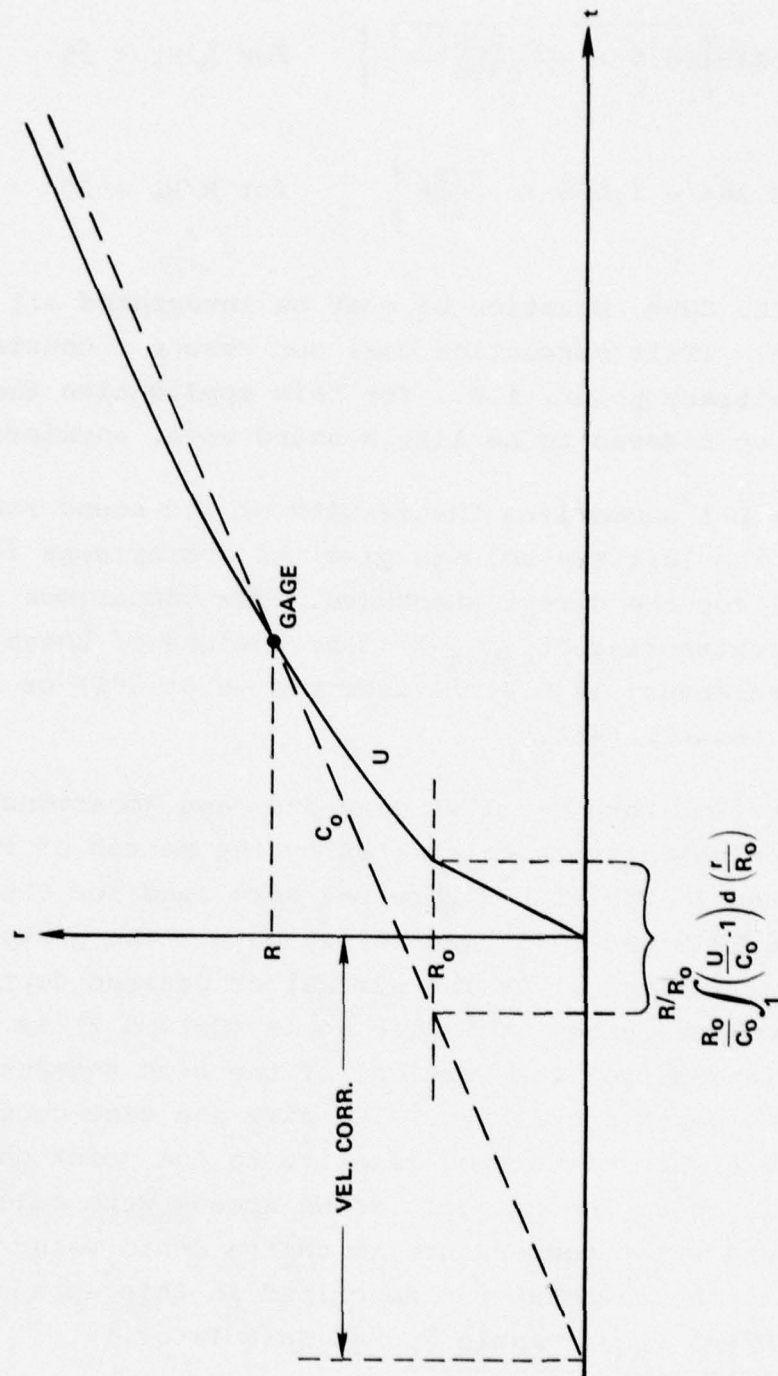


FIG. D-2 DETONATION AND SHOCKWAVE VELOCITY CORRECTIONS TO ARRIVAL TIME

$$\frac{U}{c_0} - 1 = \text{EXP} \left\{ 8.84 - \sqrt{60.9 + \frac{\ln R/R_0}{.0376}} \right\} \quad \text{for } R/R_0 \leq 25 \quad (\text{D4a})$$

$$\frac{U}{c_0} - 1 = \text{EXP} \left\{ -3.264 - 1.098 \ln \frac{R/R_0}{25} \right\} \quad \text{for } R/R_0 > 25^* \quad (\text{D4b})$$

To calculate VEL. CORR. Equation D3 must be integrated all the way out to the gage. (This correction does not assume a constant value beyond some arbitrary point, i.e., for this application the shock-wave cannot be considered to be like a sound wave, anywhere.)

Table D-1 summarizes the results of the sound ranging computations. The last two columns give the comparisons for the time of arrival for the direct shockwave. The comparison is easily understood by subtracting  $\Delta t_{\text{sound}}$  from both sides of Equation D1. The maximum discrepancy is 0.4 milliseconds (Shot 786) or a spatial discrepancy of about 2 feet.

Tables D-2 thru D-7 list cage and gage locations for the 1975 test series which were calculated by the method of this appendix. The values listed in Tables D-2 thru D-7 were used for the present analysis of the 1973 and 1975 test series data. The distance along the support wire (Column 1) is the nominal or desired depth of the fish cage or pressure gage. The wire angle (Column 2) is the calculated deviation from the vertical of the wire segment attached to the preceding depth coordinate. The cage and gage coordinates (Columns 3 thru 6) are calculated relative to the point on the water surface directly above the charge. Sound speeds were calculated from salinity and water temperature at charge depth using Del Grosso's equation.<sup>13</sup> (All the computations described in this appendix were done using an HP-65 Programmable Pocket Calculator.)

\*This straight line log-log extrapolation beyond the range of Sternberg and Walker's calculation should be adequate out to at least  $R/R_0 = 1000$ .

13. Del Grosso, V. A., "New Equation for the Speed of Sound in Natural Waters (with Comparisons to Other Equations)", J. Acoust. Soc. Am., October 1974

TABLE D-1  
SUMMARY OF SOUND RANGING COMPUTATIONS

SHOT	W (LBS)	DOB (FT)	Xo (FT)	WIRE ANGLE		SHOCK VELOCITY & FIRING DELAY CORRECTIONS			
				CHARGE SUPPORT (DEG)	CAGES* (DEG)	VELOCITY CORR. (MSEC)	FIRING DELAY (MSEC)	TOTAL (MSEC)	$\Delta t_{MEAS}$ - $\Delta t_{SOUND}$ (MSEC)
782	70.4	30	300	0°	0°	-.95	.31	-.64	-----**
783	70.2	30	200	0°	-10.5°	-.91	.31	-.60	-.97
784	71.6	30	300	0°	+11°	-.95	.31	-.64	-.66
785	1.25	29.9	40	-5°	-11°	-.23	.31	.08	-.27
786	1.26	29.5	40	-10°	-30°	-.23	.31	.08	-.35
787	72.2	10	300	0°	0°	-.95	.31	-.64	-.58

\* ANGLE NEAR WATER SURFACE

\*\* FIRING PULSE NOT RECORDED



TABLE D-2

## CORRECTED CAGE AND GAGE LOCATIONS

SHOT 782

Charge: 70.4 lbs pentolite

Charge wire length: 30 feet

Charge wire angle: 0 degrees

Charge depth: 30 feet

Charge-to-gage line distance: 300 feet

Sound speed: 4850 ft/sec

Water depth\*: 156 feet

WIRE DISTANCE	WIRE ANGLE	CAGE AND GAGE COORDINATES			
		HOR. RANGE	DEPTH	HOR. RANGE	DEPTH
(FEET)	(DEG.)	(FEET)	(FEET)	(METERS)	(METERS)
0	---	300	0.0	91.4	0.0
5	0	300	5.0	91.4	1.5
10	0	300	10.0	91.4	3.0
15	0	300	15.0	91.4	4.6
40	0	300	40.0	91.4	12.2
45	0	300	45.0	91.4	13.7
50	0	300	50.0	91.4	15.2
55	0	300	55.0	91.4	16.8
57.5	0	300	57.5	91.4	17.5
77.5	0	300	77.5	91.4	23.6
87.5	0	300	87.5	91.4	26.7
97.5	0	300	97.5	91.4	29.7

\*Calculated from times of arrival of bottom reflection.

TABLE D-3

## CORRECTED CAGE AND GAGE LOCATIONS

SHOT 783

Charge: 70.2 lbs pentolite

Charge wire length: 30 feet

Charge wire angle: 0 degrees

Charge depth: 30 feet

Charge-to-gage line distance: 200 feet

Sound speed: 4857 ft/sec

Water depth\*: 152 feet

WIRE DISTANCE	WIRE ANGLE	CAGE AND GAGE COORDINATES			
		HOR. RANGE	DEPTH	HOR. RANGE	DEPTH
(FEET)	(DEG.)	(FEET)	(FEET)	(METERS)	(METERS)
0	---	200.0	0.0	61.0	0.0
5	-10.5	199.1	4.9	60.7	1.5
10	-10.5	198.2	9.8	60.4	3.0
15	-10.5	197.3	14.7	60.1	4.5
40	-10.5	192.7	39.3	58.7	12.0
45	-10.5	191.8	44.2	58.5	13.5
50	-10.5	190.9	49.2	58.2	15.0
55	-10.5	190.0	54.1	57.9	16.5
60	-10.5	189.1	59.0	57.6	18.0
80	-10.5	185.4	78.7	56.5	24.0
90	- 8	184.0	88.6	56.1	27.0
100	- 5	183.2	98.5	55.8	30.0

\*Calculated from times of arrival of bottom reflection.

TABLE D-4

## CORRECTED CAGE AND GAGE LOCATIONS

SHOT 784

Charge: 71.6 lbs pentolite

Charge wire length: 30 feet

Charge wire angle: 0 degrees

Charge depth: 30 feet

Charge-to-gage line distance: 300 feet

Sound speed: 4866 ft/sec

Water depth\*: 135 feet

WIRE DISTANCE	WIRE ANGLE	CAGE AND GAGE COORDINATES			
		HOR. RANGE	DEPTH	HOR. RANGE	DEPTH
(FEET)	(DEG.)	(FEET)	(FEET)	(METERS)	(METERS)
0	---	300.0	0.0	91.4	0.0
5	11	301.0	4.9	91.7	1.5
10	11	301.9	9.8	92.0	3.0
20	10	303.6	19.7	92.5	6.0
30	10	305.4	29.5	93.1	9.0
40	9	306.9	39.4	93.5	12.0
45	8	307.6	44.3	93.8	13.5
50	6	308.2	49.3	93.9	15.0
55	4	308.5	54.3	94.0	16.6
60	3	308.8	59.3	94.1	18.1
80	2	309.5	79.3	94.3	24.2
90	1	309.6	89.3	94.4	27.2
100	1	309.8	99.3	94.4	30.3

\*Calculated from times of arrival of bottom reflection.



TABLE D-5

## CORRECTED CAGE AND GAGE LOCATIONS

SHOT 785

Charge: 1.25 lbs pentolite

Charge wire length: 30 feet

Charge wire angle: -5 degrees

Charge depth: 29.9 feet

Charge-to-gage line distance: 40 feet

Sound speed: 4864 ft/sec

Water depth\*: 160 feet

WIRE DISTANCE	WIRE ANGLE	CAGE AND GAGE COORDINATES			
		HOR. RANGE	DEPTH	HOR. RANGE	DEPTH
(FEET)	(DEG.)	(FEET)	(FEET)	(METERS)	(METERS)
0	---	42.6	0.0	13.0	0.0
5	-11	41.7	4.9	12.7	1.5
10	-11	40.7	9.8	12.4	3.0
20	-11	39.3	19.7	12.0	6.0
30	- 7	38.1	29.6	11.6	9.0
40	- 7	37.1	39.6	11.3	12.1
50	- 5	36.0	49.5	11.0	15.1
60	- 4	35.0	59.5	10.7	18.1
70	- 2	33.9	69.4	10.3	21.2
80	+ 2	34.1	79.4	10.4	24.2
90	+ 5	34.4	89.4	10.5	27.2
100	+ 5	35.1	99.4	10.7	30.3

\*Calculated from times of arrival of bottom reflection.

TABLE D-6

## CORRECTED CAGE AND GAGE LOCATIONS

SHOT 786

Charge: 1.26 lbs pentolite

Charge wire length: 30 feet

Charge wire angle: -10 degrees

Charge depth: 29.5 feet

Charge-to-gage line distance: 40 feet

Sound speed: 4886 ft/sec

Water depth\*: 115 feet

WIRE DISTANCE	WIRE ANGLE	CAGE AND GAGE COORDINATES			
		HOR. RANGE	DEPTH	HOR. RANGE	DEPTH
(FEET)	(DEG.)	(FEET)	(FEET)	(METERS)	(METERS)
0	---	45.2	0.0	13.8	0.0
5	-30	42.7	4.3	13.0	1.3
10	-30	40.2	8.7	12.3	2.7
20	-24	36.1	17.8	11.0	5.4
30	-19	32.9	27.3	10.0	8.3
40	-15	30.3	36.9	9.2	11.2
50	-12	28.2	46.7	8.6	14.2
55	-10	27.4	51.6	8.4	15.7
60	-10	26.5	56.5	8.1	17.2
65	- 8	25.8	61.5	7.9	18.7
70	- 6	25.3	66.5	7.7	20.3
75	- 4	24.9	71.5	7.6	21.8
80	- 2	24.7	76.4	7.5	23.3

\*Calculated from times of arrival of bottom reflection.

TABLE D -7

## CORRECTED CAGE AND GAGE LOCATIONS

SHOT 787

Charge: 72.2 lbs pentolite

Charge wire length: 10 feet

Charge wire angle: 0 degrees

Charge depth: 10 feet

Charge-to-gage line distance: 300 feet

Sound speed: 4922 ft/sec

Water depth\*: 148 feet

WIRE DISTANCE	WIRE ANGLE	CAGE AND GAGE COORDINATES			
		HOR. RANGE	DEPTH	HOR. RANGE	DEPTH
(FEET)	(DEG.)	(FEET)	(FEET)	(METERS)	(METERS)
0	---	300	0	91.4	0.0
5	0	300	5	91.4	1.5
10	0	300	10	91.4	3.0
40	0	300	40	91.4	12.2
50	0	300	50	91.4	15.2
55	0	300	55	91.4	16.8
60	0	300	60	91.4	18.3
70	0	300	70	91.4	21.3
80	0	300	80	91.4	24.4
90	0	300	90	91.4	27.4
100	0	300	100	91.4	30.5

\*Calculated from times of arrival of bottom reflection.



## APPENDIX E

## NOTE ON FISH CLOSE TO THE WATER SURFACE

According to the bladder oscillation model for explosion injury, as the fishes' depth tends to zero near the water surface the kill probability should also tend to zero regardless of how high the incident pressure. Eventually, however, for fish at the water surface and sufficiently close to the charge, the bladder oscillation model must break down and a different mechanism for injury must take over. Apparently, this happens so close to the charge, and to the water surface, to be of little practical importance, since results reported by the Lovelace Foundation<sup>4</sup> show no evidence of such a transition for 149 gm Carp (length  $\cong$  21 cm) at a depth of 5 cm subjected to 5.58 megapascals (810 psi) incident pressure.

A possible close-in non-bladder injury mechanism is tissue damage due directly to compression by the incident shockwave. If this is the case, tissue damage probably also occurs due to the pressure wave (generally an order of magnitude greater) emitted by the oscillating swim bladder. Assuming that this is the meaning of the ratio,  $AMIN/A_i$ , in the damage parameter  $Z$ , we rewrite Equation 3.1.3 in terms of the adiabatic compression ratio,  $PMIN/p_o$ , as

$$X = -100 \ln \left( \frac{PMIN}{P_i} \right)^{-\frac{1}{3\gamma}} \quad (E1)$$

where  $PMIN$  is the maximum value of the oscillating bladder pressure (corresponding to radius  $AMIN$  at the first compression),  $p_i$  is the initial ambient pressure, and  $\gamma$ , the adiabatic exponent for air. Using E1 we then rewrite 3.1.5 as

$$Z = \frac{100}{3\gamma} \ln P_{MIN}/p_i + 100 \ln A_{MAX}/A_i \quad (E2)$$

Note that Equation E2 is equivalent to 3.1.5. It is just our point of view that has changed.

Now let us suppose, for fish very close to the water surface, that the shockwave peak overpressure  $P_{MAX}$  is the only tissue damaging pressure. The damage parameter by this mechanism equivalent to Equation E2 is then given by

$$Z_{P_{MAX}} = \frac{100}{3\gamma} \ln \left[ \frac{P_{MAX}}{p_i} + 1 \right] \quad (E3)$$

where  $P_{MIN}$  is replaced by  $P_{MAX} + p_i$  and the second term drops out. Note that  $Z_{P_{MAX}}$  must always be smaller than  $Z$  calculated by Equation 3.1.5 except for those cases--the ones of interest here--where the pressure wave is of such short duration that the transient response of the swimbladder is suppressed\*. Thus, when in doubt which damage parameter to use-- $Z_{P_{MAX}}$  (Equation E3) or  $Z$  (Equation 3.1.5)--calculate both parameters, and use the greater value.

Finally, we estimate the overpressure level,  $P_{MAX}$ , associated with the assumption that all the damage corresponding to the damage parameter  $Z_{P_{MAX}}$  is due directly to tissue compression by the incident shockwave. Solving E3 for  $P_{MAX}$  we get

\* Since  $Z_{P_{MAX}}$  is equivalent to the damage parameter  $X$  (Equation 3.1.3) calculated from the non-oscillatory steady-state response of an infinitely small bubble to an overpressure  $P_{MAX}$  of finite rise time.

$$P_{MAX} = p_i \text{ EXP } [ (3\gamma Z_{P_{MAX}}/100) - 1 ] \quad (E4)$$

Setting  $p_i = 1$  atmosphere ( $1.014 \times 10^5$  pascals) and  $Z_{P_{MAX}} = 125$  (50% kill value--Equation 3.2.1) we get

$$P_{MAX} = 19.2 \text{ MPa } (=2790 \text{ psi}) \quad (E5)$$

(approximately 24 charge diameters)

for the overpressure level  $P_{MAX}$  corresponding to 50% kill by this mechanism to fish which are very close to the water surface.



DISTRIBUTION

Naval Biosciences Laboratory  
Naval Supply Center Oak  
Oakland, CA 94625  
Attn: Louis H. DiSalvo  
LTJG John F. Wyman

Commanding Officer  
Naval Underwater Systems Center  
Newport, RI 02840  
Attn: Roy R. Manstan, Code EA 11

Naval Ship Research and Development Center  
Underwater Explosions Research Division  
Portsmouth, VA 23709  
Attn: LCDR R. H. Burt  
Richard Oliver

Commander  
Naval Ocean Systems Center  
San Diego, CA 92152  
Attn: G. B. Anderson  
S. Yamamoto, Code 406  
D. A. Wilson  
F. G. Wood, Code 40  
Code 6565  
Michael H. Salazar  
Jack W. Hoyt  
J. D. Warner, Code 2531  
William C. Cummings, Code 4013

Naval Ocean Systems Center  
Hawaii Laboratory  
P.O. Box 997, Kailua, Oahu  
Hawaii, 96734  
Attn: Evan C. Evans, III  
Head Marine Environmental Management Office

Officer in Charge  
New London Laboratory  
Naval Underwater Systems Center  
New London, CT 06320  
Attn: Albert B. Brooks  
Charles L. Brown, Jr., Code TA13

Commanding Officer  
Naval Explosive Ordnance Disposal Facility  
Indian Head, MD 20640  
Attn: Library Division  
Lionel A. Dickinson, Code 5D  
Richard Burdette  
Lyle Malotky

Commanding Officer  
Naval Explosive Ordnance Disposal School  
Indian Head, MD 20640  
Attn: LCDR E. W. McConnell

Commander  
David W. Taylor Naval Ship Research  
and Development Center  
Bethesda, MD 20034  
Attn: Library, Code 5641

Commanding Officer  
Naval Coastal Systems Laboratory  
Panama City, FL 32401  
Attn: Code 350  
John A. Brasewell, Code 773  
Everett L. Richards, Code 721

Officer in Charge  
Civil Engineering Laboratory  
Naval Construction Battalion Center  
Port Hueneme, CA 93043  
Attn: Code L70  
Code L71  
Code L43  
Code L65

Commanding Officer  
Naval Air Station  
Patuxent River, MD 20670  
Attn: A. L. Clark, Environmental Protection Coordinator  
Public Works Department

Commander  
Naval Sea Systems Command  
Washington, D. C. 20362  
Attn: SEA-033  
SEA-0332  
SEA-332B  
SEA-09G32  
SEA-03B

2

U. S. Army Engineer District  
100 McAllister Street  
San Francisco, CA 94102  
Attn: Tom Crews, III, Environmental Branch

Edgewood Arsenal  
Edgewood, MD 21010  
Attn: David Kramer  
Harold Sommer  
Allen E. Hilsmeier

U. S. Army Engineer Division, Pacific Ocean  
Environmental Section  
Bldg. 230, Ft. Shafter  
APO San Francisco 96558  
Attn: Michael T. Lee, Biologist

Director  
Waterways Experiment Station  
P. O. Box 631  
Vicksburg, MS 39180  
Attn: Technical Library  
J. N. Strange  
Kim Davis  
WESNE

ADTC/DLV  
Eglin AFB, FL 32542  
Attn: J. C. Cornette

National Marine Fisheries Service  
Auke Bay Biological Laboratory  
P. O. Box 155  
Auke Bay, AK 99821  
Attn: Theodore Merrell

National Marine Fisheries Service  
Water Resources Division  
P. O. Box 1668  
Juneau, AK 99801  
Attn: Dale R. Evans, Chief

National Marine Fisheries Service  
Southwest Fisheries Center  
P. O. Box 271  
La Jolla, CA 92037

Department of Commerce  
National Oceanic and Atmospheric Administration  
Washington Science Center, Bldg. 5  
6010 Executive Blvd.  
Rockville, MD 20852  
Attn: Donald P. Martineau, Deputy Associate Administrator  
for Marine Resources  
CAPT Scott E. Drummond, Room 918  
CDR John G. McMillan, USN  
LTJG Richard A. Zachariason, Room 805  
Sidney T. Smith, Room 100  
Milton S. Arnostam  
Emmett S. Hill, Jr.  
Fletcher F. Echard, AD1X3



Department of Commerce  
Biological Laboratory  
Milford, CT 06460

Department of the Interior  
1107 NE 45th Street  
Suite 110  
Seattle, WA 98105  
Attn: Karen Bachman  
Mark L. Holmes

Department of the Interior  
Bureau of Sports Fisheries and Wildlife  
Interior Building  
Washington, D. C. 20240  
Attn: John S. Gottschalk, Director

Bureau of Commercial Fisheries  
Interior Building  
Washington, D. C. 20240  
Attn: Philip M. Roedel, Director

State of Maryland  
Fish and Wildlife Administration  
Annapolis, MD 21404  
Attn: Charles Frisbie  
Barbara Holden

State of North Carolina  
Department of Natural and Economic Resources  
Division of Marine Fisheries  
Box 769  
Morehead City, NC 28557  
Attn: Willard Lane, Artificial Reef Program  
Jim Tyler, Artificial Reef Program

South Carolina Marine Resources Division  
2024 Maybank Highway  
Charleston, SC 29412  
Attn: Michael D. McKenzie

Trust Territory Environmental Protection Board  
P. O. Box 215  
Yap, W.C.I. 96943  
Attn: M. Falanruw, Staff Ecologist

Howard J. King, E-2  
580 Taylor Avenue  
Annapolis, MD 21401

State of Alaska  
Department of Fish and Game  
333 Raspberry Road  
Anchorage, AK 99502  
Attn: Lance L. Trasky, Fisheries Research Biologist

Deputy Commissioner  
Alaska Department of Fish and Game  
Support Building  
Juneau, AK 99801  
Attn: Joseph R. Blum

State of Alaska  
Department of Fish and Game  
Habitat Section  
333 Raspberry Road  
Anchorage, AK 99501

Department of Fish and Game  
Wildlife Protection Branch  
1416 Ninth Street  
Sacramento, CA 95814

State of California  
Marine Resources Division  
350 Golden Shore  
Long Beach, CA 90802  
Attn: Doyle Gates, Regional Manager

State of Florida  
Department of Natural Resources  
Larson Building  
Tallahassee, FL 32304

State of Louisiana  
Wildlife and Fisheries Commission  
P. O. Box 44095, Capital Station  
Baton Rouge, LA 70804  
Attn: Fred Dunham

Virginia Institute of Marine Science  
Gloucester Point, VA 23062  
Attn: William J. Hargis, Director

University of Washington  
College of Fisheries  
Fisheries Research Institute  
Seattle, WA 98195  
Attn: Dave R. Gibbons  
Charles Simenstad, Biologist

Director  
Woods Hole Oceanographic Institution  
Woods Hole, MA 02543  
Attn: Bostwick Ketchum  
Gifford C. Ewing  
Earl E. Hays  
Library

Director  
Scripps Institution of Oceanography  
La Jolla, CA 92037  
Attn: Fred Spiess

School of Oceanography  
Oregon State University  
Corvallis, OR 97331  
Attn: A. G. Carey, Jr.  
Librarian

Chesapeake Bay Institute  
The Johns Hopkins University  
Baltimore, MD 21218

Chesapeake Biological Laboratory  
P. O. Box 38  
Solomons, MD 20688  
Attn: T. S. Y. Koo  
Joseph A. Mihursky  
Martin L. Wiley  
John S. Wilson

Marine Physical Laboratory, S10/UCSD  
Bldg. 106, Naval Undersea Center  
San Diego, CA 92106  
Attn: Charles B. Bishop

University of Hawaii at Manoa  
Hawaii Institute of Marine Biology  
P. O. Box 1346, Coconut Island  
Kaneohe, HI 96744  
Attn: George H. Balazs, Jr., Marine Biologist

Department of Biology  
Juniata College  
Huntingdon, PA 16652  
Attn: Robert L. Fisher

Marine Resources Division  
California State Fisheries Lab  
350 South Magnolia  
Long Beach, CA 30802  
Attn: Robert Kanlen



Argus Pressure Grouting Services, Inc.  
22000 Ryan Road  
Warren, MI 48091  
Attn: Albin Gronowicz, President

Hydronautics  
7210 Pindell School Road  
Laurel, MD 20910  
Attn: Norman Shapira

Robert E. Eckels & Associates  
Consulting Engineers  
2101 Youngfield  
Golden, CO 80401

Woodward Clyde Consultant  
Box 1149  
Orange, CA 92668  
Attn: Jack Kiker

B.O.C. Sub Ocean Services  
1022 Wirt Road  
Houston, TX 77055  
Attn: Thomas L. Kirchberg

Lovelace Biomedical & Environmental Research  
Institute, Inc.  
P. O. Box 5890  
Albuquerque, NM 87115  
Attn: Donald R. Richmond  
E. Royce Fletcher  
Robert K. Jones  
John T. Yelverton

Meteorology Research, Inc.  
464 West Woodbury Road  
Altadena, CA 91001  
Attn: George Woffinder

Mount Auburn Research Associates, Inc.  
385 Elliot Street  
Newton, MA 02164  
Attn: Sheldon L. Kahalas

Tetra Tech, Inc.  
630 N. Rosemead Blvd.  
Pasadena, CA 91107  
Attn: Li-San Hwang

Explo Precision Engineering Corporation  
Manager of Technical Services  
Gretna, LA 70053  
Attn: John J. Ridgeway

NSWC/WOL TR 76-155

Crisfield Laboratory  
Box 351  
Crisfield, MD 21817  
Attn: M. W. Paparella

Defense Documentation Center  
Cameron Station  
Alexandria, VA 22314

12

Office of Naval Research  
Washington, D.C. 20350  
Code 482

TO AID IN UPDATING THE DISTRIBUTION LIST  
FOR NAVAL SURFACE WEAPONS CENTER, WHITE  
OAK TECHNICAL REPORTS PLEASE COMPLETE THE  
FORM BELOW:

TO ALL HOLDERS OF NSWC/WOL/TR 76-155  
by John F. Goertner, Code R-14

DO NOT RETURN THIS FORM IF ALL INFORMATION IS CURRENT

---

A. FACILITY NAME AND ADDRESS (OLD) (Show Zip Code)

---

NEW ADDRESS (Show Zip Code)

---

B. ATTENTION LINE ADDRESSES:

---

C.

☐ REMOVE THIS FACILITY FROM THE DISTRIBUTION LIST FOR TECHNICAL REPORTS ON THIS SUBJECT.

---

D.

NUMBER OF COPIES DESIRED \_\_\_\_\_



DEPARTMENT OF THE NAVY  
NAVAL SURFACE WEAPONS CENTER  
WHITE OAK, SILVER SPRING, MD. 20910

OFFICIAL BUSINESS  
PENALTY FOR PRIVATE USE, \$300

POSTAGE AND FEES PAID  
DEPARTMENT OF THE NAVY  
DOD 316



COMMANDER  
NAVAL SURFACE WEAPONS CENTER  
WHITE OAK, SILVER SPRING, MARYLAND 20910

ATTENTION: CODE R-14